

Republic of Iraq
Ministry of Higher Education & Scientific Research
University of Kerbala
College of Engineering
Electrical & Electronic Engineering



Controller Design of Two-Wheeled Robotic Vehicle Based on Fuzzy Logic Technique

**A Thesis Submitted to the Department of Electrical & Electronic Engineering,
University of Kerbala in Partial Fulfilment of the Requirements for the Degree of
Master of Science (MSC) in Electrical Engineering**

By

Yomna Sabah Hussein

Supervised by

Assist. Prof. Dr. Haider Galil Kamil

Assist. Prof. Dr. Ahmed Abdulhadi Ahmed

1443A.H.

2022A.D.

بِسْمِ اللَّهِ الرَّحْمَنِ الرَّحِيمِ

وَأَنْ لَّيْسَ لِلْإِنْسَانِ إِلَّا مَا سَعَى ﴿39﴾ وَأَنْ سَعْيُهُ سَوْفَ يُرَى ﴿40﴾
ثُمَّ يُجْزَاهُ الْجَزَاءَ الْأَوْفَى ﴿41﴾

صَدَقَ اللَّهُ الْعَظِيمِ

سورة النجم

SUPERVISOR CERTIFICATE

I certify that this thesis entitled "**Controller Design of Two-Wheeled Robotic Vehicle Based on Fuzzy Logic Technique**", which is prepared by "**Yomna Sabah Hussein**", under my supervision at University of Kerbala in partial fulfillment of the requirements for the degree of Master of Science in Electrical Engineering.

Signature:



Assist. Prof. Dr. Haider Galil Kamil

(First Supervisor)

Date: 10/5 / 2022

Signature:



Assist. Prof. Dr. Ahmed Abdulhadi Ahmed

(Second Supervisor)

Date: 10/5 / 2022

LINGUISTIC CERTIFICATION

I certify that this thesis entitled "**Controller Design of Two-Wheeled Robotic Vehicle Based on Fuzzy Logic Technique**" which is prepared by "**Yomna Sabah Hussein**", under my linguistic supervision. It was amended to meet the English style.

Signature: 

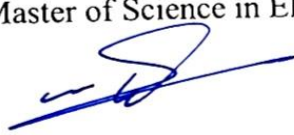
Dr. Ahmed Selmán Altuma

Date: 10 / 5 / 2022

EXAMINATION COMMITTEE CERTIFICATION

We certify that we have read the thesis entitled "**Controller Design of Two-Wheeled Robotic Vehicle Based on Fuzzy Logic Technique**" and as an examining committee, we examined the student "**Yomna Sabah Hussein**" in its content and in what is connected with it and that in our opinion it is adequate as a thesis for the degree of Master of Science in Electrical Engineering.

Signature:



Assist. Prof. Dr. Haider Galil Kamil
(First Supervisor)

Date: 10 / 5 / 2022

Signature:



Assist. Prof. Dr. Ahmed Abdulhadi Ahmed
(Second Supervisor)

Date: 10 / 5 / 2022

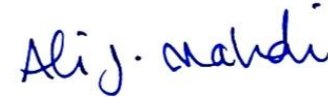
Signature:



Dr. Dhirgaam A. Kadhim
(Member)

Date: 10 / 5 / 2022

Signature:



Assist. Prof. Dr. Ali Jafer Mahdi
(Member)

Date: 10 / 5 / 2022

Signature:



Assist. Prof. Dr. Hayder Mahdi Abdulridha
(Chairman)

Date: 11 / 5 / 2022

Approval of the Department of Electrical
and Electronic Engineering

Signature:




Name: Prof. Dr. Haider Ismael Shahadi

(Head of Electrical and Electronic
Engineering Dept.)

Date: 12 / 5 / 2022

Approval of Deanery of the College of
Engineering/ University of Kerbala.

Signature:



Name: Prof. Dr. Laith Sh. Rasheed

(The Dean of the College of Engineering)

Date: 12 / 5 / 2022

ACKNOWLEDGMENT

I would express my highest praises to Allah S.W.T for the good health and strength that helped me to achieve this goal.

My deepest gratitude and appreciation to my supervisor **Dr Haider Galil Kamil**, for his useful guidance, time, and helpful insightful comments to complete this thesis.

I would like to thank **Dr Ahmed Abdulhadi Ahmed**, for providing valuable assistance during this thesis.

I came to know so many new things; I am really thankful to them.

A special thanks to my parents, my sister, and my brother, who helped and encouraged me throughout my life.

DEDICATION

To

My father who is always there whenever I need him, thank you for making me able to get success.

My mother my first teacher, who believe in me and being my comfort in the hours of sadness. Your prayers was what sustained me this far.

(I hope that this achievement will complete a part of the dream you had for me all those many years ago when you chose to give me the best education you could)

My sister Noor Al-Huda and my brother Maithm, we will be there for one another at all times.

Abstract

This thesis presents the control system for two-wheeled robot vehicles with an extendable payload. The robot structure is based on a double inverted pendulum mechanism. The system comprises five degrees of freedom (left wheel, right wheel, first link, second link, and movable payload). The vehicle has the ability to lift the payload to the demanded height, which provides more flexibility further, ensuring comfortability and protection for users with maintaining system stability while manoeuvring in different environments.

The dynamic model of the system is derived using the Euler-Lagrange equations. Since the model is strong coupling and nonlinear, it posed challenges for controlling the parts of the system, including the upright balancing of the intermediate body and angular displacement of the wheels and lifting the payload to the demanded height.

Various control methods are adopted to study the system stabilisation of the two-wheeled robot vehicle. The first is a combination of Proportional Integral Derivative (PID) and Proportional Derivative (PD) techniques that were tuned manually to develop the stabilisation behaviour of the designed model. The second is the Fuzzy Logic Control (FLC) system. The third control technique is the hybrid control system comprising PID-PD and FLC structure. The PID and PD assist in achieving stable response, but with higher control effort exerted by the wheels motors that reach more than 300N.m. It nevertheless remains essential to decrease the exerted control effort to stabilise the system. The reduction of the controller's efforts was noticed in all system parts with a stable response when a system is designed with a fuzzy logic controller with a significant decrease in the left and right wheels motors less than 45N.m. Then a hybrid control system combined PID, PD, and FLC were designed to improve the system's overall response without affecting the system stability.

A comparative assessment based on the system specifications, including settling time, rise time, overshoot, peak time, and steady-state error, is presented to obtain the best controllers for the proposed system.

The robustness of the control system was tested by applying disturbance forces with different amplitudes, and the maximum disturbance force applied was 350N at each part of the robot vehicle to study the control system's ability to cope with various forces applied.

The simulation of the two-wheeled robot vehicle with a movable payload designed with different control systems is implemented using MATLAB/Simulink environment.

Table of Contents

Abstract	8
Table of Contents	I
Abbreviations	IV
List of Tables	V
List of Figures	VI
Nomenclature	IX
Chapter One	1
Introduction	1
1.1 Overview	1
1.2 Problem Statement	1
1.3 Objectives of the Study	2
1.4 Research Methodology	3
1.5 Thesis Layout	4
Chapter Two	5
Literature Review	5
2.1 Introduction	5
2.2 Literature Review	5
Chapter Three	11
System Description and Mathematical Modelling	11
3.1 Introduction	11
3.2 System Description	12
3.3 System Mathematical Modelling	13
3.4 System Performance	19
3.5 Summary	23

Chapter Four	24
Controller Design with Different Control Strategy	24
4.1 Introduction	24
4.2 Control Design	25
4.2.1 PID Control Design	25
4.2.2 Fuzzy Logic Control Design	40
4.2.3 Hybrid Control Design	56
4.3 Summary	72
Chapter Five	73
Control System Robustness Under Disturbance	73
5.1 Introduction	73
5.2 Disturbance Force with Various Amplitudes	73
5.2.1 Disturbance Applied on the Left Wheel	74
5.2.2 Disturbance Applied on the Right Wheel	76
5.2.3 Disturbance Applied on the First Link	78
5.2.4 Disturbance Applied on the Second Link	80
5.2.5 Disturbance Applied on the Payload	82
5.3 Summary	85
Chapter Six	86
Conclusion, Contribution, and Future works	86
6.1 Conclusion	86
6.2 Contribution	87
6.3 Future Works	88
References	89
APPENDICES	99

APPENDIX-A	99
APPENDIX-B	100
الخلاصة	110

Abbreviations

<i>DC</i>	<i>Direct current</i>
<i>DOF</i>	<i>Degree of Freedom</i>
<i>FLC</i>	<i>Fuzzy Logic Controllers</i>
<i>IP</i>	<i>Inverted Pendulum</i>
<i>NB</i>	<i>Negative Big</i>
<i>NS</i>	<i>Negative Small</i>
<i>PB</i>	<i>Positive Big</i>
<i>PD</i>	<i>Proportional Derivative</i>
<i>PID</i>	<i>Proportional Integral derivative</i>
<i>PS</i>	<i>Positive Small</i>
<i>Z</i>	<i>Zero</i>

List of Tables

Table 3. 1: The parameters of a two-wheeled robot vehicle with movable payload..... 18

Table 4. 1: PID gain parameters. 26

Table 4. 2: System specifications apply the first input signal using PID controllers. 30

Table 4. 3: System specifications applying the second input signal using PID controllers. 33

Table 4. 4: System specifications apply the third input signal using PID controllers..... 36

Table 4. 5: System specifications apply the fourth input signal using PID controllers.... 39

Table 4. 6: Fuzzy rules base. 41

Table 4. 7: System specifications apply the first input signal using fuzzy logic controllers. 46

Table 4. 8: System specifications applying the second input signal using fuzzy logic controllers 49

Table 4. 9: System specifications apply the third input signal using fuzzy logic controllers. 52

Table 4. 10: System specifications applying the fourth input signal using fuzzy logic controllers..... 55

Table 4. 11: PID gain parameters. 57

Table 4. 12: Fuzzy rules base. 57

Table 4. 13: System specifications applying the first input signal using hybrid controllers 62

Table 4. 14: System specifications apply the second input signal using hybrid controllers. 65

Table 4. 15: System specifications apply the third input signal using hybrid controllers 68

Table 4. 16: System specifications apply the fourth input signal using hybrid controllers. 71

List of Figures

Figure 3. 1: The schematic diagram of the robot vehicle.....	12
Figure 3. 2: payload input signal.....	19
Figure 3. 3: System open-loop response with the first input signal.	19
Figure 3. 4: Payload input signal.....	20
Figure 3. 5: System open-loop response with the second input signal.	20
Figure 3. 6: Payload input signal.....	21
Figure 3. 7: System open-loop response with the third input signal.	21
Figure 3. 8: Payload input signal.....	22
Figure 3. 9: System open-loop response with the fourth input signal.....	22
Figure 4. 1: The block diagram using PID controllers.....	26
Figure 4. 2: The first input signal applied on the payload.....	27
Figure 4. 3: System response of PID controllers.....	28
Figure 4. 4: System exerted effort using PID controllers.....	29
Figure 4. 5: The second input signal applied on the payload.....	30
Figure 4. 6: System response of PID controllers.....	31
Figure 4. 7: System exerted effort using PID controllers.....	32
Figure 4. 8: The third input signal applied on the payload.....	33
Figure 4. 9: System response of PID controllers.....	34
Figure 4. 10: System exerted effort using PID controllers.....	35
Figure 4. 11: The fourth input signal applied on the payload.	36
Figure 4. 12: System response of PID controllers.....	37
Figure 4. 13: System exerted effort using PID controllers.....	38
Figure 4. 14: The system block diagram using the fuzzy logic controller.	41
Figure 4. 15: Gaussian membership function with two inputs and one output.....	42
Figure 4. 16: The first input signal applied on the payload.....	43
Figure 4. 17: System response using a fuzzy logic controller.....	44
Figure 4. 18: System exerted effort using a fuzzy logic controller.	45
Figure 4. 19: The second input signal applied on the payload.....	46
Figure 4. 20: System response using a fuzzy logic controller.....	47

Figure 4. 21: System exerted effort using a fuzzy logic controller. 48

Figure 4. 22: The third input signal applied on the payload. 49

Figure 4. 23: System response using a fuzzy logic controller. 50

Figure 4. 24: System exerted effort using a fuzzy logic controller. 51

Figure 4. 25: The fourth input signal applied on the payload. 52

Figure 4. 26: System response using a fuzzy logic controller. 53

Figure 4. 27: System exerted effort using a fuzzy logic controller. 54

Figure 4. 28: The system block diagram using hybrid controllers. 56

Figure 4. 29: Gaussian membership function with two inputs and one output. 58

Figure 4. 30: The first input signal applied on the payload. 59

Figure 4. 31: System response using hybrid controllers. 60

Figure 4. 32: System exerted effort using hybrid controllers. 61

Figure 4. 33: The second input signal applied on the payload. 62

Figure 4. 34: System response using hybrid controllers. 63

Figure 4. 35: System exerted effort using hybrid controllers. 64

Figure 4. 36: The third input signal applied on the payload. 65

Figure 4. 37: System response using hybrid controllers. 66

Figure 4. 38: System exerted effort using hybrid controllers. 67

Figure 4. 39: The fourth input signal applied on the payload. 68

Figure 4. 40: System response using hybrid controllers. 69

Figure 4. 41: System exerted effort using hybrid controllers. 70

Figure 5. 1: Disturbance applied on the left wheel with different amplitudes. 74

Figure 5. 2: The control system effort with disturbance forces applied on the left wheel.
..... 75

Figure 5. 3: Disturbance applied on the right wheel with different amplitudes. 76

Figure 5. 4: The control system effort with disturbance forces applied on the right wheel.
..... 77

Figure 5. 5: Disturbance applied on the first link with different amplitudes. 78

Figure 5. 6: The control system effort with disturbance forces applied on the first link. 79

Figure 5. 7: Disturbance applied on the second link with different amplitudes. 80

Figure 5. 8: The control system effort with disturbance forces applied on the second link.
..... 81

Figure 5. 9: Disturbance applied on the payload with different amplitudes. 82

Figure 5. 10: The control system effort with disturbance forces applied on the payload.83

Nomenclature

<i>Variables and Units</i>	<i>Description</i>
$L_{M(t)}(m)$	Distance from the centre of mass to the payload
$L_{2u(t)}(m)$	Distance from the centre of mass to the upper part of 2 nd link
$L_a(m)$	Linear actuator position
$L_1(m)$	The half length of the 1 st link
$H(m)$	Distance between two wheels
$Q(m)$	The linear actuator displacement
$M_1(Kg)$	Mass of the 1 st link
$M_m(Kg)$	The motor mass that driving the 2 nd link
$M_{2l}, M_{2u}(Kg)$	The lower-upper parts mass of the 2 nd link
$M_a(Kg)$	Linear actuator mass
$M(Kg)$	Mass of the payload
$M_w(Kg)$	Mass of the wheels
$T_R, T_L(N.m)$	Torques driving left-right wheels
$T_m(N.m)$	The motor torque
$F_a(N)$	The linear actuator force
$F_f(N)$	The linear actuator frictional force
$F_d(N)$	The external force
$\theta_1(rad)$	The angle of the 1 st link
$\theta_2(rad)$	The angle of the 2 nd link
$\phi(rad)$	The angle measured around the Z-axis
$\delta_R, \delta_L(m)$	The angular displacement of both wheels
$J_1(Kg.m^2)$	Mass-moment of inertia of the 1 st link
$J_{2u}, J_{2l}(Kg.m^2)$	Mass-moment of inertia of the 2 nd link upper-lower parts
$J_a(Kg.m^2)$	Mass-moment of inertia for the actuator
$J_M(Kg.m^2)$	Mass-moment of inertia for the payload
$J_w(Kg.m^2)$	Mass-moment of inertia for both wheels
$J_{IB}(Kg.m^2)$	Mass-moment of inertia for the intermediate body

Chapter One

Introduction

1.1 Overview

In recent years, the interest in studying the inverted pendulum (IP) systems has increased due to system complexity and non-linearity [1] [2] [3]. Many robots operate on the principle of an IP system and used in many applications. The two-wheeled robot vehicles one of the IP system applications became a standard topic for researchers and engineers because of the control system challenges [4] [5] [6]. The IP system plays a vital role as a benchmark in control system engineering. This role is due to its high complexity, non-linearity, and strong-coupling model [7] [8]. A two-wheeled robot vehicle has the exact specifications as an IP structure due to the unbalanced of the system. Previous research has reflected the development of many applications based on the inverted pendulum system, including the design of a classical pendulum on a cart [9] [10] [11] [12]. The field of this study attractive many researchers for many reasons involve: (1) Enable evolution of motion problems for a two-wheeled robot based on double IP with movable payload; (2) It is considered a principle to test various control techniques and a basis to develop multiple applications such as advanced personal transporters and balancing two-wheelchairs.

1.2 Problem Statement

Currently, the problem of balancing an inverted pendulum is used as a benchmark for the control algorithms, which is one of the most widely used for under-actuated systems. The system becomes more complicated with increased links that increase the degrees of freedom and the complexity of the system. The multi links systems present challenging and control problems such as double inverted pendulum [2] [13] [14] and triple inverted pendulum [15] [16] [17].

Due to the system complexity, the multi links systems provide helpful testbeds for evaluation, validation, and comparison between different control techniques. Studying such systems enables many researchers to design controllers for inverted pendulum systems. There have been many research papers that have focused on the applications based

on inverted pendulum systems. The Segway robot [18] [19] is a two-wheeled mobile robot used as human transport that is considered one of the most critical applications of the IP systems [20]. Wheelchairs on two wheels helped the person to reach the extended height, which is very complicated in modelled and controlled due to independent mobility that can be used by disabled people and becoming a necessary part of their lives [5], furthermore the flying inverted pendulum is one of IP system applications [21]. These applications and others provide a highly designer challenge because of the system's imbalanced and unstable nature.

This work presents the modelling and controlling of the two-wheeled robot vehicle with two links. The vehicle was designed with a movable payload that expanded the system degrees of freedom, attached to the intermediate body, increasing system complexity and non-linearity. The robot vehicle can extend the payload to the required height and achieve the desired motion while keeping the two links at the upright position. The research investigated and implemented different control approaches to confirm the complexity and highly non-linearity of the two-wheeled vehicle.

1.3 Objectives of the Study

This research aimed to design various control systems for stabilising a two-wheeled robot vehicle with a movable payload based on the concept of double links inverted pendulum.

The following objectives can be summarised as follows:

- To simulate and analyse the open loop response and test the system's behaviour by applying different input signals on the payload actuator.
- To design different controllers that enable the stabilising and balancing of the system.
- To validate the control system's stability by applying various force input signals.
- To evaluate the robustness of the controller for stabilising the system and rejecting external disturbances applied separately on each part of the robot vehicle.

1.4 Research Methodology

- Reviewing and understanding most related papers in the field of inverted pendulum systems and their applications, controlled with different control techniques.
- The Euler-Lagrange modelling approach was used to derive the mathematical model for minimising the complexity of the robot vehicle with five degrees of freedom.
- The system of the robot vehicle simulated and verified using MATLAB/Simulink environment.
- Design different control techniques further evaluate the system performance in terms of the system response characteristics.
- Finally, test the system robustness by applying external disturbance with different amplitudes on the two-wheeled robot vehicle with a movable payload.

1.5 Thesis Layout

Chapter 2 begins with relevant reviews of inverted pendulum systems with single and multiple links and their applications further focuses on different control systems used for the system stabilisation.

Chapter 3 presented the system description and the mathematical model of the two-wheeled robot with a movable payload capable of manoeuvring on flat surfaces, including the equation's derivation using the Euler Lagrange approach. The system motion introduced five non-linear differential equations due to the system's five degrees of freedom moving on flat surfaces.

Chapter 4 tests the system performance and different control system techniques designed for system stabilisation. The controller types used include PID-PD, FLC, and hybrid controllers (PID, PD, and FLC). Furthermore, a comparative study presented the proposed control systems regarding the responses characteristics and control effort.

Chapter 5 evaluates the proposed model's system robustness by applying external disturbances with different amplitudes.

Chapter 6 summarises and evaluates the study's findings, explains the study's contributions, and provides suggestions for future work.

Chapter Two

Literature Review

2.1 Introduction

This chapter reviews the relevant work of the study based on the IP system and associated with under-actuated control systems. The presented works of literature based on the IP has focused on different control systems and embedding various control techniques. Several works of literature described single, double, and triple inverted pendulum systems. Many applications based on inverted pendulum systems, were used to facilitate difficulties faced the human. The researchers have been implemented various control techniques concerning inverted pendulum systems focused on designing a control system to solve the problems of system stabilisation. Some of them focused on tracking controllers while others designed the balancing and stabilisation controllers for the upright balancing.

2.2 Literature Review

There have been many studies that have established the dynamic model of the inverted pendulum system. Some authors have presented the Lagrange equation of motion using kinetic and potential energy. Researchers published papers describing the dynamics of the IP systems using the Lagrange equation for modelling complex, non-linearity, and strong coupling systems such as **F Phelps et al. (1965)** [22], **Z Lijuan et al. (2006)** [23], and **J Wu et al. (2021)** [24].

K Furta et al. (1980) [25] have presented double IP on an inclined rail. An optimal control system based on servo control theory is designed for the proposed model. The experimental results have proven effectiveness for the model within an inclined angle. Furthermore, the results match with linearized model simulation. Several researchers have examined double IP systems, such as **H Niemann and J Poulsen (2005)** [26], **V Mohan et al. (2017)** [27].

W chen et al. (1998) [28] designed a fuzzy logic control system of an inverted pendulum. The simulation results evaluate the fuzzy logic controller and compare it with the conventional controller. The fuzzy controller successfully kept the pole upright under

different conditions and improved the performance compared to the conventional controller.

J Yi and N Yubazaki (2000) [1] introduced a control strategy using FLC for stabilising the inverted pendulum on a cart. The proposed controller is executed in parallel to control the pendulum angle's position and the cart's motion. According to the simulation results show that the control system can stabilise a wide range of the inverted pendulum within 9s.

J Wang (2001) [29] the researcher applied PID for inverted pendulum system stabilisation. The proposed controller is designed with three types of inverted pendulum starting with one PID, two, and three PID controllers design. The simulation results explain that the three types of the inverted pendulum are very powerful and successfully stabilise the system with good performance and provide robustness to the large and fast disturbance.

A Delibasi and I Kucukdemiral (2007) [30] this paper presented a robust PID controller for double inverted pendulum on cart stabilisation. The goal of the control system used is to make the cart move horizontally while the double links of the intermediate body are balanced at the upright position. The experimental results show that the PID controller successfully stabilised the model and rejected the applied external disturbance.

Some researchers have utilized a two-wheeled mobile robot based on IP systems such as **J Li et al. (2008)** [31], **Z Guo et al. (2014)** [32], **S Kim and S Kwon (2015)** [6].

T Ren et al. (2008) [33] have presented motion control of two-wheeled mobile robots. Researchers proposed a PID controller tuned automatically for the system stabilisation and following the desired motion. The simulation results illustrate the effectiveness of the control system.

K M Goher et al. (2011) [34] proposed a two-wheeled robot vehicle with an intermediate body based on an inverted pendulum system with a virtual payload. The system is controlled with two types of controllers, including the conventional PD and hybrid fuzzy

controller with PD. The two control techniques successfully stabilised the proposed model. An external disturbance is applied, which affect the balancing of the intermediate body. The design of the control systems successfully deals with unexpected external disturbances.

A Yadav et al. (2011) [35] authors used PID and a different combination of a fuzzy logic controller for controlling the inverted pendulum. The simulation results of the PID and fuzzy successfully stabilised the pendulum angle. The fuzzy and PD was better than the PID controller. Moreover, the combination of fuzzy PD+I is approximately the same as fuzzy PD+PID. The control system fuzzy PD+PID improved the settling time by 37.5%, which explains that this controller gives better performance when compared with other combinations of fuzzy controllers to stabilise the inverted pendulum.

J Wu and W Zhang. (2011) [36] have proposed a two-wheeled self-balancing robot vehicle based on an inverted pendulum system. The system used pole placement and fuzzy logic controllers, and both controllers provide good stability for the model with a short settling time and low overshoot. The fuzzy logic control system obtains better dynamic performance and can successfully achieve self-balance control of the model and prevent the robot from falling down.

A.M. Almeshal et al. (2012) [37] used PID-PD and hybrid controllers, including FLC+PD and FLC+PID, to stabilise the two-wheeled robot vehicle and an intermediate body comprised of two links based on a double inverted pendulum with movable payload. The control systems approaches stabilised the robot vehicle. An external disturbance force with 80N was applied on the tilt angles of both links to test the intermediate body stability. The system successfully copes with external disturbance. However, the hybrid controllers showed improved simulation results than the PID-PD controllers.

A. M. Almeshal et al. (2012) [38] have designed a hybrid fuzzy logic control strategy to balance the two-wheeled robot vehicle with two links attached to a movable payload based on a double IP system. The authors applied disturbance force with different amplitudes on

the first and second links of the intermediate body. The maximum disturbance applied is 300N. The simulation results have been proven the robustness of the controllers to overcome the external disturbances.

F.Dai et al. (2014) [39] this research is about a two-wheeled robot moving on a sloped surface. The presented model was designed with two degrees of freedom, one for the robot's centre of gravity moved forward and backwards. The other one can tilt the robot body in the vertical plane when the robot spins quickly. Two PID controllers ensure that the robot body is stabilised at the upright position and rejected the external disturbances are applied. Simulation results show that the robot can move on a sloped surface with a small pitch angle.

A triple IP system presented by **H G Kamil et al. (2015)** [40] where the authors have designed a robot gymnast with three joints. The proposed model mimics the acrobat with two DC motors at the shoulders and hip joints. Researchers employed an optimisation technique include the Bees Algorithm to select the robot gymnast's optimal parameters to control the swing from down to the upright situation. The simulation results successfully achieve the robot gymnast's faster and smoother swing up. In a similar vein **H G Kamil et al. (2017)** [41] proposed controlling of three links robot manipulator. The main challenge is to pose the three links at the upright position. The study's main strength is the quick time to reach the upright position.

M Shehu et al. (2016) [42] proposed a single-link IP system on a cart. Researchers proposed to design three controllers for upright stabilisation and tracking controls of the IP system. PID, LQR and pole placement are proposed. System simulation results illustrated the performance of the control systems in terms of system characteristics and disturbance rejection.

A Kharola (2016) [43] this paper presents a two-wheeled inverted pendulum robot controlled using a fuzzy logic controller. The model is comprised of a chassis mounted on two movable wheels. The fuzzy logic controller shows excellent performance in terms of

system characteristics. The controller of the wheels controls the system within 9s and has zero steady-state error.

P Patil et al. 2016 [44] this paper introduced stabilisation and controlling inverted pendulum on cart moving on an inclined surface. The control systems used are the PID controller and fuzzy logic controller and compared between the two controllers in terms of system specifications, including settling time, overshoot, and steady-state error. The simulation results obtained good results in both controllers, but better performance is shown in the PID controller over the fuzzy logic controller.

S Shubhank et al. (2017) [45] have used a PID control strategy for the self-balancing robot. The robot with a two-wheeled vehicle based on an inverted pendulum system. The proposed control system, maintain self-balancing the robot and moving forward further rejected external disturbances. This model can be used in several applications, including healthcare, agriculture fields, airports, and intelligent robot guide.

R Eini et al. (2018) [46] researchers have proposed a paper about controlling a rotational IP system designed with an adaptive Fuzzy Logic Controller (FLC). The adaptive FLC is considered efficient due to the wide range of the system associated with uncertainties. Simulation results had shown that the adaptive FLC performed efficiently for stabilising the IP system.

K Pankaj et al. (2018) [47] have represented a comparative study of various control systems used for balancing the IP system. A Proportional Derivative, Fuzzy Logic Controller, Neural Networks, and Adaption based Neuro-Fuzzy Inference System are all used to balance the IP. The simulation results illustrated that the Fuzzy controller and Neural Networks respond better than the PD controller regarding settling time and peak overshoot. This method demonstrated the effectiveness over competing methods accordingly combined the advantages of Fuzzy controller and Neural Networks.

I Siradjuddin (2018) [48] were proposed an underactuated and highly unstable inverted pendulum on a cart. The authors derived the mathematical model using the Euler Lagrange equation. A PID control system used for the system stabilisation and the control system parameters has been chosen the appropriate values to ensure the system's stability. From the simulation results, the pendulum reaches the desired position within 2s; further, the cart response settles less than 4s.

A Zimit et al. (2018) [49] this research is about self-balancing two-wheeled robot vehicles. The researcher used a PID controller to balance the robot at the upright position and follow the trajectory path. The mathematical model of the robot was developed by using the Euler Lagrange equation. The experimental results have shown the successful performance of the control system used with low cost and flexible design.

M Heidar et al. (2021) [50] this paper provides a hybrid control system that combines fuzzy and PD controllers to stabilise the inverted pendulum system on a cart. The hybrid control system controls the displacement of the cart and the pendulum angle. The simulation results obtained acceptable performance for the control system used in stabilising the motion of the inverted pendulum.

N Nguyen et al. (2021) [51] they proposed a nonlinear hybrid controller for stabilising a rotary inverted pendulum system that guarantees faster swing up and good stabilisation performance. The hybrid control system combined the fuzzy- Linear Quadratic Regulator approaches to derive the arm at zero position and simultaneously stabilise the pendulum at the upright position. The experimental results have shown the effectiveness of a nonlinear hybrid controller system.

These works of literature review and understand the most related papers in the field of inverted pendulum systems and their applications, controlled with different control techniques, including PID, FLC, and hybrid control systems. The literature has proven the effectiveness of the proposed control systems used in the inverted pendulum system and their applications.

Chapter Three

System Description and Mathematical Modelling

3.1 Introduction

This chapter presents the system description and the mathematical model of a two-wheeled robot vehicle with a movable payload. The robot vehicle is capable of manoeuvring on flat surfaces. The two-wheeled robot vehicle with double joints is a complex coupled system and it's very difficult to achieve system stabilisation. The main fundamental issues with this study are the ability to control the movement of the two-wheeled robot vehicle with movable payload by determining the system mathematical equations, analyse and controlling the motion. The system equations of motion were derived using the Euler Lagrange of motion to determine the system dynamics.

In this study, the model comprises two wheels and two links with a movable payload that can be lifted to demand height. The movable payload provides the system flexibility and increases the system's complexity.

The system performance was investigated using five non-linear differential equations and examined if the proposed model required a controller for the proposed model stabilisation. Section 3.2 presents a description of the proposed system with schematic diagrams illustrating the two-wheeled robot's main parts. Section 3.3 explains the mathematical model derivation of the robot vehicle when moving on flat surfaces. Section 3.4 analyses and investigates system performance behaviour with different input signals.

3.2 System Description

This section explains the system description with a schematic diagram of the proposed model shown, in Figure 3.1. The system consists of two wheels and an intermediate body comprised of two links connected to the payload that can move to the demanded height. The robot vehicle drives these wheels using two DC motors, with a further motor driving the second link; these motors help the system be stabilised at the upright position. A single actuator in the middle of the second link of the intermediate body lifts the payload to the required height. The robot vehicle thus has five Degrees of Freedom (DOF): the translational motion of the two wheels, the two links of the system, and the movable payload linear actuator. The angles of both links, the first being θ_1 and the second θ_2 , were measured from the Z -axis, representing the intermediate body being in the upright position or inclined to only a small degree, depending on the controller design. Q is the linear displacement of the payload measured from the O_2 position along with the second link. The vehicle moves linearly in the XY plane due to the angular displacement of both wheels, the left δ_L and the right δ_R . These are the main five parts of the two-wheeled robot vehicle [37].

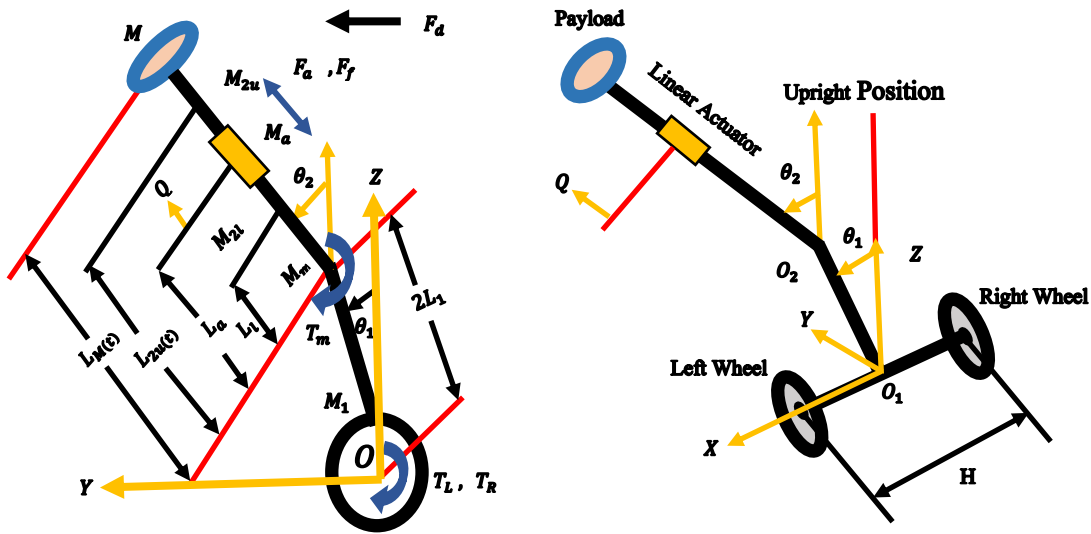


Figure 3. 1: The schematic diagram of the robot vehicle.

3.3 System Mathematical Modelling

The mathematical modelling of the system was derived using the Euler Lagrange equation. Many researchers described the dynamics of the applications based on IP systems using the Lagrange equation due to modelling complex, non-linearity, and strong coupling systems [22][23] [24]. This method offers a simple approach to determining a complex systems model [23] [52]. The Lagrange equation employs both kinetic energy and potential energy that are solved for motion [53] using an equation as follows:

$$\frac{d}{dt} \left(\frac{\partial L}{\partial \dot{q}_i} \right) - \frac{\partial L}{\partial q_i} = Q_i \quad (3.1)$$

Where:

$L = T_T - V_T$ The Lagrange function.

Q_i = The force vector.

q_i = The coordinate vector.

T_T = The total kinetic energy.

V_T = The total potential energy.

The system has five degrees of freedom, so the selected coordinates are:

$$q_i = [\delta_L \quad \delta_R \quad \theta_1 \quad \theta_2 \quad Q] \quad (3.2)$$

The force vector is defined as:

$$Q_j = [T_{LT} \quad T_{RT} \quad 0.5(T_{LT}+T_{RT}) \quad T_{MT} \quad F_{aT}] \quad (3.3)$$

Where:

$$T_{LT} = T_L - T_{fL} \quad (3.4)$$

$$T_{RT} = T_R - T_{fR} \quad (3.5)$$

$$T_{MT} = T_M - T_{fM} \quad (3.6)$$

$$F_{aT} = F_a - F_{fa} \quad (3.7)$$

T_{fL} = The frictional moments of the left wheel.

T_{fR} = The frictional moments of the right wheel.

T_{fM} = Frictional moments of the intermediate body.

F_{fa} = Actuator frictional force.

The expressions of total kinetic energy and total potential energy are:

$$T_T = T_1 + T_{2l} + T_{2u} + T_m + T_a + T_M + T_c + T_\phi \quad (3.8)$$

$$V_T = V_1 + V_{2l} + V_{2u} + V_m + V_M + V_a \quad (3.9)$$

The derivative of kinetic energy can be observed as follows:

$$T_1 = \frac{1}{2} M_1 \left(\left(\frac{R_w}{2} (\dot{\delta}_L + \dot{\delta}_R) + L_1 \dot{\theta}_1 \cos \theta_1 \right)^2 + (L_1 \dot{\theta}_1 \sin \theta_1)^2 \right) + \frac{1}{2} J_1 \dot{\theta}_1^2 \quad (3.10)$$

$$T_m = \frac{1}{2} M_m \left(\left(\frac{R_w}{2} (\dot{\delta}_L + \dot{\delta}_R) + 2L_1 \dot{\theta}_1 \cos \theta_1 \right)^2 + (L_1 \dot{\theta}_1 \sin \theta_1)^2 \right) + \frac{1}{2} J_m \dot{\theta}_1^2 \quad (3.11)$$

$$T_{2l} = \frac{1}{2} M_{2l} \left(\left(\frac{R_w}{2} (\dot{\delta}_L + \dot{\delta}_R) + 2L_1 \dot{\theta}_1 \cos \theta_1 + L_{2l} \dot{\theta}_2 \cos \theta_2 \right)^2 + (2L_1 \dot{\theta}_1 \sin \theta_1 + L_{2l} \dot{\theta}_2 \sin \theta_2) \right) + \frac{1}{2} J_{2l} \dot{\theta}_2^2 \quad (3.12)$$

$$T_a = \frac{1}{2} M_a \left(\left(\frac{R_w}{2} (\dot{\delta}_L + \dot{\delta}_R) + 2L_1 \dot{\theta}_1 \cos \theta_1 + L_{2l} \dot{\theta}_2 \cos \theta_2 \right)^2 + (2L_1 \dot{\theta}_1 \sin \theta_1 + 2L_{2l} \dot{\theta}_2 \sin \theta_2) \right) + \frac{1}{2} J_a \dot{\theta}_2^2 \quad (3.13)$$

$$T_{2u} = \frac{1}{2} M_{2u} \left(\dot{Q}^2 \left(\frac{R_w}{2} (\dot{\delta}_L + \dot{\delta}_R) + 2L_1 \dot{\theta}_1 \cos \theta_1 + 2L_{u(t)} \dot{\theta}_2 \cos \theta_2 \right)^2 + (2L_1 \dot{\theta}_1 \sin \theta_1 + L_{2u(t)} \dot{\theta}_2 \sin \theta_2) \right) + \frac{1}{2} J_{2u} \dot{\theta}_2^2 \quad (3.14)$$

$$T_M = \frac{1}{2}M \left(\dot{Q}^2 \left(\frac{R_w}{2} (\dot{\delta}_L + \dot{\delta}_R) + 2 L_1 \dot{\theta}_1 \cos \theta_1 + 2 L_{M(t)} \dot{\theta}_2 \cos \theta_2 \right)^2 + (2 L_1 \dot{\theta}_1 \sin \theta_1 + L_{2M(t)} \dot{\theta}_2 \sin \theta_2)^2 \right) + \frac{1}{2} J_M \dot{\theta}_2^2 \quad (3.15)$$

$$T_c = (M_w R_w^2 + J_w) (\dot{\delta}_L^2 + \dot{\delta}_R^2) \quad (3.16)$$

$$T_\phi = \frac{1}{2} (2J_w + J_{IB}) \dot{\phi}^2 \quad (3.17)$$

Simplifying the total kinetic energy is expressed as:

$$T_T = C_{21} (\dot{\delta}_L^2 + \dot{\delta}_R^2) + C_{22} \dot{\delta}_L \dot{\delta}_R + \frac{1}{2} C_8 \dot{Q}^2 + \frac{1}{2} C_{16} \dot{\theta}_2^2 + C_{18} \dot{\theta}_1^2 + \frac{1}{2} (C_{20} + C_{12} Q + C_8 Q^2) \dot{\theta}_2^2 + C_9 \frac{R_w}{2} L_1 \dot{\theta}_1 (\dot{\delta}_L + \dot{\delta}_R) \cos \theta_1 + \frac{R_w}{2} (C_{10} + C_8 Q) (\dot{\delta}_L + \dot{\delta}_R) \dot{\theta}_2 \cos \theta_2 + 2 L_1 (C_{10} + C_8 Q) \dot{\theta}_1 \dot{\theta}_2 \cos(\theta_1 - \theta_2) \quad (3.18)$$

The Potential energy of the system is expressed as:

$$V_1 = M_1 g L_1 \cos \theta_1 \quad (3.19)$$

$$V_m = 2M_{m1} g L_1 \cos \theta_1 \quad (3.20)$$

$$V_{2l} = M_{2l} g (2L_1 \cos \theta_1 + L_{2l} \cos \theta_2) \quad (3.21)$$

$$V_{2u} = M_{2u} g (2L_1 \cos \theta_1 + 2L_{2u(t)} \cos \theta_2) \quad (3.22)$$

$$V_a = M_a g (2L_1 \cos \theta_1 + 2L_{2l} \cos \theta_2) \quad (3.23)$$

$$V_M = M g (2L_1 \cos \theta_1 + 2L_{2M(t)} \cos \theta_2) \quad (3.24)$$

Where:

$$L_{2u(t)} = 2L_{2l} + L_{2u} + Q \quad (3.25)$$

$$L_{M(t)} = 2L_{2l} + 2L_{2u} + Q \quad (3.26)$$

After simplifying the total potential energy of the system:

$$V_T = C_3 g \cos \theta_1 + (C_{15} + C_8 Q) g \cos \theta_2 \quad (3.27)$$

The Lagrange function can be written as:

$$L = T_T - V_T \quad (3.28)$$

After substituting T_T and V_T , the Lagrange of the system is defined as:

$$\begin{aligned} L = & C_{21}(\dot{\delta}_L^2 + \dot{\delta}_R^2) + C_{22}\dot{\delta}_L\dot{\delta}_R + \frac{1}{2}C_8\dot{Q}^2 + \frac{1}{2}C_{16}\dot{\theta}_2 + C_{18}\dot{\theta}_1^2 + \frac{1}{2}(C_{20} + C_{12}Q + \\ & C_8Q^2)\dot{\theta}_2^2 + C_9\frac{R_w}{2}L_1\dot{\theta}_1(\dot{\delta}_L + \dot{\delta}_R)\cos\theta_1 + \frac{R_w}{2}(C_{10} + C_8Q)(\dot{\delta}_L + \\ & \dot{\delta}_R)\dot{\theta}_2\cos\theta_2 + 2L_1(C_{10} + C_8Q)\dot{\theta}_1\dot{\theta}_2\cos(\theta_1 - \theta_2) - C_3g\cos\theta_1 + (C_{15} + \\ & C_8Q)g\cos\theta_2 \end{aligned} \quad (3.29)$$

After calculating each system coordinate, the equations of motion of the system are generated as follows:

$$\frac{d}{dt}\left(\frac{\partial L}{\partial \dot{\delta}_L}\right) - \frac{\partial L}{\partial \delta_L} = T_L - T_{fL} \quad (3.30)$$

$$\frac{d}{dt}\left(\frac{\partial L}{\partial \dot{\delta}_R}\right) - \frac{\partial L}{\partial \delta_R} = T_R - T_{fR} \quad (3.31)$$

$$\frac{d}{dt}\left(\frac{\partial L}{\partial \dot{\theta}_1}\right) - \frac{\partial L}{\partial \theta_1} = 0.5(T_{LT} + T_{RT}) \quad (3.32)$$

$$\frac{d}{dt}\left(\frac{\partial L}{\partial \dot{\theta}_2}\right) - \frac{\partial L}{\partial \theta_2} = T_M - T_{FM} - L_d F_d \quad (3.33)$$

$$\frac{d}{dt}\left(\frac{\partial L}{\partial \dot{Q}}\right) - \frac{\partial L}{\partial Q} = F_a - F_{fa} \quad (3.34)$$

The mathematical system model was derived [54], and five non-linear differential equations were yielded:

$$\begin{aligned} 2C_{21}\ddot{\delta}_L + C_{22}\ddot{\delta}_R + C_9\frac{R_w}{2}L_1\ddot{\theta}_1\cos\theta_1 - C_9\frac{R_w}{2}L_1\dot{\theta}_1^2\sin\theta_1 + \frac{R_w}{2}(C_{10} + C_8Q)\ddot{\theta}_2\cos\theta_2 - \frac{R_w}{2}(C_{10} + \\ C_8Q)\dot{\theta}_2^2\sin\theta_2 + \frac{R_w}{2}C_8\dot{Q}\dot{\theta}_2\cos\theta_2 = T_L - T_{fL} \end{aligned} \quad (3.35)$$

$$\begin{aligned} 2C_{21}\ddot{\delta}_R + C_{22}\ddot{\delta}_L + C_9\frac{R_w}{2}L_1\ddot{\theta}_1\cos\theta_1 - C_9\frac{R_w}{2}L_1\dot{\theta}_1^2\sin\theta_1 + \frac{R_w}{2}(C_{10} + C_8Q)\ddot{\theta}_2\cos\theta_2 - \frac{R_w}{2}(C_{10} + \\ C_8Q)\dot{\theta}_2^2\sin\theta_2 + \frac{R_w}{2}C_8\dot{Q}\dot{\theta}_2\cos\theta_2 = T_R - T_{fR} \end{aligned} \quad (3.36)$$

$$\begin{aligned}
& 2C_{18}\ddot{\theta}_1 + C_9 \frac{R_w}{2} L_1 (\ddot{\delta}_L + \ddot{\delta}_R) \cos \theta_1 - C_9 \frac{R_w}{2} L_1 (\dot{\delta}_L + \dot{\delta}_R) \dot{\theta}_1 \sin \theta_1 + 2L_1 (C_{10} + C_8 Q) \dot{\theta}_2 \cos(\theta_1 - \theta_2) - \\
& 2L_1 (C_{10} + C_8 Q) \dot{\theta}_1 \dot{\theta}_2 \sin(\theta_1 - \theta_2) + 2L_1 (C_{10} + C_8 Q) \dot{\theta}_2^2 \sin(\theta_1 - \theta_2) + 2L_1 C_8 \dot{Q} \dot{\theta}_2 \cos(\theta_1 - \theta_2) + \\
& C_9 \frac{R_w}{2} L_1 \dot{\theta}_1^2 (\dot{\delta}_L + \dot{\delta}_R) \sin \theta_1 + 2L_1 (C_{10} + C_8 Q) \dot{\theta}_1^2 \dot{\theta}_2 \sin(\theta_1 - \theta_2) - C_3 g \dot{\theta}_1 \sin \theta_1 = 0.5 (T_{LT} + T_{RT})
\end{aligned} \tag{3.37}$$

$$\begin{aligned}
& C_{20}\ddot{\theta}_2 + (C_{12} \dot{Q} + 2C_8 Q) \dot{\theta}_2 + (C_{12} Q + C_8 Q^2) \ddot{\theta}_2 + \frac{R_w}{2} (C_{10} + C_8 Q) (\ddot{\delta}_L + \ddot{\delta}_R) \cos \theta_2 - \frac{R_w}{2} (C_{10} + \\
& C_8 Q) (\dot{\delta}_L + \dot{\delta}_R) \dot{\theta}_2 \sin \theta_2 + C_8 \frac{R_w}{2} \dot{Q} (\dot{\delta}_L + \dot{\delta}_R) \cos \theta_2 + 2L_1 (C_{10} + C_8 Q) \dot{\theta}_1 \cos(\theta_1 - \theta_2) - 2L_1 (C_{10} + \\
& C_8 Q) \dot{\theta}_1^2 \sin(\theta_1 - \theta_2) + 2L_1 (C_{10} + C_8 Q) \dot{\theta}_1 \dot{\theta}_2 \sin(\theta_1 - \theta_2) + 2C_8 L_1 \dot{\theta}_1 \dot{\theta}_2 \cos(\theta_1 - \theta_2) + \frac{R_w}{2} (C_{10} + \\
& C_8 Q) (\dot{\delta}_L + \dot{\delta}_R) \dot{\theta}_2^2 \sin \theta_2 - (C_{15} + C_8 Q) g \dot{\theta}_2 \sin \theta_2 - 2L_1 (C_{10} + C_8 Q) \dot{\theta}_1 \dot{\theta}_2^2 \sin(\theta_1 - \theta_2) = T_M - T_{FM} - \\
& L_d F_d
\end{aligned} \tag{3.38}$$

$$\begin{aligned}
& C_8 \ddot{Q} - \frac{1}{2} (C_{12} + 2C_8 Q) \dot{\theta}_2^2 - C_8 \frac{R_w}{2} \dot{\theta}_2 (\dot{\delta}_L + \dot{\delta}_R) \cos \theta_2 - 2L_1 C_8 \dot{\theta}_1 \dot{\theta}_2 \cos(\theta_1 - \theta_2) + C_8 g \cos \theta_2 = F_a - \\
& F_{fa}
\end{aligned} \tag{3.39}$$

A mathematical model of the two-wheeled system with an extendable payload that can manoeuvre on flat surfaces has been derived using the Euler Lagrange equations. The system yields five non-linear differential equations built to describe the system dynamics. The five degrees of freedom calculated using:

$$DOF = m(N - 1 - J) + \int_{i=1}^J f_i$$

where N is number of bodies and J is number of joints.

The constant parameters C are given in APPENDIX-A. The system simulation parameters reported by [55] that based on standard dimensions of a two-wheeled robot vehicle illustrated in Table 3.1.

Table 3. 1: The parameters of a two-wheeled robot vehicle with movable payload.

Variable	Value	Unit
M_m	0.3	Kg
J_w	0.225	$Kg.m^2$
R_w	0.3	m
M_l	3	Kg
J_1	0.003025	$Kg.m^2$
M_{2l}	1.5	Kg
M_{2u}	1.5	Kg
J_{2u}	0.005	$Kg.m^2$
J_{2l}	0.005	$Kg.m^2$
M	70	Kg
J_M	1	$Kg.m^2$

3.4 System Performance

The system was investigated using five non-linear differential equations with different force input signals were implemented at the payload to test the system's stability.

The first input signal is illustrated in Figure 3.2.

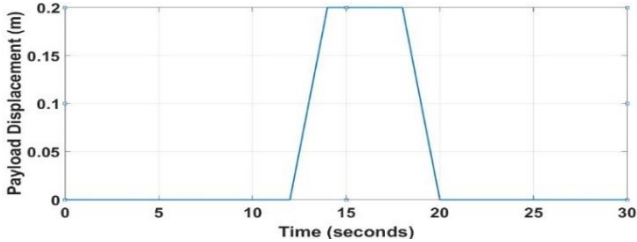


Figure 3. 2: payload input signal.

The open-loop system response was unstable, as shown in Figure 3.3.

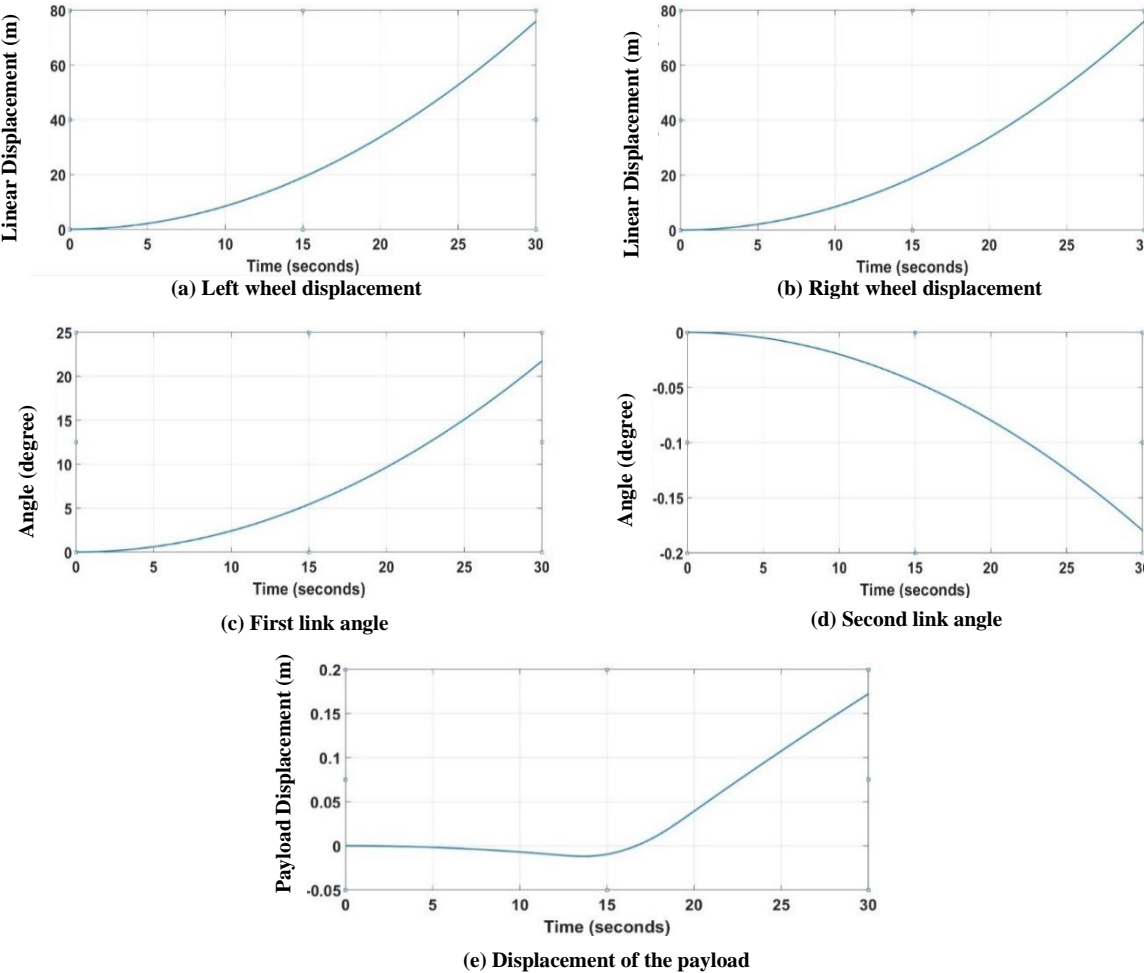


Figure 3. 3: System open-loop response with the first input signal.

The second input signal illustrated in Figure 3.4.

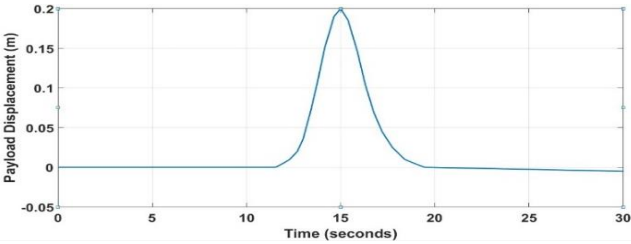


Figure 3. 4: Payload input signal.

The open-loop system response was unstable, as shown in Figure 3.5.

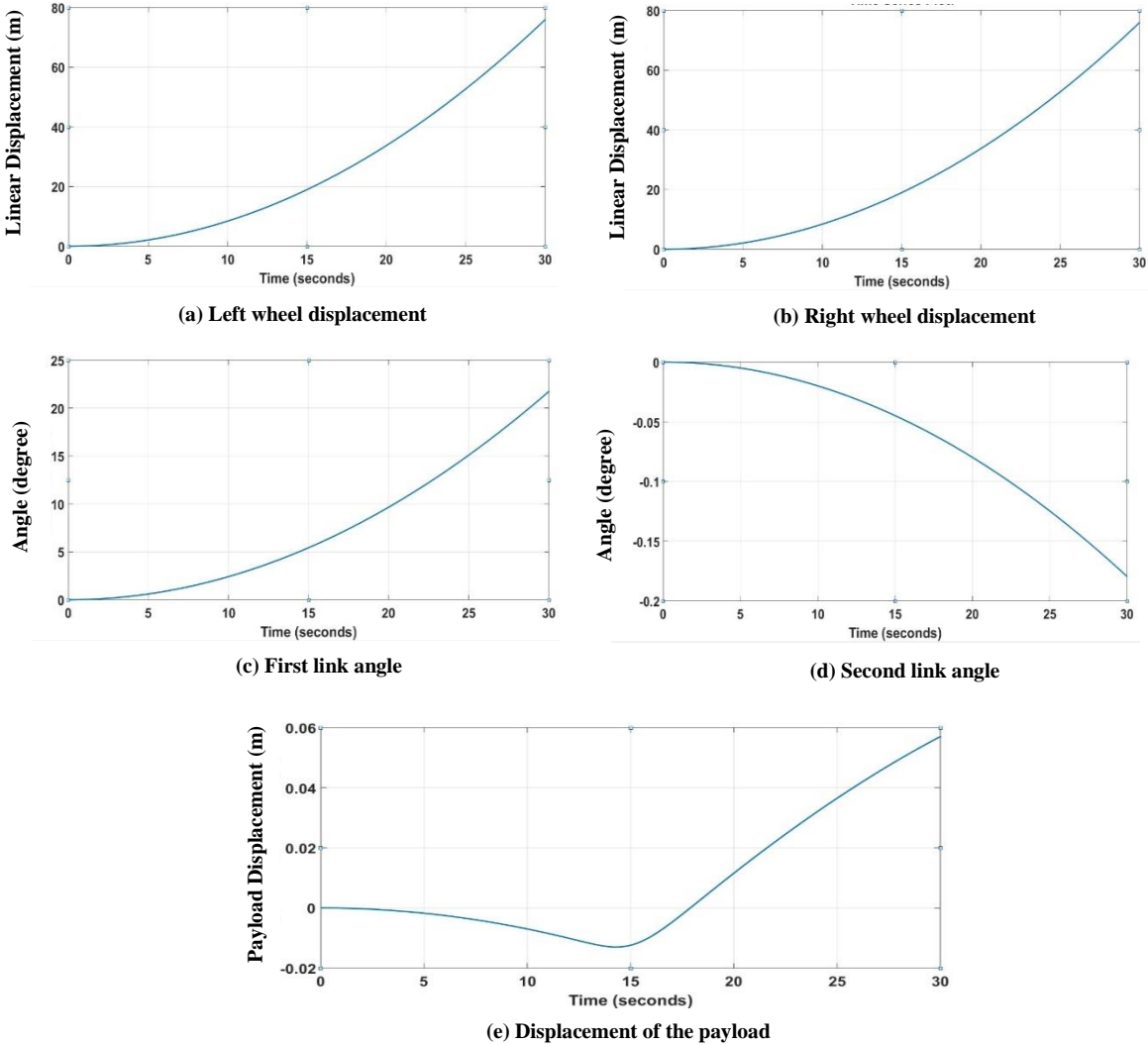


Figure 3. 5: System open-loop response with the second input signal.

The third input signal is illustrated in Figure 3.6.

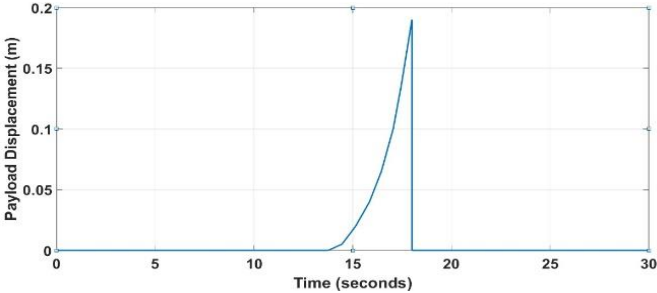


Figure 3. 6: Payload input signal.

The open-loop system response was unstable, as shown in Figure 3.7.

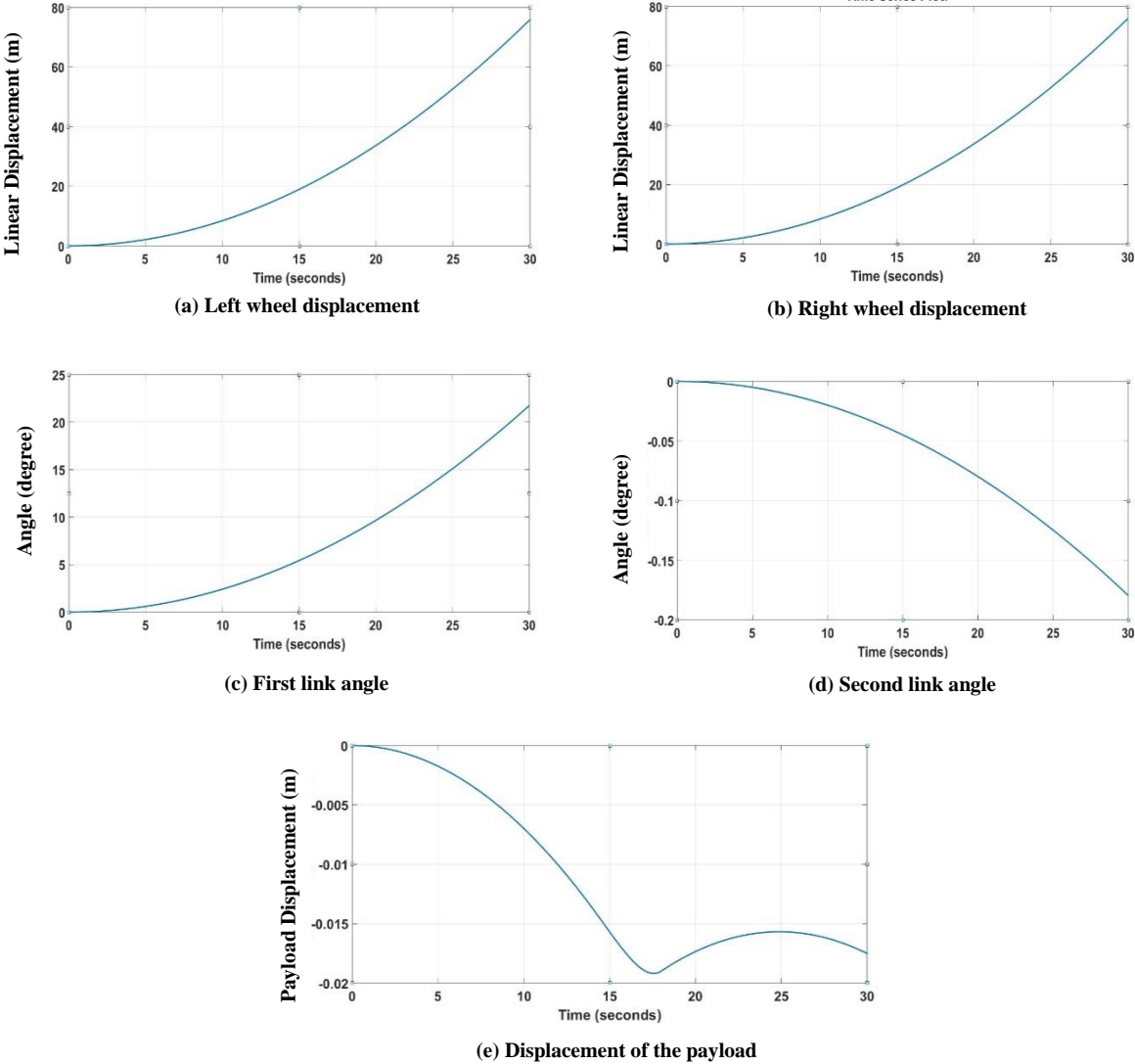


Figure 3. 7: System open-loop response with the third input signal.

The fourth input signal is illustrated in Figure 3.8.

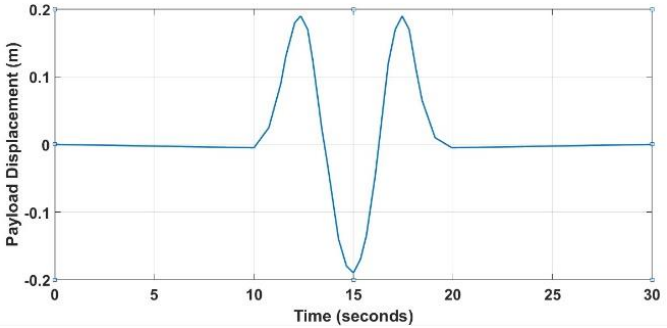


Figure 3. 8: Payload input signal.

The open-loop system response was unstable, as shown in Figure 3.9.

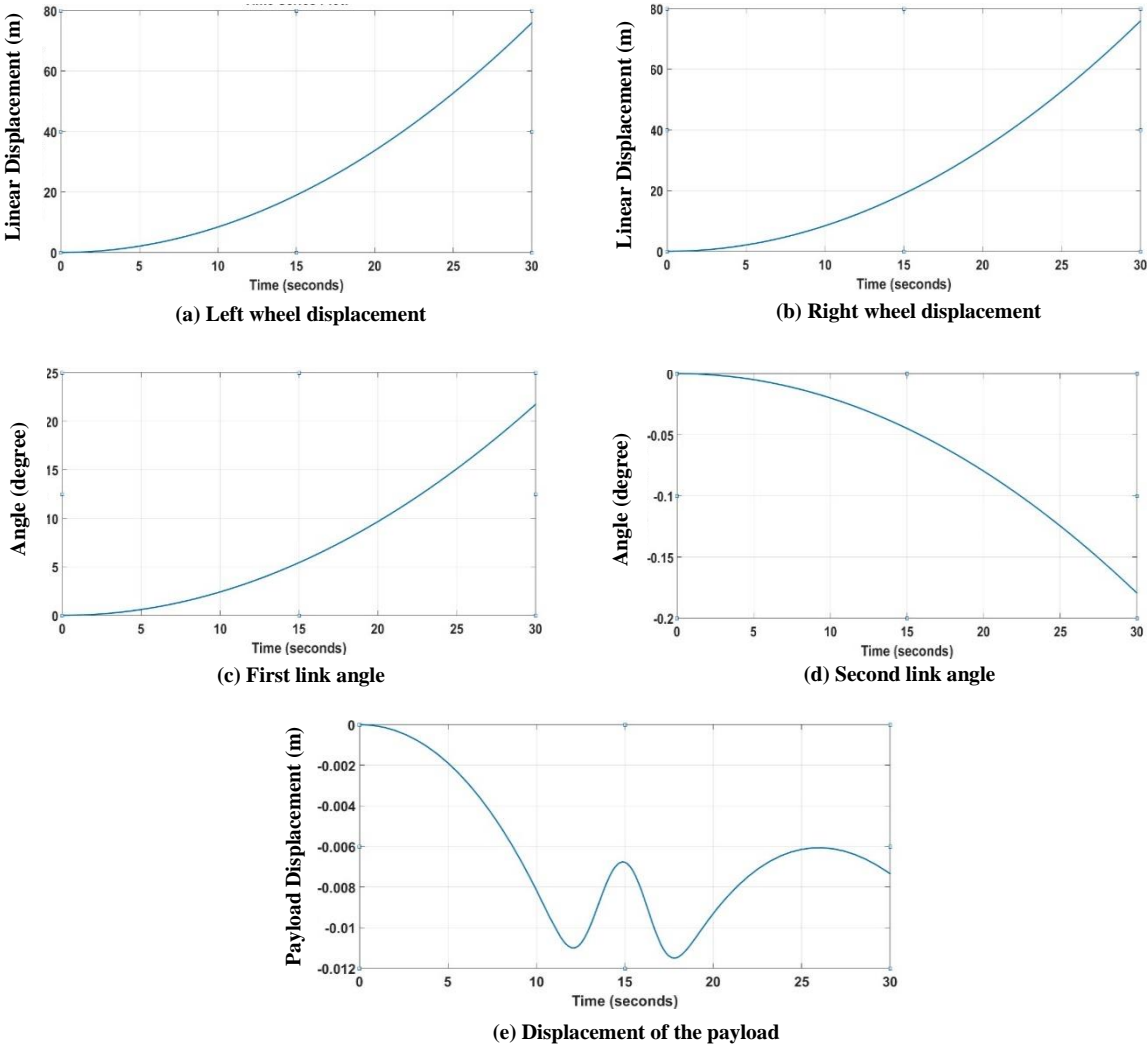


Figure 3. 9: System open-loop response with the fourth input signal.

From the simulation results, the system responses with different input signals applied at the payload actuator were initially unstable with all five parts including the left wheel, right wheel, first link, second link, and payload actuator. This highlighted the need to design an appropriate control system to achieve system stabilisation.

3.5 Summary

This chapter aims to design a robot vehicle with two wheels. The system has five degrees of freedom. The description and components of the system have been obtained. The mathematical model of a two-wheeled robot vehicle moving on flat surfaces was derived based on the Euler Lagrange method describing the system dynamics. The derived mathematical model yields the five non-linear differential equations, which have been simulated and confirmed that the system was unstable. The next chapter will demonstrate the system behaviour with various control system approaches.

Chapter Four

Controller Design with Different Control Strategy

4.1 Introduction

The double inverted pendulum systems have the characteristics of non-linearity, complexity, and instability. Many researchers have increased their interest in controlling the systems based on the inverted pendulum. Stabilising a system based on a double inverted pendulum is a complex challenge that demonstrates the control method's effectiveness. A lot of researchers have been presented on controlling this type of system [56] [57] [58].

This chapter analyses the system performance and tests the system response. Then different control techniques are designed to evaluate the model behaviour. The proposed control systems investigated the five parts of the model to test the effect of the controller stability. In addition, a comparative examination of the simulation results has been considered.

Chapter four is organised as follows. Section 4.2 presents the control system design, divided into three sub sections. The first Section 4.2.1 focused on using a PID-PD controllers. The second Section 4.2.2 used a Fuzzy Logic controller; the third Section 4.2.3 used a hybrid controller combined with PID-PD and Fuzzy Logic controllers.

4.2 Control Design

In this section, controllers were designed to control all five parts, including both wheels, left and right, the inclination angle of the first and second links, and the payload linear actuator. In this study, different input signals were applied to the movable payload to validate the system's stability. The wheels were assumed to move within 0.8m while both links of the intermediate body of the system were retained as upright to ensure system stabilisation. Various controllers are proposed, including PID, PD, FLC, and hybrid control systems, which will be designed to achieve system stability.

4.2.1 PID Control Design

This section implements a Proportional Integral Derivative (PID) control strategy for system stabilisation. PID controller is one of the most widely used control systems which provide dependable and stable performance for most systems [59] [60] [61]. The proposed controller is a commonly used control system because it is simple and easy to tune, further providing robust performance [62] [29] [63]. The proportional term, integral term, and derivative term were all employed on the PID controller consisting of three gain parameters, K_p , K_d , and K_i , tuned to develop stabilisation behaviour [64] [65]. The proportional term will increase the control signal for the same rate of error, the integral term to reduce steady-state errors, and the derivative term to reduce the overshoot [45] [66][67].

Many researchers have been used PID controllers in different applications to achieve the desired performance. Since many control systems using PID control have proved satisfactory results in their applications, it is still used over the years in most process control [29] [45] [68] [69].

PID and Proportional Derivative (PD) controllers are used in this study. For this model design, the first link and payload actuator were controlled using the PD controller, with the control parameters tuned progressively to achieve the desired performance.

Figure 4.1 illustrates the position of five loops: two loops for each wheel, two loops for both links, and one loop for the payload linear actuator.

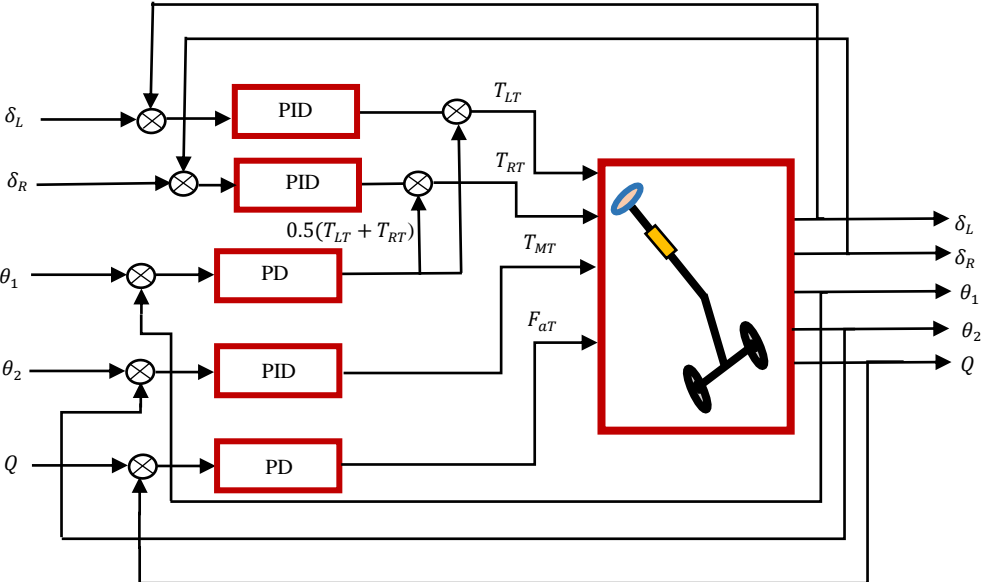


Figure 4. 1: The block diagram using PID controllers.

Table 4.1 shows the PID and PD controllers gain parameters that make the system most stable. These gain parameters were chosen after tuning progressively, which successfully stabilised the system model parts.

Table 4. 1: PID gain parameters.

Loop	PID Gains		
	Kp	Kd	Ki
Left Wheel	40	20	0.1
Right Wheel	40	20	0.1
First Link Angle	30	15	0
Second Link Angle	20	15	10
Payload Actuator	60	25	0

4.2.1.1 Results Using PID Controllers.

Different force input signals were applied on the payload actuator to validate the control system's stability and study the system behaviour. The payload actuator follows the input signal as shown in the following tests.

Test 1: Simulation results applying first input signal on the payload.

This step is used for investigating the stabilisation of the two-wheeled robot vehicle with a movable payload by applying the input signal illustrated in Figure 4.2. The simulation results illustrated in Figure 4.3 explain that the system successfully stabilised with the first input signal applied. And the system control effort for all systems parts is illustrated in Figure 4.4.

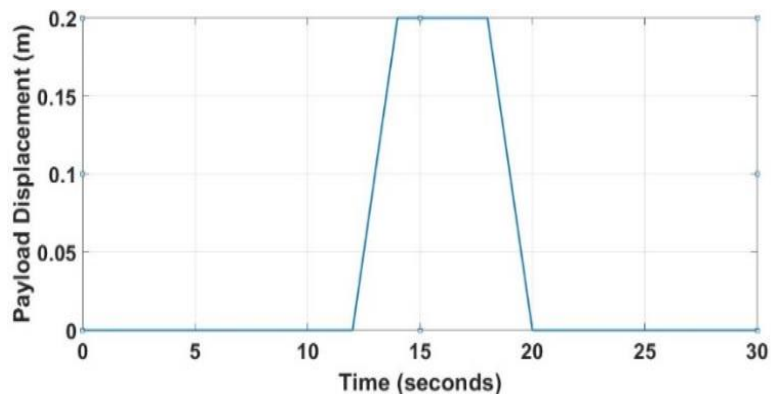


Figure 4. 2: The first input signal applied on the payload.

The simulation results for the system response using the PID-PD controllers are illustrated in Figure 4.3.

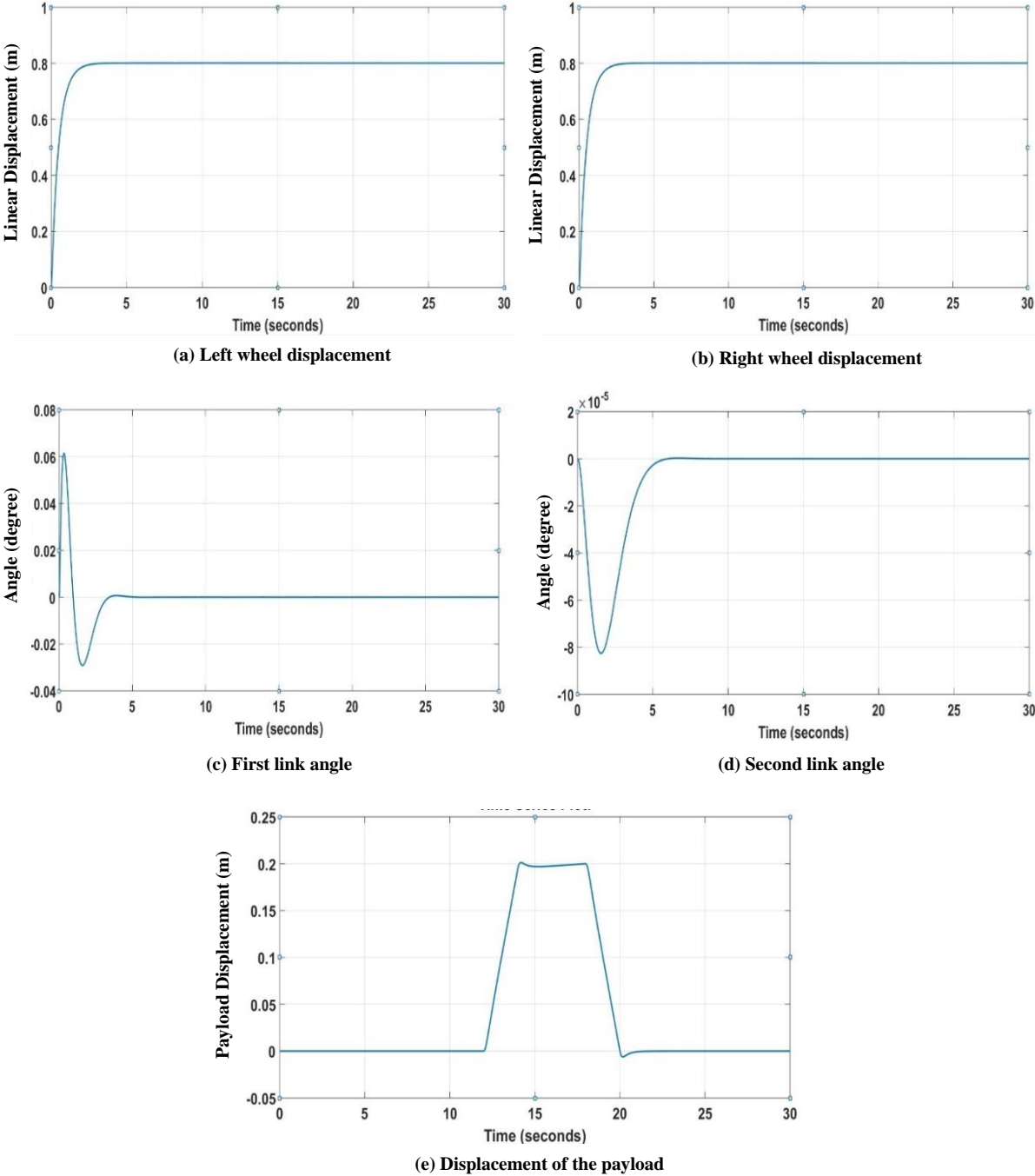
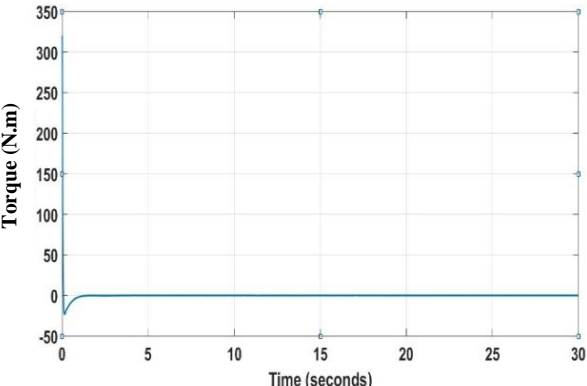
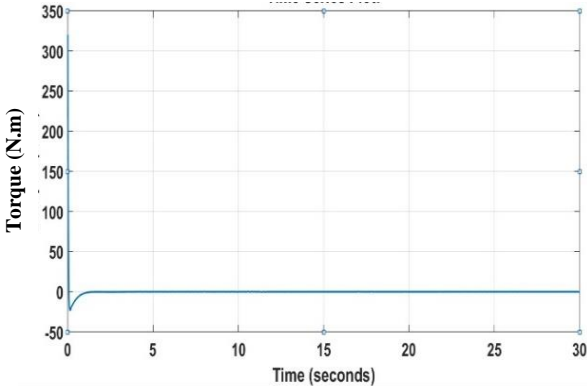


Figure 4. 3: System response of PID controllers.

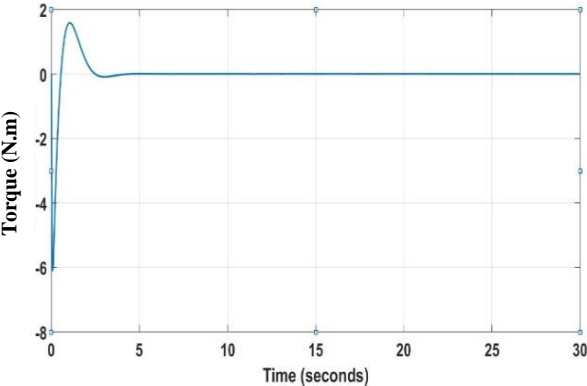
The exerted effort of the controllers required to stabilise the system is represented in Figure 4.4.



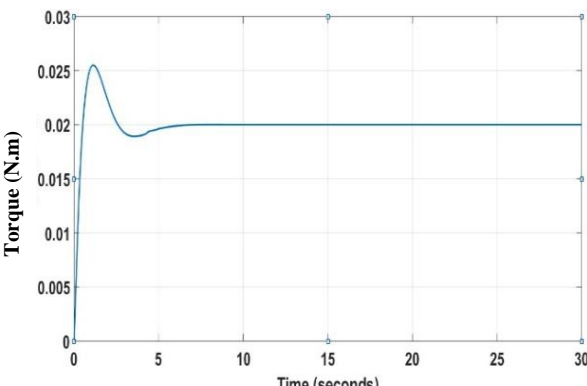
(a) Control effort of the left wheel



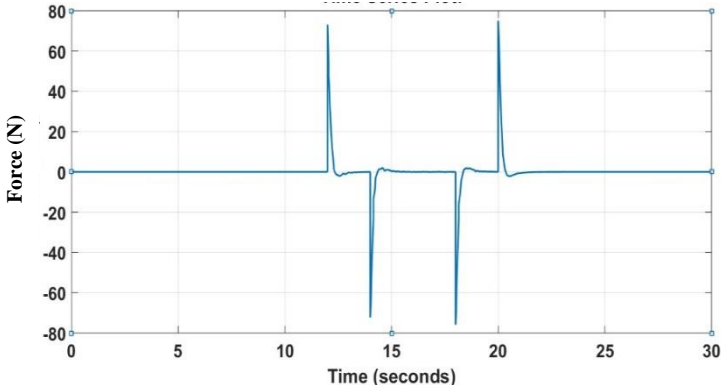
(b) Control effort of the right wheel



(c) Control effort of the first link



(d) Control effort of the second link



(e) Control effort of the payload

Figure 4. 4: System exerted effort using PID controllers.

The control system stabilised and balanced the two-wheeled robot vehicle with a movable payload. The wheels settle at 0.7261s with 0.481% overshoot. The first link of the intermediate body reached settling time at 3.1952s, and the second link settled at 5.2356s, as illustrated in Table 4.2.

Table 4. 2: System specifications apply the first input signal using PID controllers.

	Rise Time	Settling Time	Overshoot	Peak Time	Steady State Error
Left Wheel	1.061s	0.7261s	0.481%	10.859s	-0.0009138
Right Wheel	1.061s	0.7261s	0.481%	10.859s	-0.0009138
First Link	0.088s	3.1952s	64.634%	0.351s	-6.104e-6
Second Link	2.270s	5.2356s	0.505%	6.729s	-1.972e-18
Payload	1.557s	20.402s	1.579%	14.150s	5.556e-6

Test 2: Simulation results with the second input signal.

In this case, the second input signal is applied to the payload actuator, as shown in Figure 4.5. Figure 4.6 shows the control system response after applying the second input signal. And the control system effort is illustrated in Figure 4.7.

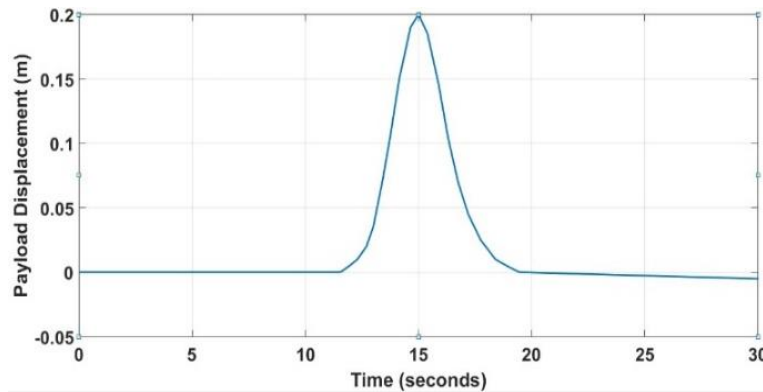


Figure 4. 5: The second input signal applied on the payload.

The simulation results for the system response using the PID-PD controllers are illustrated in Figure 4.6.

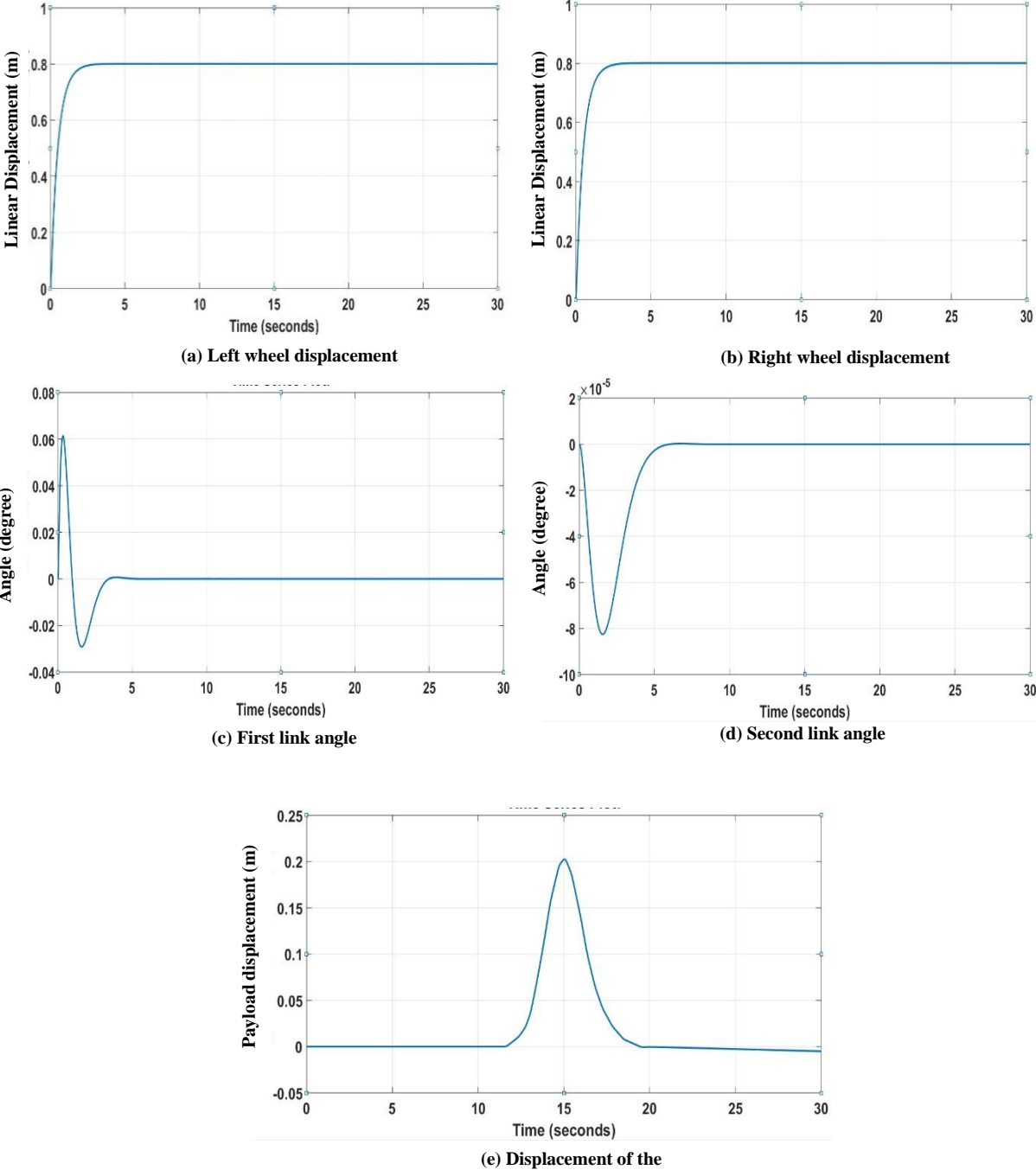


Figure 4. 6: System response of PID controllers.

The exerted effort of the controllers required to stabilise the system is represented in Figure 4.7.

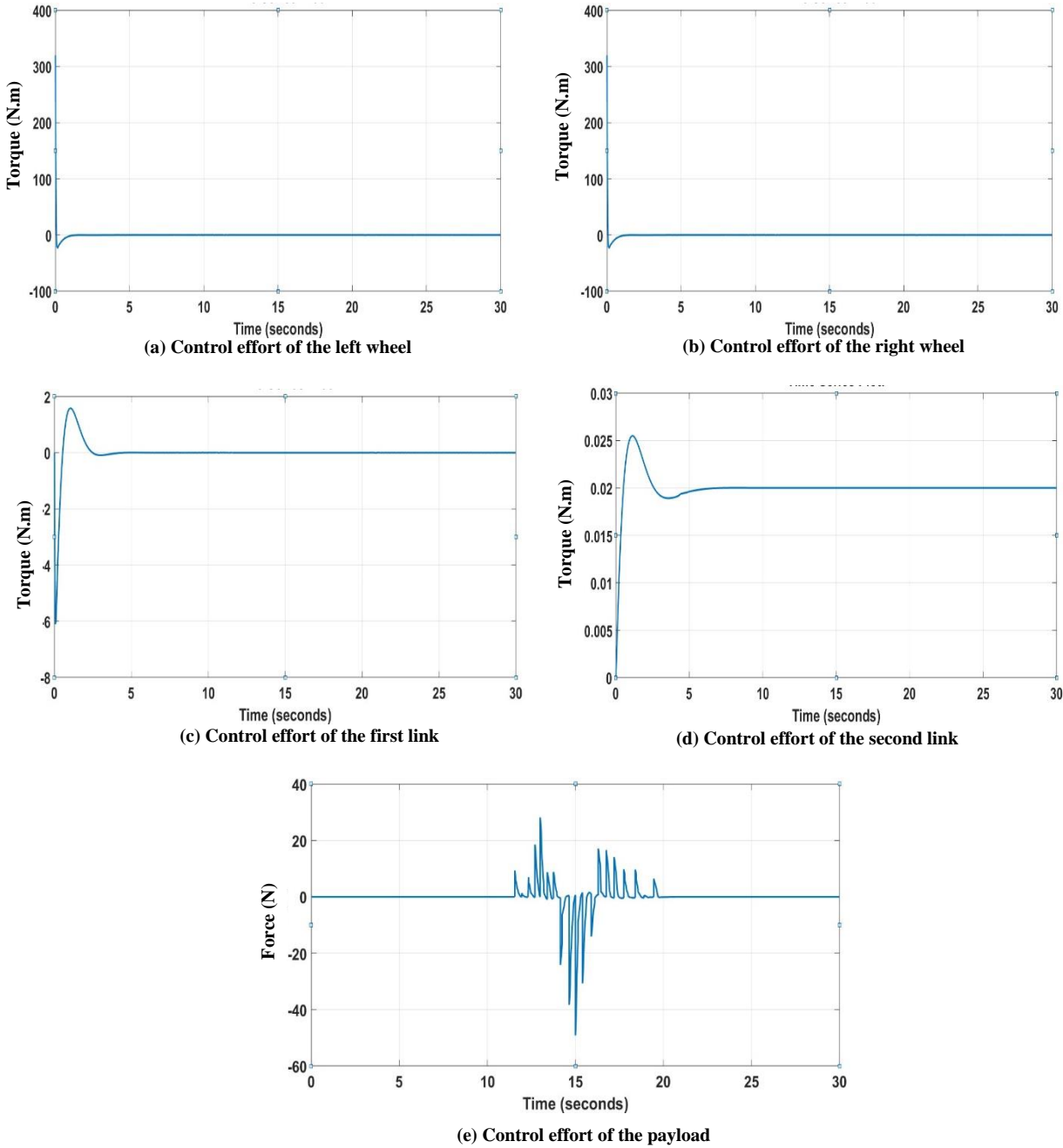


Figure 4. 7: System exerted effort using PID controllers.

The controllers stabilised the robot vehicle with the second input signal applied at the payload actuator. The most interesting finding was that the controller effort was less than the first input signal, this is can be explained due to the shape of the applied input signal. The system specifications are illustrated in Table 4.3.

Table 4. 3: System specifications applying the second input signal using PID controllers.

	Rise Time	Settling Time	Overshoot	Peak Time	Steady State Error
Left Wheel	1.061s	0.7261s	0.481%	10.859s	-0.0009138
Right Wheel	1.061s	0.7261s	0.481%	10.859s	-0.0009138
First Link	0.088s	3.1952s	64.634%	0.351s	-6.104e-6
Second Link	2.270s	5.2356s	0.505%	6.729s	-1.972e-18
Payload	1.396s	21.2138s	59.836%	15.040s	5.556e-6

Test 3: Simulation results with the third input signal.

In this case, the third input signal is applied to the payload actuator, as shown in Figure 4.8. Figure 4.9 shows the control system response after applying the second input signal and the control system effort illustrated in Figure 4.10.

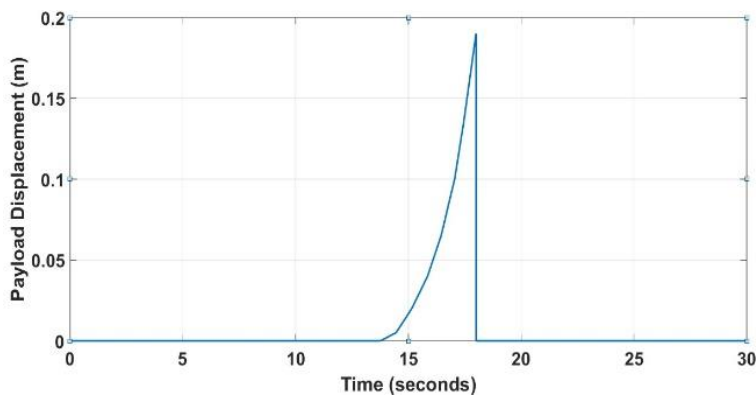


Figure 4. 8: The third input signal applied on the payload.

Simulation results for the system response using the PID-PD controllers are illustrated in Figure 4.9.

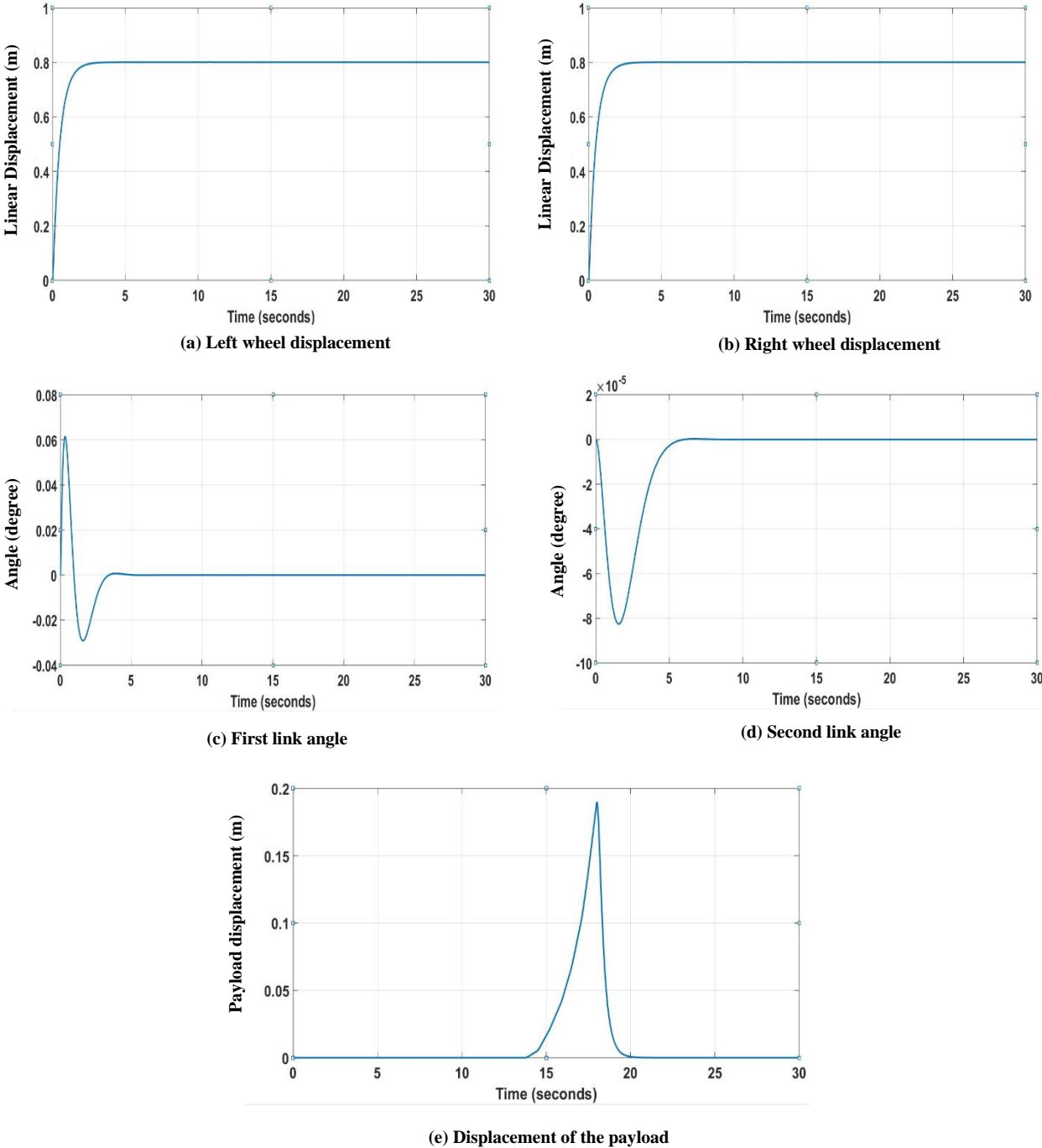


Figure 4. 9: System response of PID controllers.

The exerted effort of the controllers required to stabilise the system is represented in Figure 4.10.

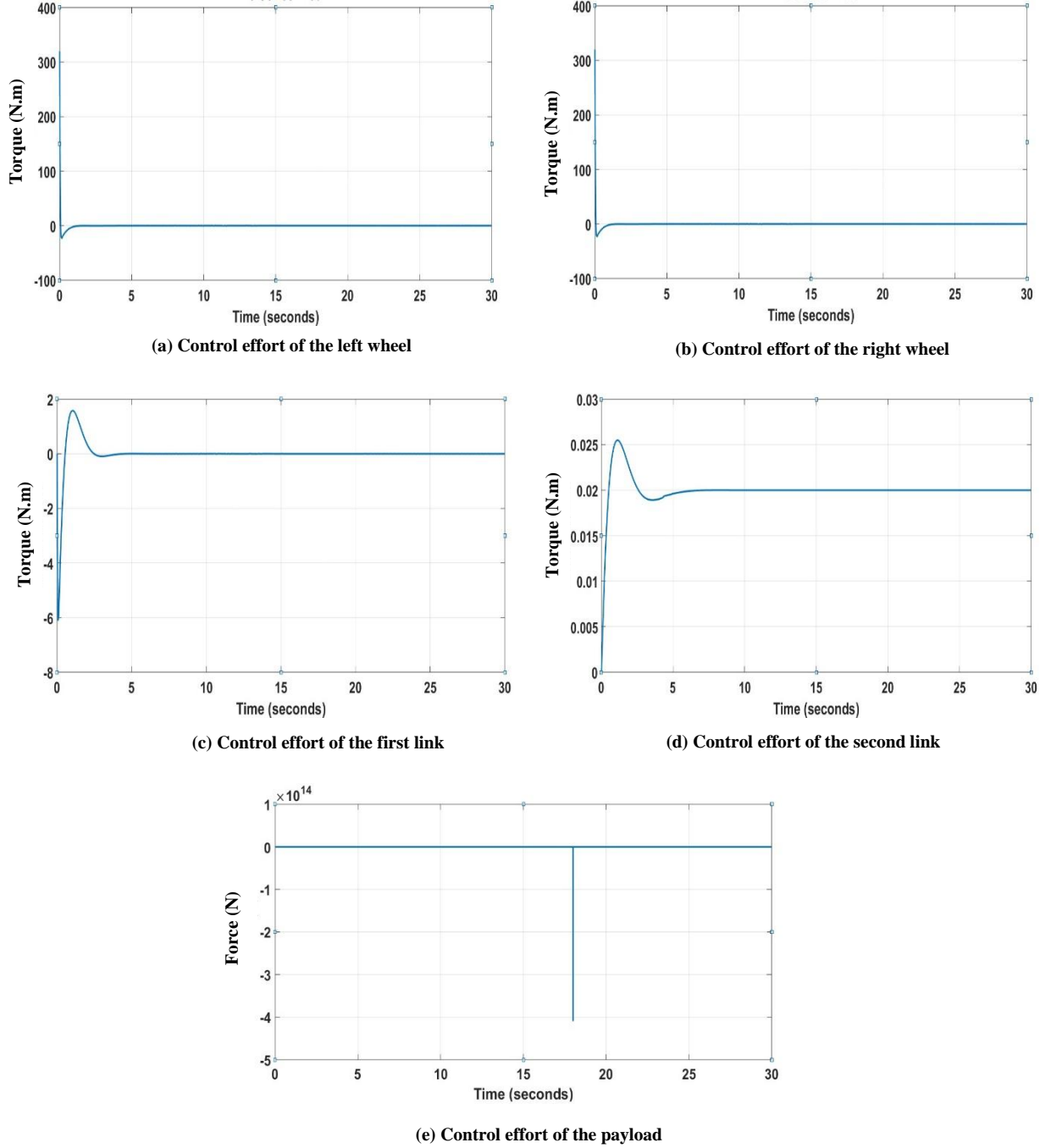


Figure 4. 10: System exerted effort using PID controllers.

The controller successfully stabilised the robot vehicle with the second input signal applied. Figure 4.10 illustrates the very high control effort exerted for the payload stabilisation. When the signal reaches the maximum point, it suddenly goes back to zero, making the controller require higher effort for the payload stabilisation. The system specifications are illustrated in Table 4.4 are the same as the previous signals except for the specifications of the payload linear actuator

Table 4. 4: System specifications apply the third input signal using PID controllers.

	Rise Time	Settling Time	Overshoot	Peak Time	Steady State Error
Left Wheel	1.061s	0.7261s	0.481%	10.859s	0.0739
Right Wheel	1.061s	0.7261s	0.481%	10.859s	0.0739
First Link	0.088s	3.1952s	64.634%	0.351s	3.1952
Second Link	2.270s	5.2356s	0.505%	6.729s	5.2356
Payload	2.659s	19.4200s	0.505%	18.009s	5.556e-6

Test 4: Simulation results with the fourth input signal.

The fourth test applied the input signal illustrated in Figure 4.11. The system's response using PID-PD controllers is shown in Figure 4.12, and the system controller efforts are shown in Figure 4.13.

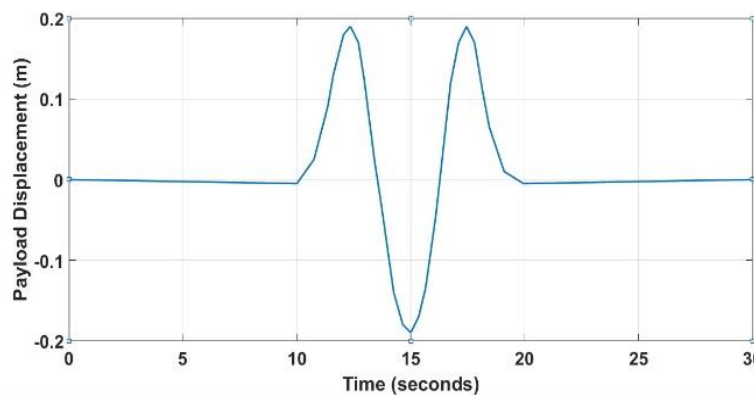


Figure 4. 11: The fourth input signal applied on the payload.

The simulation results for the system response using the PID-PD controllers are illustrated in Figure 4.12.

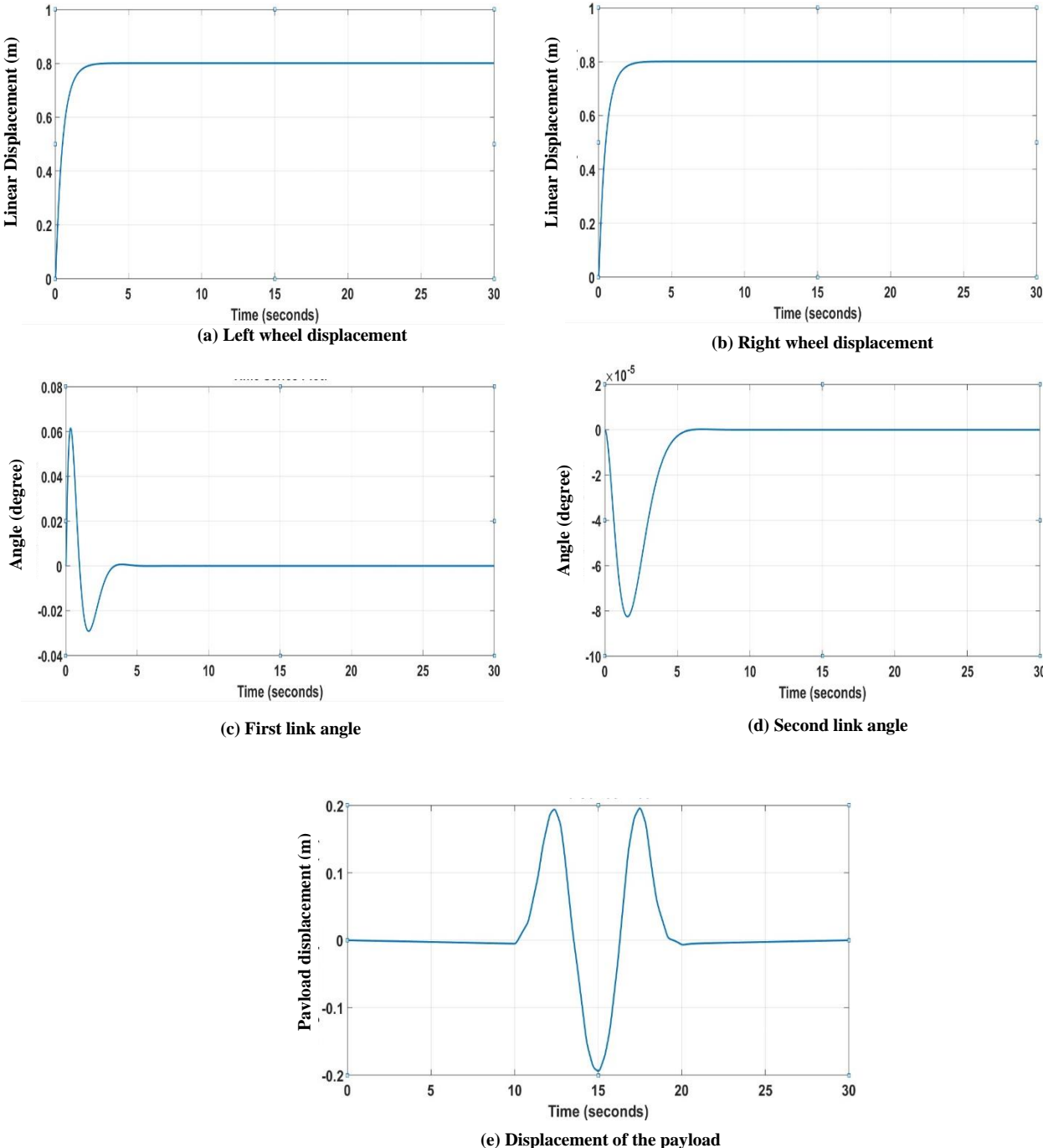


Figure 4. 12: System response of PID controllers.

The exerted effort of the controllers required to stabilise the system is represented in Figure 4.13.

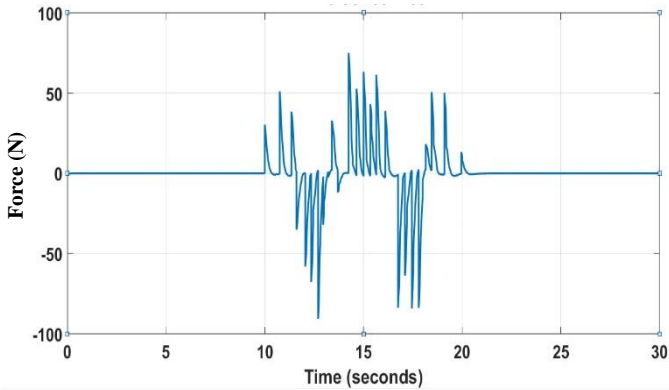
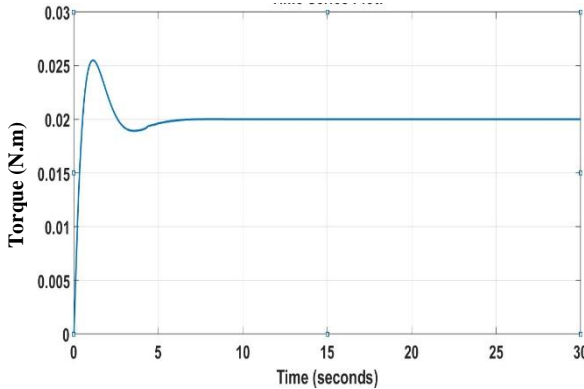
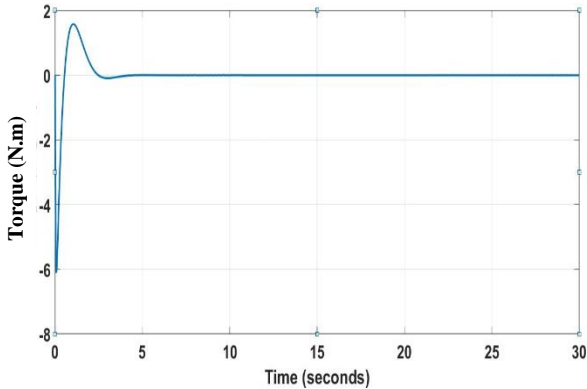
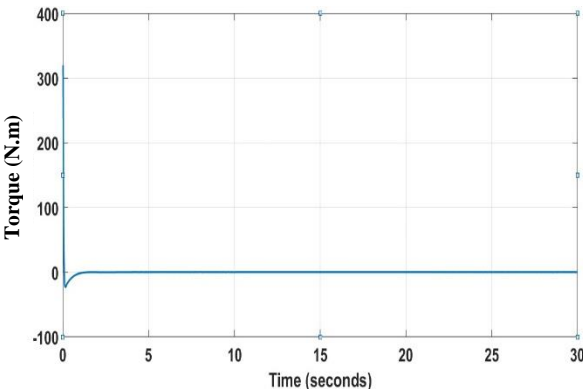
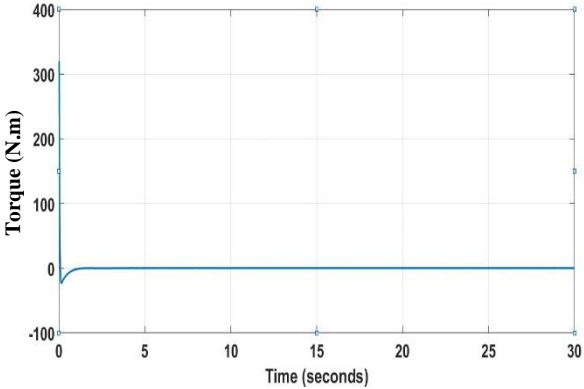


Figure 4.13: System exerted effort using PID controllers.

The controller successfully stabilised the robot vehicle with the fourth input signal applied at the payload actuator. Table 4.5 explains the system specifications designed with PID-PD controllers.

Table 4. 5: System specifications apply the fourth input signal using PID controllers.

	Rise Time	Settling Time	Overshoot	Peak Time	Steady State Error
Left wheel	1.060s	0.7261s	0.486%	10.000s	0.0739
Right wheel	1.060s	0.7261s	0.486%	10.000s	0.0739
First Link	0.088s	3.1952s	64.634%	0.351s	3.1952
Second Link	2.270s	5.2356s	0.505%	6.729s	5.2356
Payload	0.0307s	22.1351s	58.240%	17.494s	5.556e-6

The system simulation results illustrate that the presented model with the PID-PD control systems successfully stabilised with different input signals applied on the payload linear actuator to study the system behaviour and investigate the system stability. This step validates the system and explains that the system is still stable with various input signals.

The proposed PID and PD had shown excellent performance in terms of the control system characteristics. From the simulation results, the PID and PD wheels displacement stabilised at 0.7261s without oscillation. The tilt angle of the first and the second links improved overshoot and had a faster settling time, as shown in the previous tables. The payload linear actuator force follows the proposed input signals.

The next step is to design the fuzzy logic controllers to test the system stability and the improvement of this type of controller on the system.

4.2.2 Fuzzy Logic Control Design

Fuzzy logic control (FLC) is a logical and flexible technique used to communicate with fuzzy systems where the dynamics are too complicated or unknown [70] [71] [35]. In this control system approach, the use of linguistic variables rather than numerical variables is one of its most major features whose values are natural language sentences [28] [72].

The FLC is used in digital technologies such as microcontrollers and digital signal processing [73]. For the FLC output calculations, all linguistic variables and membership functions are employed to design the rule-base that produces the fuzzy controller action [73] [74]. FLC has been applied successfully in different applications [75] [76] [77].

In this design, the FLC was designed to control each left wheel, right wheel, first link, second link, and payload actuator and this controller for each part had two inputs error and change of error, with a further output used to describe a fuzzy inference system to create the necessary fuzzy rules. The linguistic variables of the two inputs and the output could be Negative-Big (NB), Negative-Small (NS), Zero (Z), Positive-Big (PB), and Positive-Small (PS). These rules yield relevant action in FLC parts. The fuzzy logic controllers were designed with nine rules, 25 rules, and 49 rules. However, the nine and 49 rules become unstable. The proper system tuning of the FLC to stabilise the model was developed using five membership functions with 25 rules base. There are many types of membership functions such as Triangle, Trapezoidal, Gaussian, and Gaussian two membership functions. These types have been tested, but the Gaussian membership function was chosen as a way to provide smooth inputs and outputs with less control effort exerted at each part compared with the other types of membership functions.

Figure 4.14 illustrates the position of five loops: two loops for each wheel, two loops for both links, and one loop for the payload linear actuator using the fuzzy controller with five Gaussian membership functions and 25 rules base.

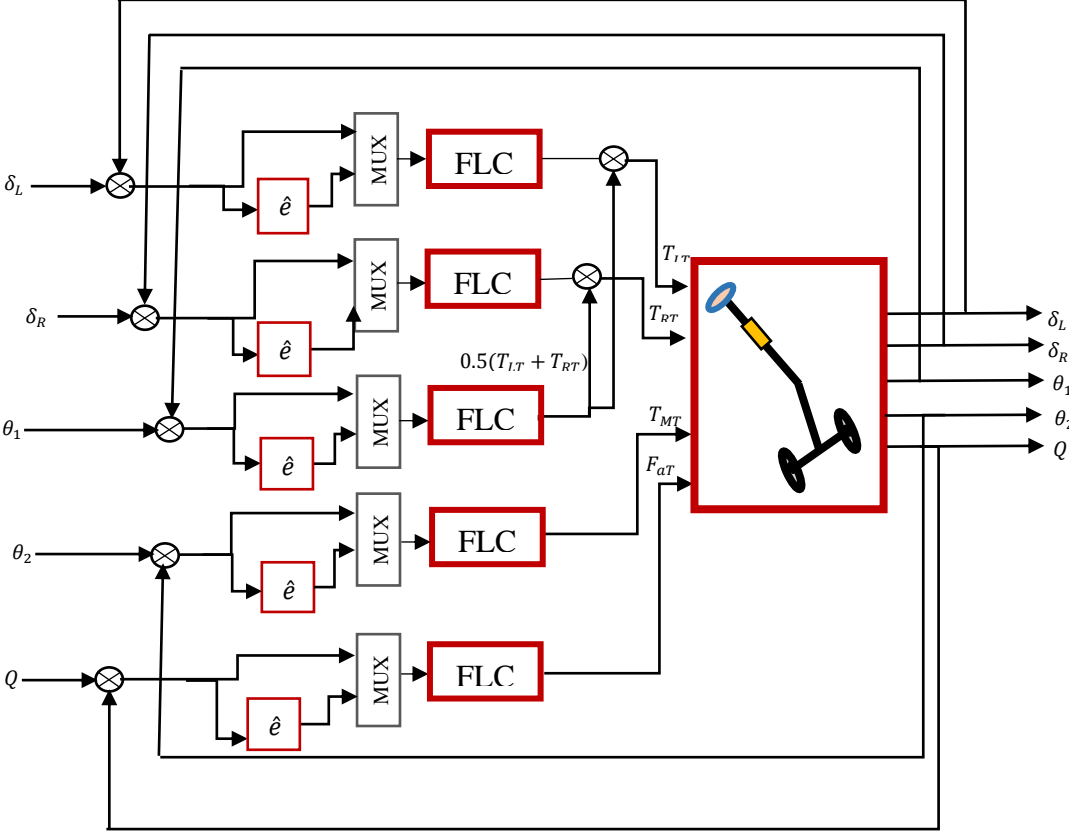


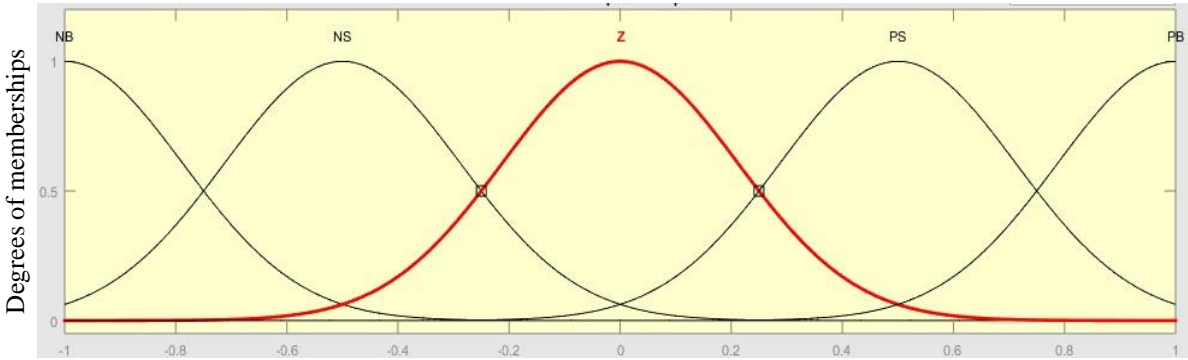
Figure 4. 14: The system block diagram using the fuzzy logic controller.

Table 4.6 presents the fuzzy rules used in the model that make the system most stable.

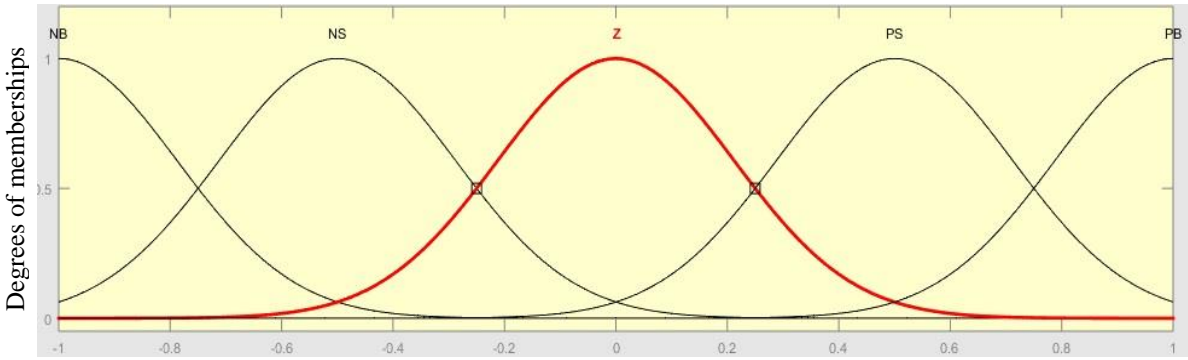
Table 4. 6: Fuzzy rules base.

e \ \hat{e}	NB	NS	Z	PS	PB
NB	NB	NB	NB	NS	Z
NS	NB	NB	NS	Z	PS
Z	NB	NS	Z	PS	PB
PS	NS	Z	PS	PB	PB
PB	Z	PS	PB	PB	PB

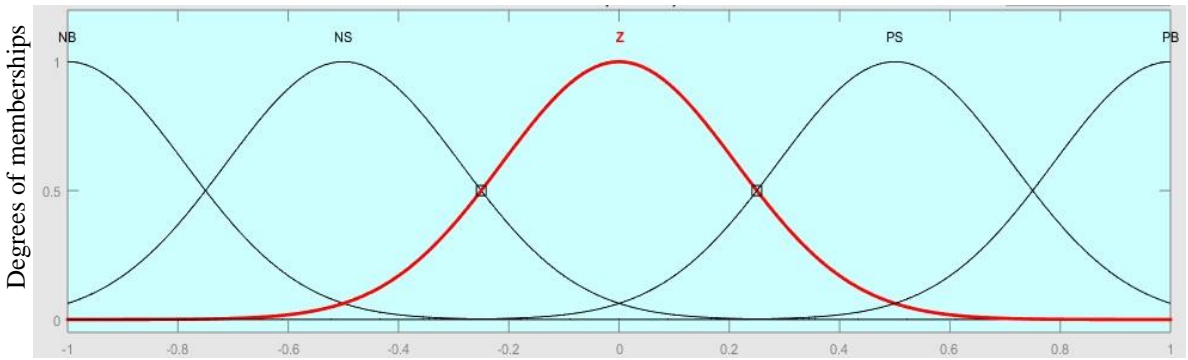
The memberships functions are illustrated in Figure 4.15.



(a) Error



(b) Change of Error



(c) Output

Figure 4. 15: Gaussian membership function with two inputs and one output.

4.2.2.1 Results Using Fuzzy Logic Controller.

The fuzzy logic control system is designed to evaluate the system's stability. This simulation results of the system response using the fuzzy logic controller and applying the first input signal as illustrated in Figure 4.16.

Test 1: Simulation results with first payload input signal

The first input signal applied on the payload actuator is illustrated in Figure 4.16. Figure 4.17 explains the system simulation result and the system control effort is shown in Figure 4.18.

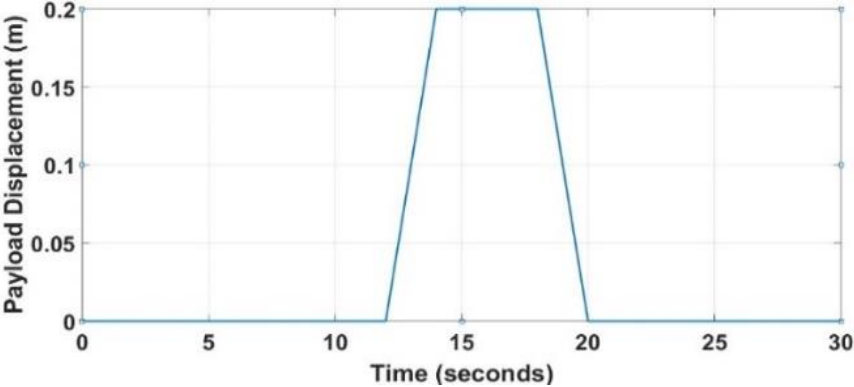


Figure 4. 16: The first input signal applied on the payload.

Simulation results for the system response using the fuzzy logic controllers are illustrated in Figure 4.17.

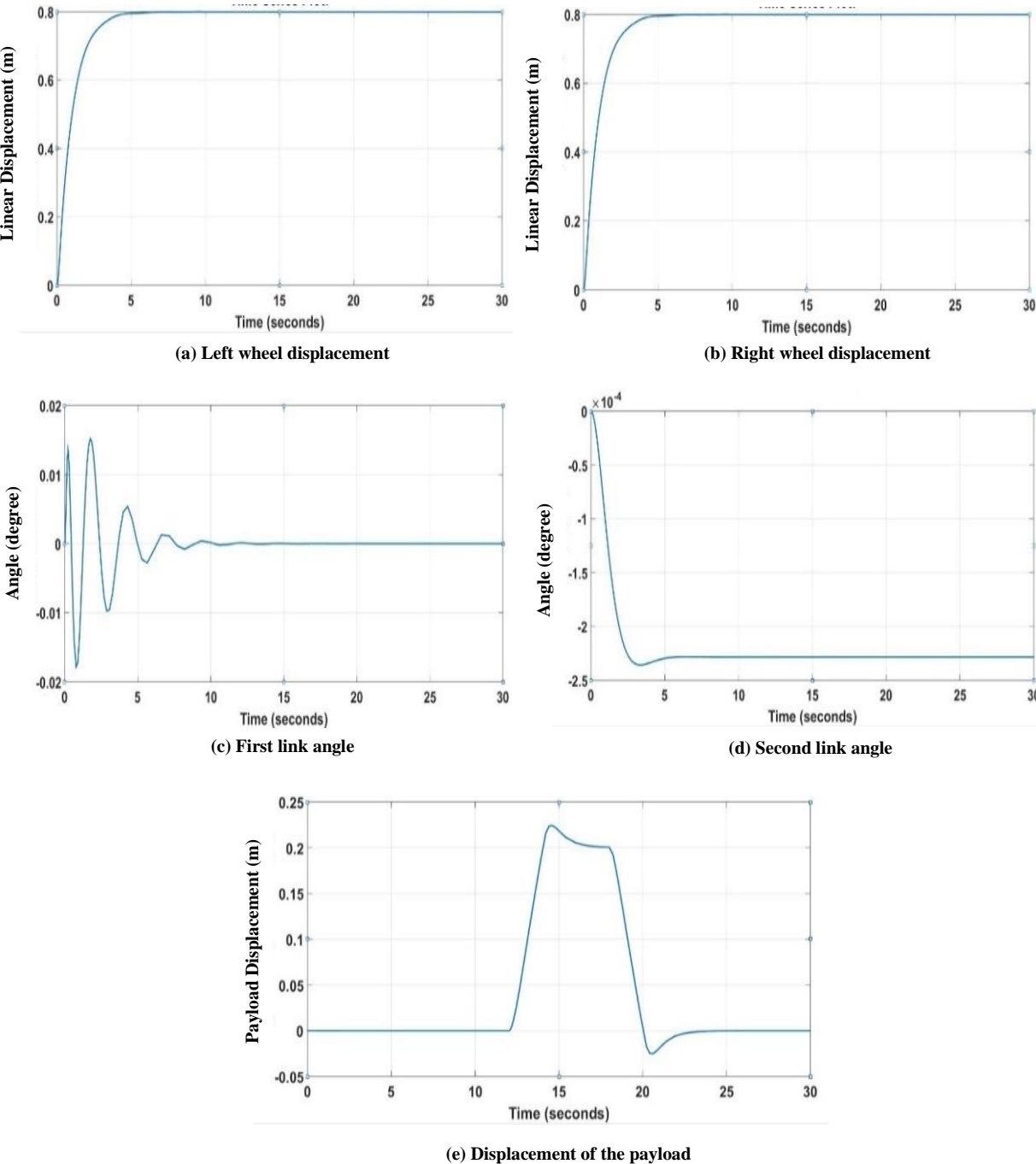


Figure 4. 17: System response using a fuzzy logic controller.

The exerted effort of the controllers required to stabilise the system is represented in Figure 4.18.

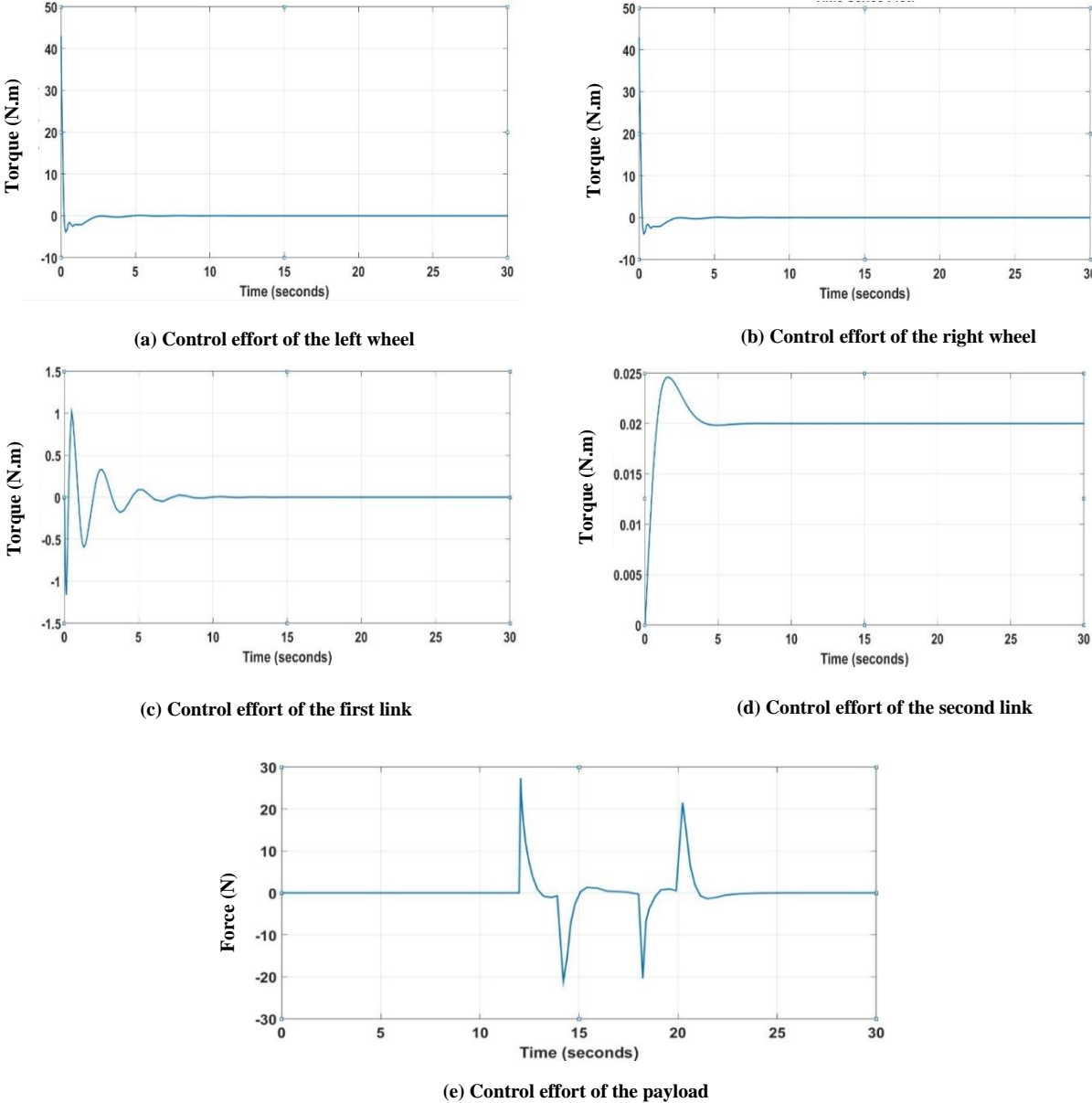


Figure 4. 18: System exerted effort using a fuzzy logic controller.

The first input signal applied on the payload actuator and designed with the fuzzy logic controller successfully stabilised. The settling time of the wheels is 3.7801s while the first link at 9.4910s and the second link stabilised at 4.1526s. The system specification is illustrated in Table 4.7.

Table 4. 7: System specifications apply the first input signal using fuzzy logic controllers.

	Rise Time	Settling Time	Overshoot	Peak Time	Steady State Error
Left Wheel	2.042s	3.7801s	0.505%	9.345s	0.0002854
Right Wheel	2.042s	3.7801s	0.505%	9.345s	0.0002854
First Link	0.3031s	9.4910s	100.294%	1.745s	-1.031e-8
Second Link	1.590s	4.1526s	1.759%	6.623s	0.0002284
Payload	1.457s	22.1763s	11.875%	14.586s	4.6e-5

Test 2: Simulation results with the second payload input signal.

The second input signal applied on the payload actuator is illustrated in Figure 4.19. Figure 4.20 explains the system simulation result and the system control effort is shown in Figure 4.21.

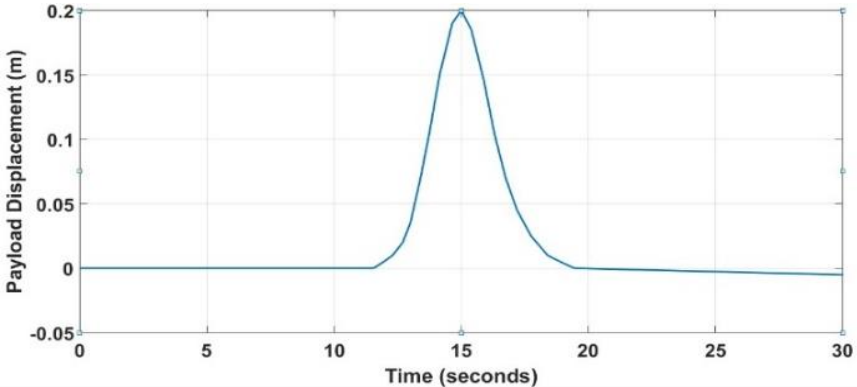


Figure 4. 19: The second input signal applied on the payload.

Simulation results for the system response using the FLC controllers are illustrated in Figure 4.20.

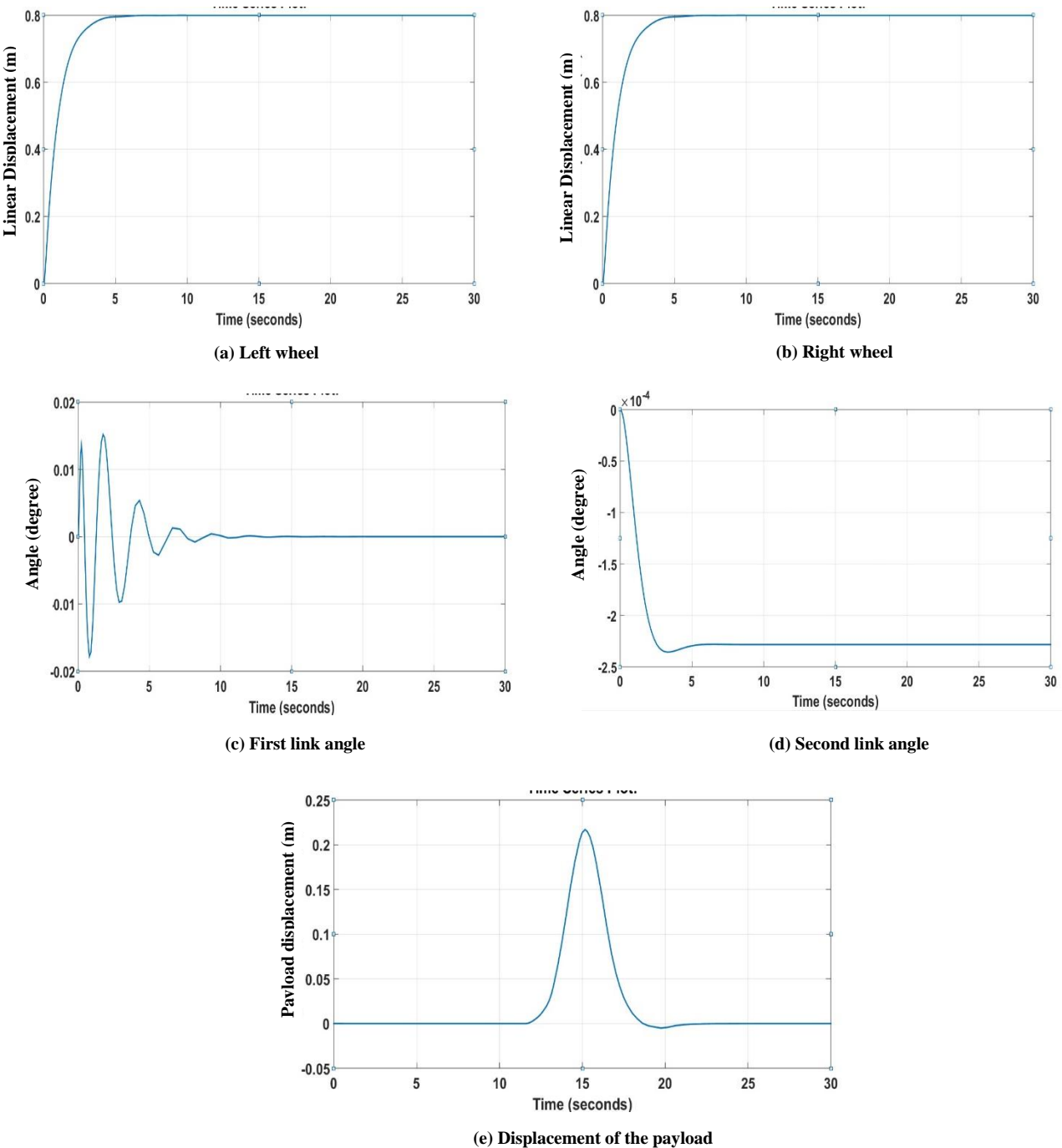


Figure 4. 20: System response using a fuzzy logic controller.

The exerted effort of the controllers required to stabilise the system is represented in Figure 4.21.

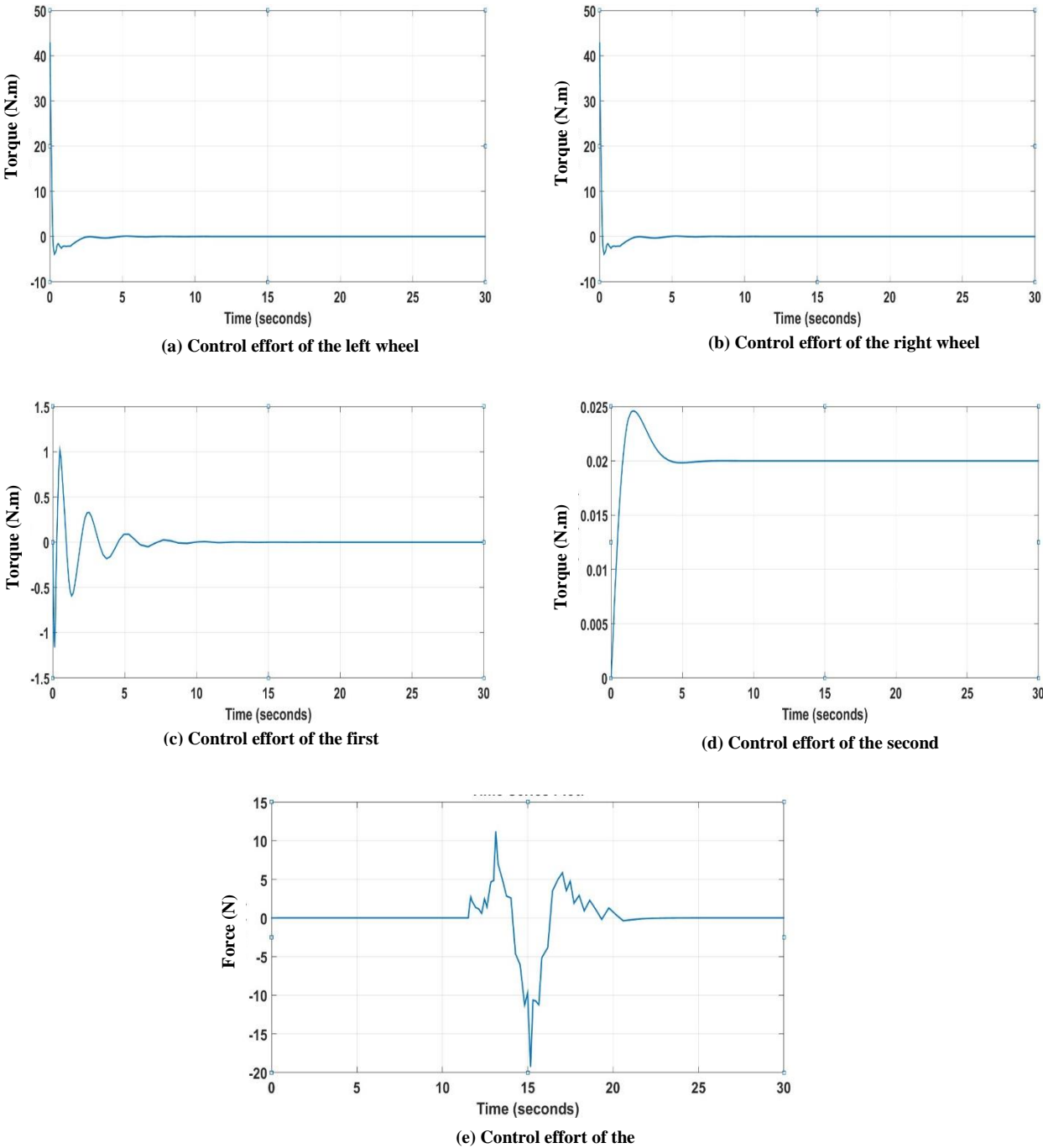


Figure 4. 21: System exerted effort using a fuzzy logic controller.

The system was stabilised with a second input signal but with higher overshoot and less control effort applied on the payload actuator than the first input signal. The system specifications are illustrated in Table 4.8.

Table 4. 8: System specifications applying the second input signal using fuzzy logic controllers

	Rise Time	Settling Time	Overshoot	Peak Time	Steady State Error
Left Wheel	2.042s	3.7801s	0.505%	9.345s	0.0002854
Right Wheel	2.042s	3.7801s	0.505%	9.345s	0.0002854
First Link	0.3031s	9.4910s	100.294%	1.745s	-1.031e-8
Second Link	1.590s	4.1526s	1.759%	6.623s	0.0002284
Payload	1.574s	20.0572s	20.370%	15.166s	4.573e-5

Test 3: Simulation results with the third payload input signal.

The third input signal applied to the payload actuator is illustrated in Figure 4.22. Figure 4.23 explains the system simulation result, and the system control effort is shown in Figure 4.24.

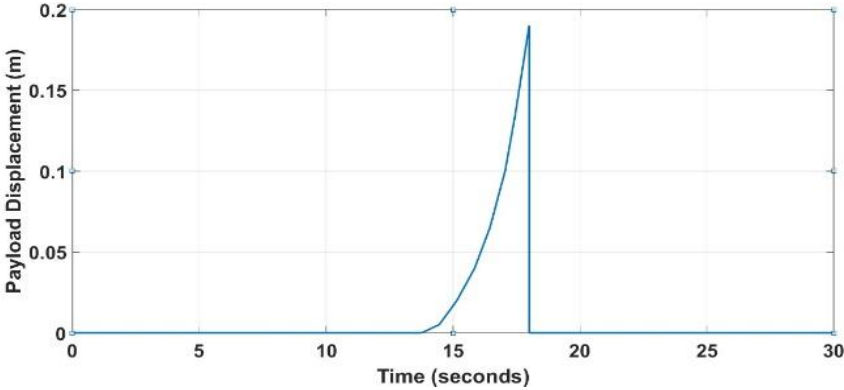


Figure 4. 22: The third input signal applied on the payload.

Simulation results for the system response using the FLC controllers are illustrated in Figure 4.23.

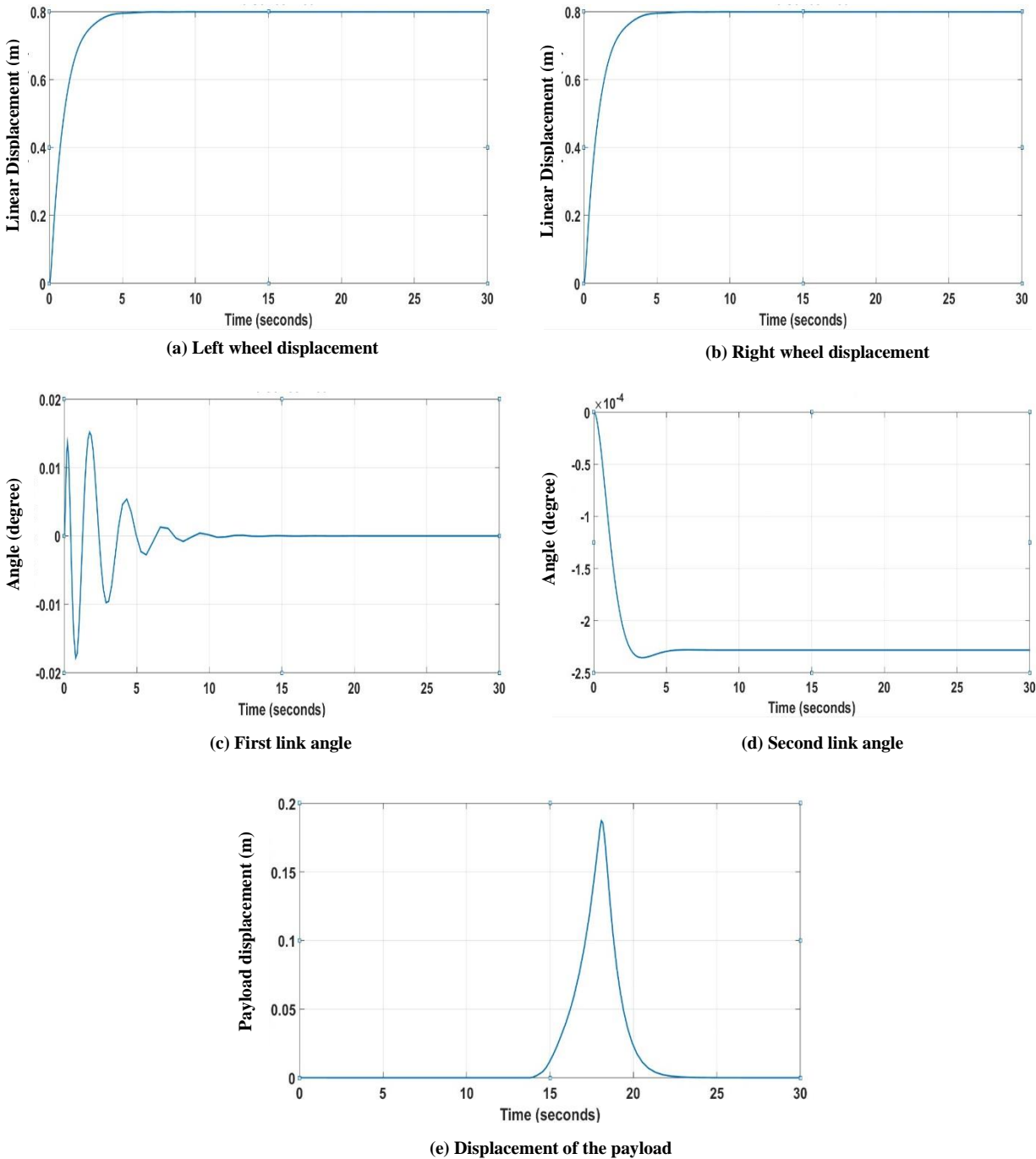


Figure 4.23: System response using a fuzzy logic controller.

The exerted effort of the controllers required to stabilise the system is represented in Figure 4.24.

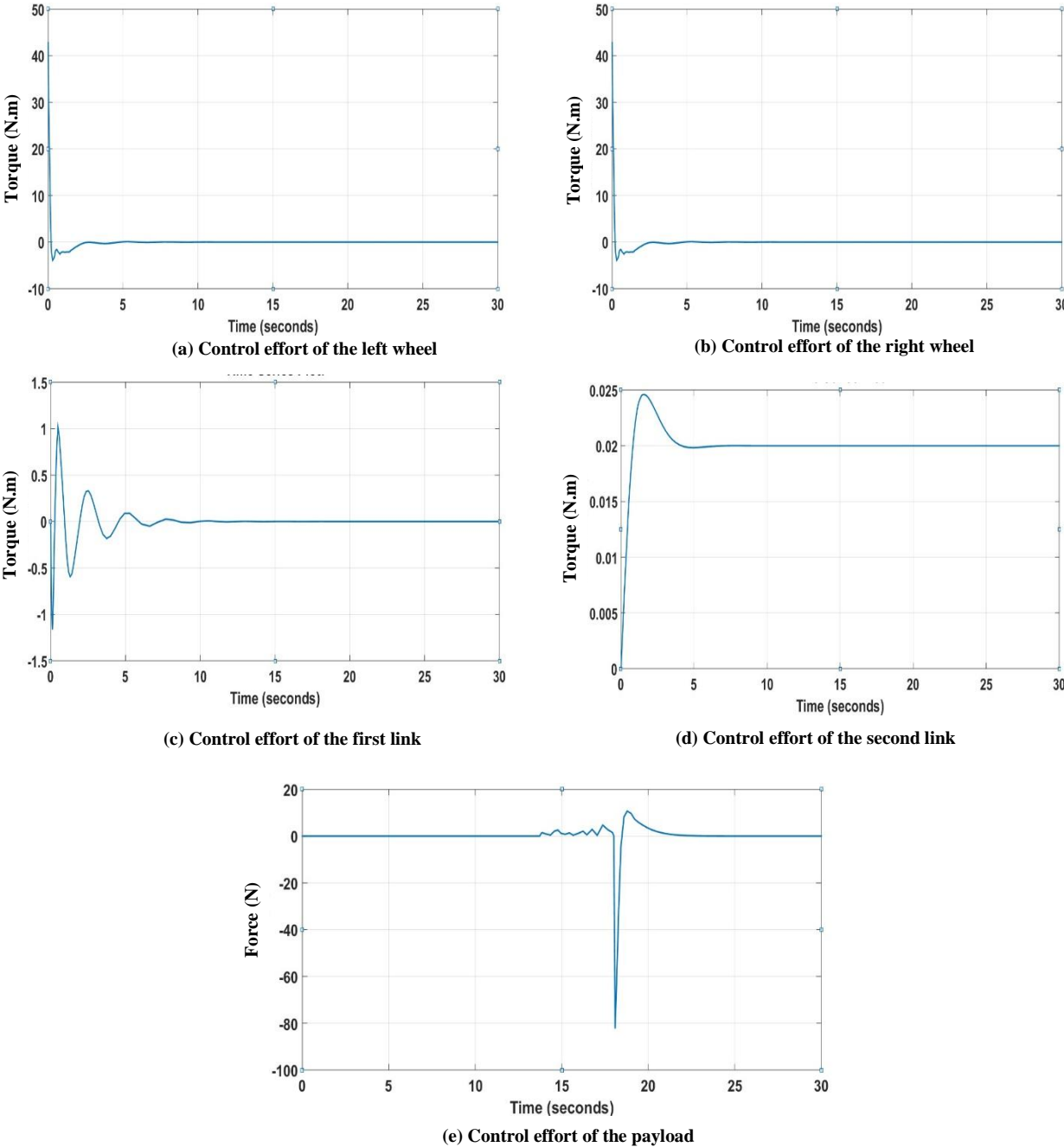


Figure 4. 24: System exerted effort using a fuzzy logic controller.

The system successfully stabilised with the third input signal but with higher controller effort on the payload actuator than the previous signals applied on the payload. The system specifications are illustrated in Table 4.9.

Table 4. 9: System specifications apply the third input signal using fuzzy logic controllers.

	Rise Time	Settling Time	Overshoot	Peak Time	Steady State Error
Left Wheel	2.042s	3.7801s	0.505%	9.345s	0.0002854
Right Wheel	2.042s	3.7801s	0.505%	9.345s	0.0002854
First Link	0.3031s	9.4910s	100.294%	1.745s	-1.031e-8
Second Link	1.590s	4.1526s	1.759%	6.623s	0.0002284
Payload	2.581s	21.375s	0.505%	18.082s	4.553e-5

Test 4: Simulation results with the fourth payload input signal.

The fourth input signal is applied on the payload actuator illustrated in Figure 4.25. Figure 4.26 explains the system simulation result, and the system control effort is shown in Figure 4.27.

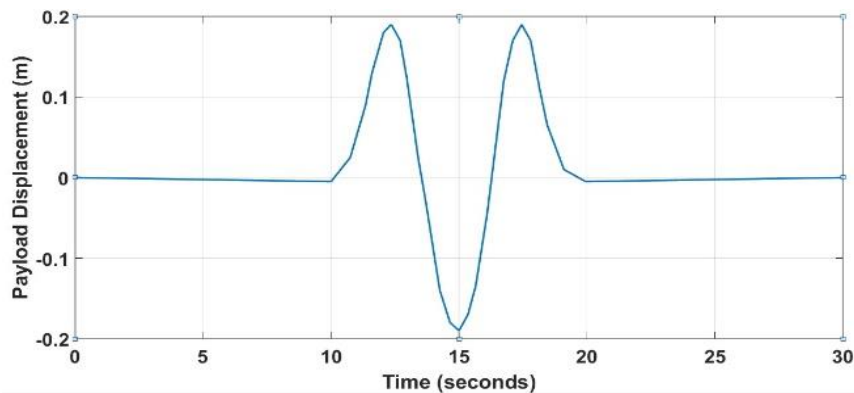


Figure 4. 25: The fourth input signal applied on the payload.

Simulation results for the system response using the FLC controllers are illustrated in Figure 4.26.

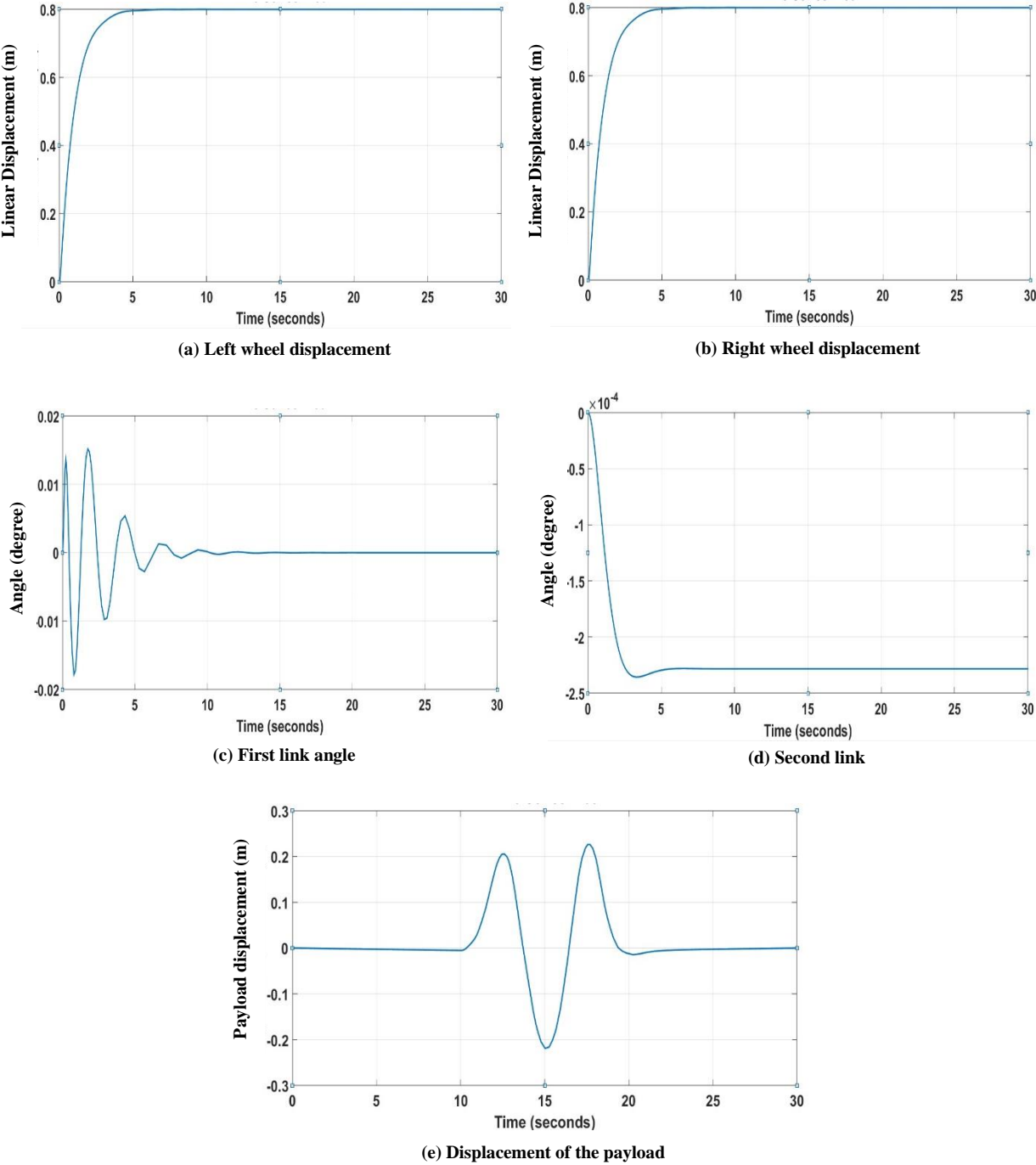


Figure 4. 26: System response using a fuzzy logic controller.

The exerted effort of the controllers required to stabilise the system is represented in Figure 4.27.

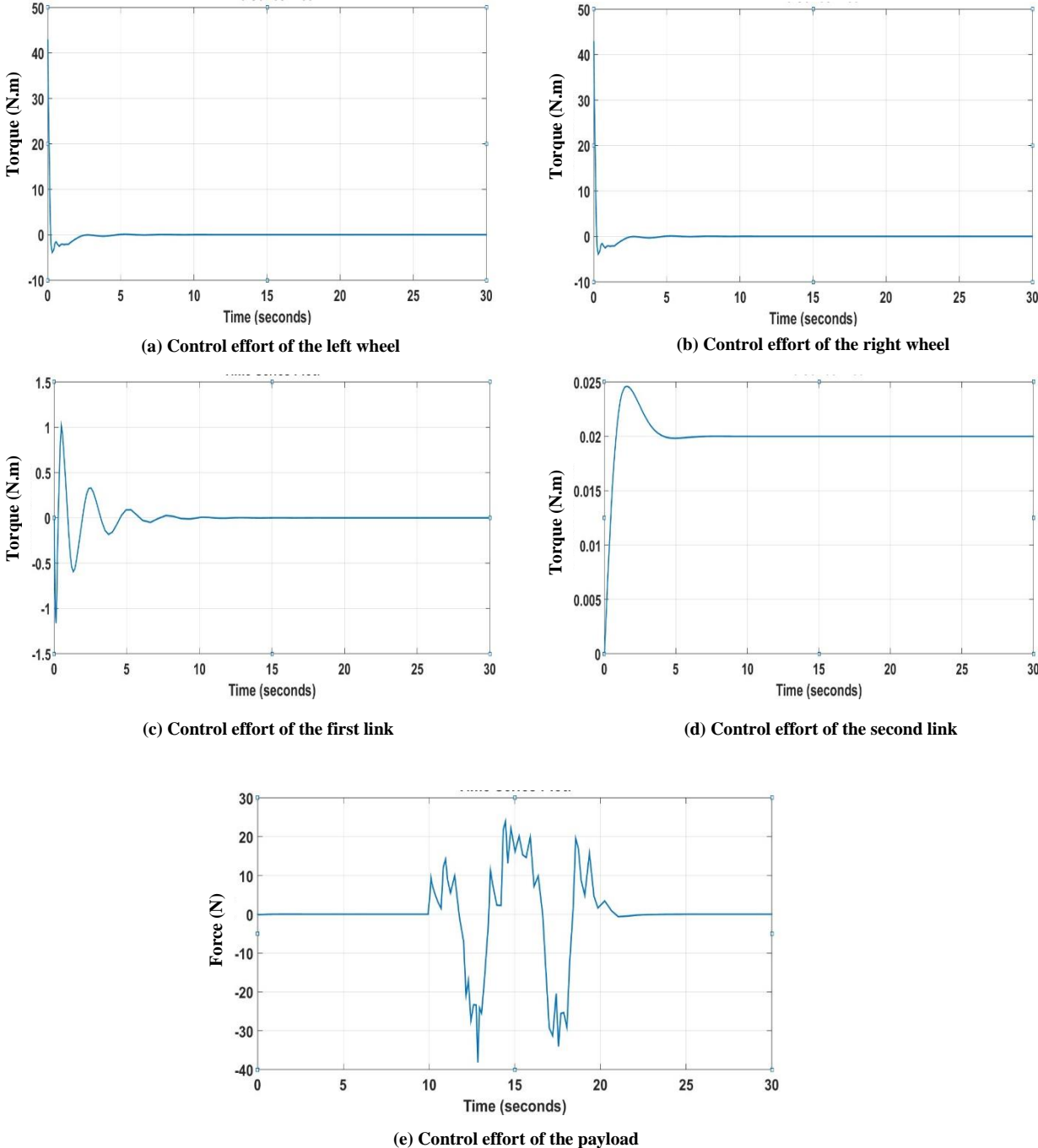


Figure 4. 27: System exerted effort using a fuzzy logic controller.

The system stabilised with the fourth input signal and the system specifications illustrated in Table 4.10.

Table 4. 10: System specifications applying the fourth input signal using fuzzy logic controllers.

	Rise Time	Settling Time	Overshoot	Peak Time	Steady State Error
Left wheel	2.042s	3.7801s	0.505%	9.345s	0.0002854
Right wheel	2.042s	3.7801s	0.505%	9.345s	0.0002854
First Link	0.3031s	9.4910s	100.294%	1.745s	-1.031e-8
Second Link	1.590s	4.1526s	1.759%	6.623s	0.0002284
Payload	0.0709s	20.0572s	726.466%	17.691s	4.58e-5

The simulation results using a fuzzy logic controller successfully stabilised the system. The left and right wheel displacement demonstrated excellent performance in the fuzzy logic controller tests, approximately the same as using the PID and PD controllers. The first and second links stabilised the intermediate body in the upright position in the fuzzy controller, with an oscillation observed in tables. The PID and PD controllers thus performed with less oscillation for the first and second links in terms of the system specifications. The system specifications in PID-PD controllers were better. In contrast, higher control efforts were exerted in PID-PD than FLC for the system stabilisation. However, it is essential to decrease the exerted effort of the controller to stabilise the system. The simulation results show that the control effort exerted for the system stabilisation resulted in a significant reduction in the FLC compared with PID-PD controllers, without affecting the system stability.

The next step is to design a hybrid control system that combines PID, PD, and FLC to check further effects and improvements concerning the system's overall response.

4.2.3 Hybrid Control Design

This section designs a hybrid controller that combines more than one control system. The hybrid control system intends to improve the system performance by combining the good specifications from the control systems used. A hybrid control system employs the beneficial sides of the proposed controllers suggested. Naturally, researchers have presented various hybrid controllers structure such as fuzzy and PID [78] [79] [80] [4].

This study implements PID, PD, and FLC controllers to improve performance. Two types of hybrid control systems are designed for the nonlinear model for two-wheeled robot vehicles with movable payload. PID with FLC is used to control both wheels, two links of the intermediate body, while the payload actuator was controlled using PD with FLC controllers.

The PID-PD control parameters are tuned progressively until the system stabilise. The FLC with two inputs includes error and change of error with one output used to describe a fuzzy inference system then create the fuzzy rules. The linguistic variable of the two inputs and output are Negative-Big (NB), Negative-Small (NS), Zero (Z), Positive-Big (PB), and Positive-Small (PS). These rules yield the action of the FLC parts. The fuzzy logic controllers were designed with nine rules, 25 rules, and 49. As well as the proper system tuning of the FLC to stabilise the model was developed using five Gaussian membership functions with 25 rules base.

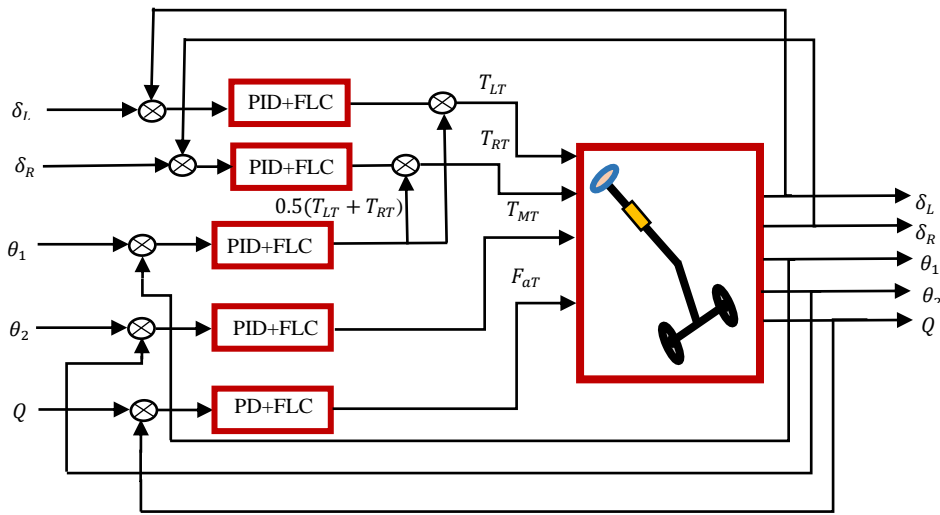


Figure 4. 28: The system block diagram using hybrid controllers.

For PID and PD tuning the gain parameters shown in Table 4.11.

Table 4. 11: PID gain parameters.

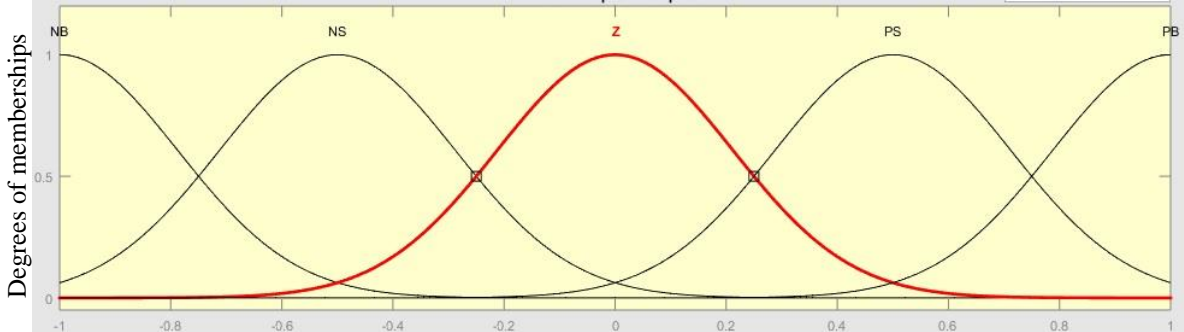
Loop	PID Gains		
	Kp	Kd	Ki
Left Wheel	50	1	0.01
Right Wheel	50	1	0.01
First Link	10	2	$0.1e^{-3}$
Second Link	6	7	0.8
Payload Actuator	20	10	0

The fuzzy logic control is of Mamdani with 25 rules base and five membership functions shown in Table 4.12 depending on the desired system performance.

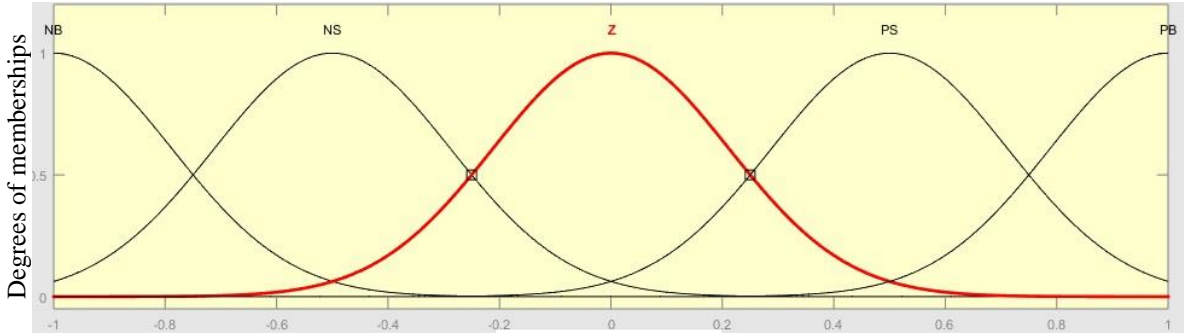
Table 4. 12: Fuzzy rules base.

\hat{e} e	NB	NS	Z	PS	PB
NB	NB	NB	NB	NS	Z
NS	NB	NB	NS	Z	PS
Z	NB	NS	Z	PS	PB
PS	NS	Z	PS	PB	PB
PB	Z	PS	PB	PB	PB

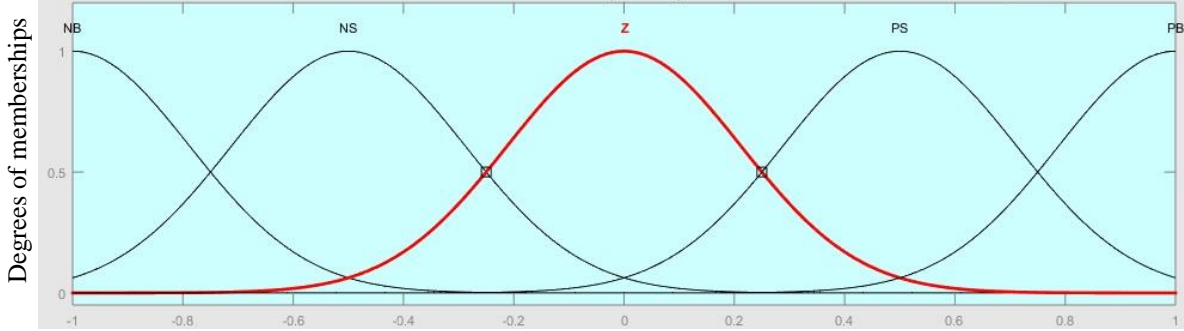
The memberships functions illustrated in Figure 4.29.



(a) Error



(b) Change of



(c) Output

Figure 4. 29: Gaussian membership function with two inputs and one output.

4.2.3.1 Results Using Hybrid Controller.

A hybrid control system is designed for system stabilisation combined with PID-PD and FLC. The system responses with various input signals will be explained in the next sections.

Test 1: Simulation results with first payload input signal.

This simulation results of the system response using hybrid controllers are illustrated in Figure 4.31 and the system controller effort observed in Figure 4.32. The first signal applied on the payload actuator is shown in Figure 4.30.

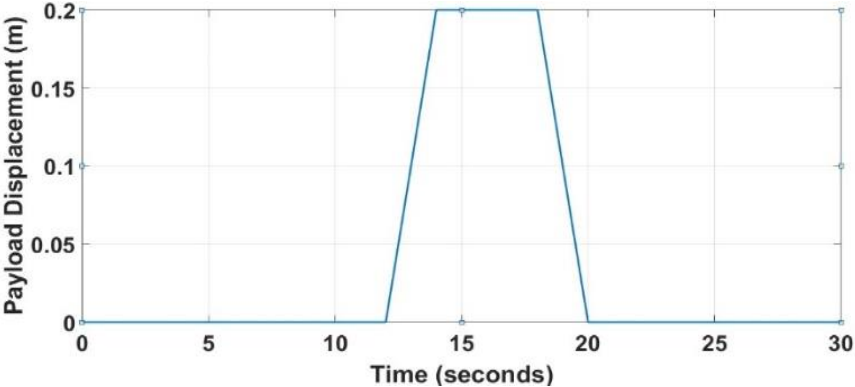


Figure 4. 30: The first input signal applied on the payload.

Simulation results for the system response using the hybrid controllers are illustrated in Figure 4.31.

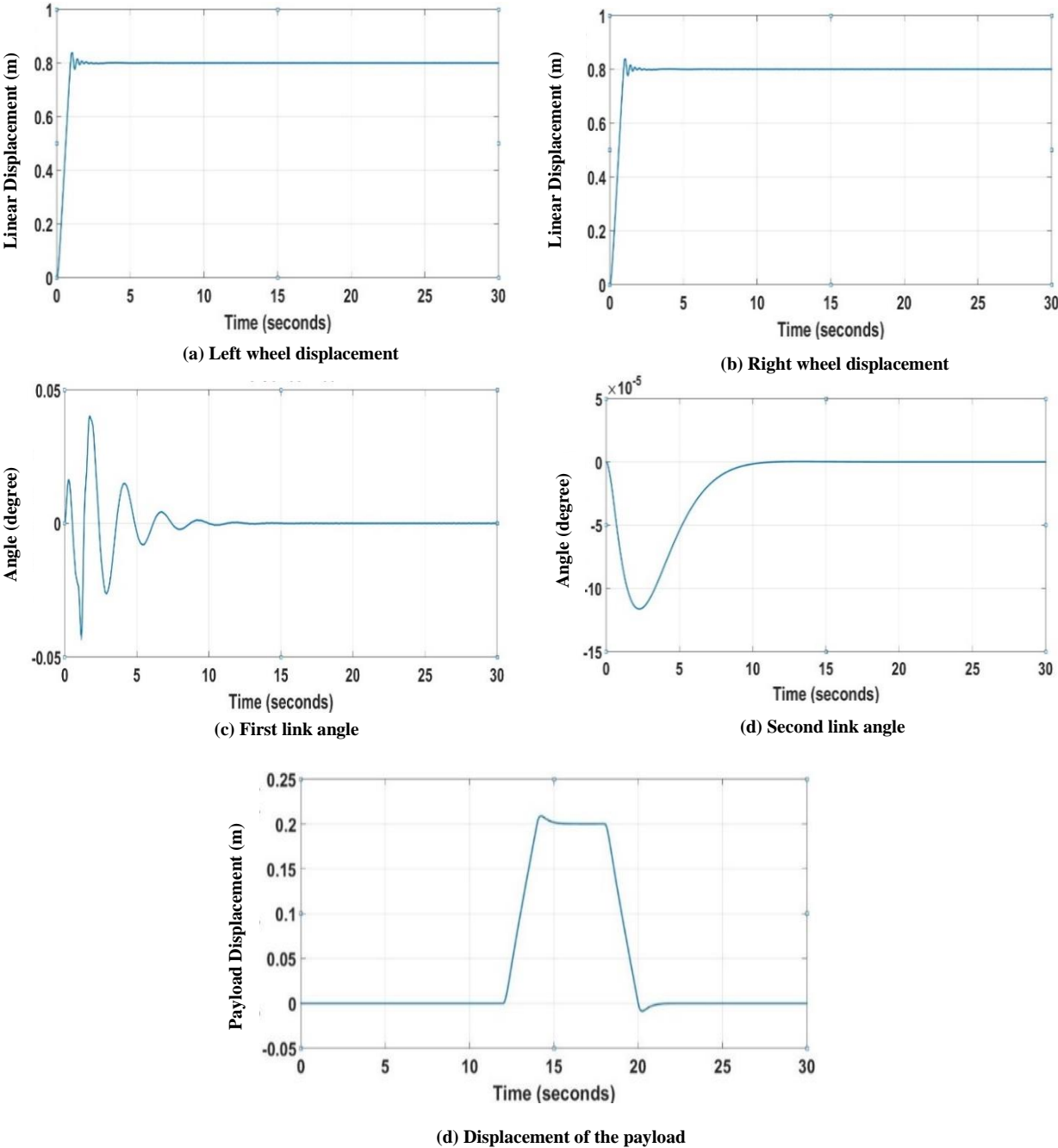


Figure 4. 31: System response using hybrid controllers.

The exerted effort of the controllers required to stabilise the system is represented in Figure 4.32.

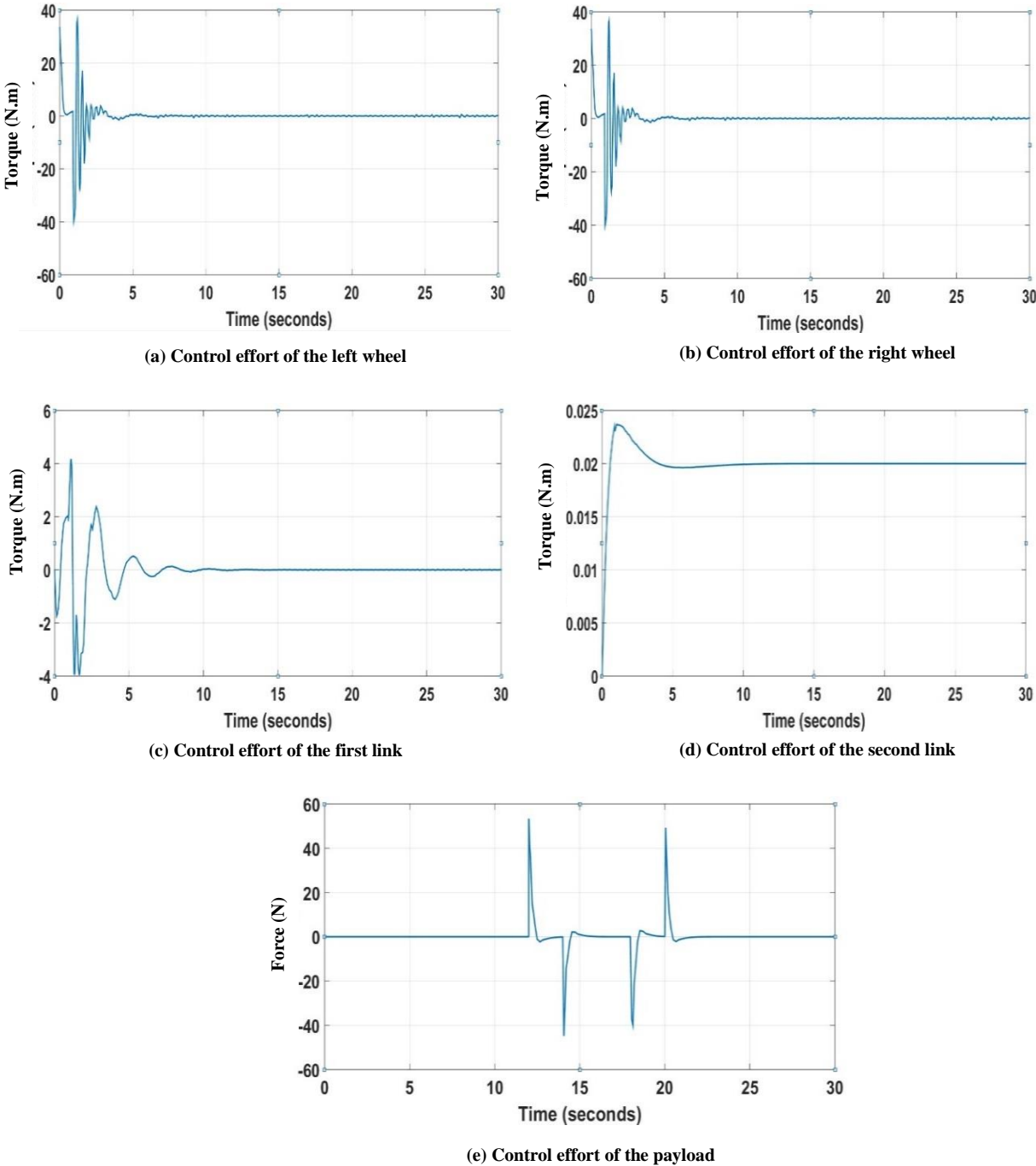


Figure 4. 32: System exerted effort using hybrid controllers.

The system successfully stabilised with the first input signal applied on the payload actuator further, the system specifications illustrated in Table 4.13.

Table 4. 13: System specifications applying the first input signal using hybrid controllers

	Rise Time	Settling Time	Overshoot	Peak Time	Steady State Error
Left Wheel	0.6694s	1.2682s	4.737%	1.055s	-5.91e-5
Right Wheel	0.6694s	1.2682s	4.737%	1.055s	-5.91e-5
First Link	0.0621s	9.5953s	99.960%	1.729s	1.813e-5
Second Link	4.529s	9.6467s	0.505%	13.270s	6.263e-11
Payload	1.497s	20.6472s	4.954%	14.280s	1.427e-5

Test 2: Simulation results with the second input signal.

The second input signal using a hybrid controller is applied on the payload actuator illustrated in Figure 4.33.

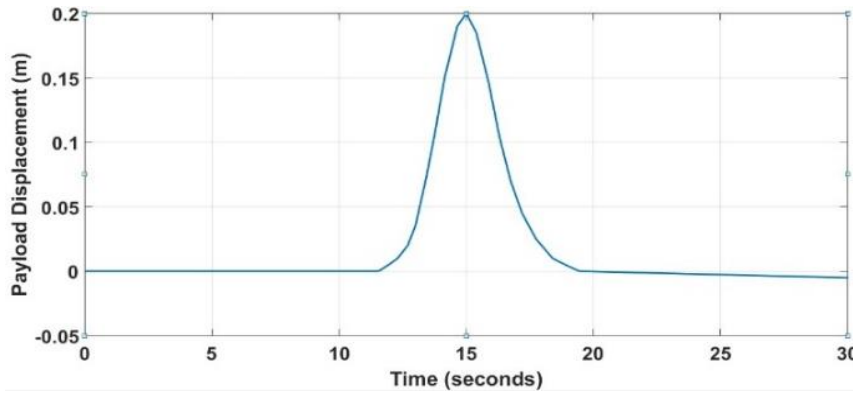


Figure 4. 33: The second input signal applied on the payload.

Simulation results for the system response using the hybrid controllers are illustrated in Figure 4.34.

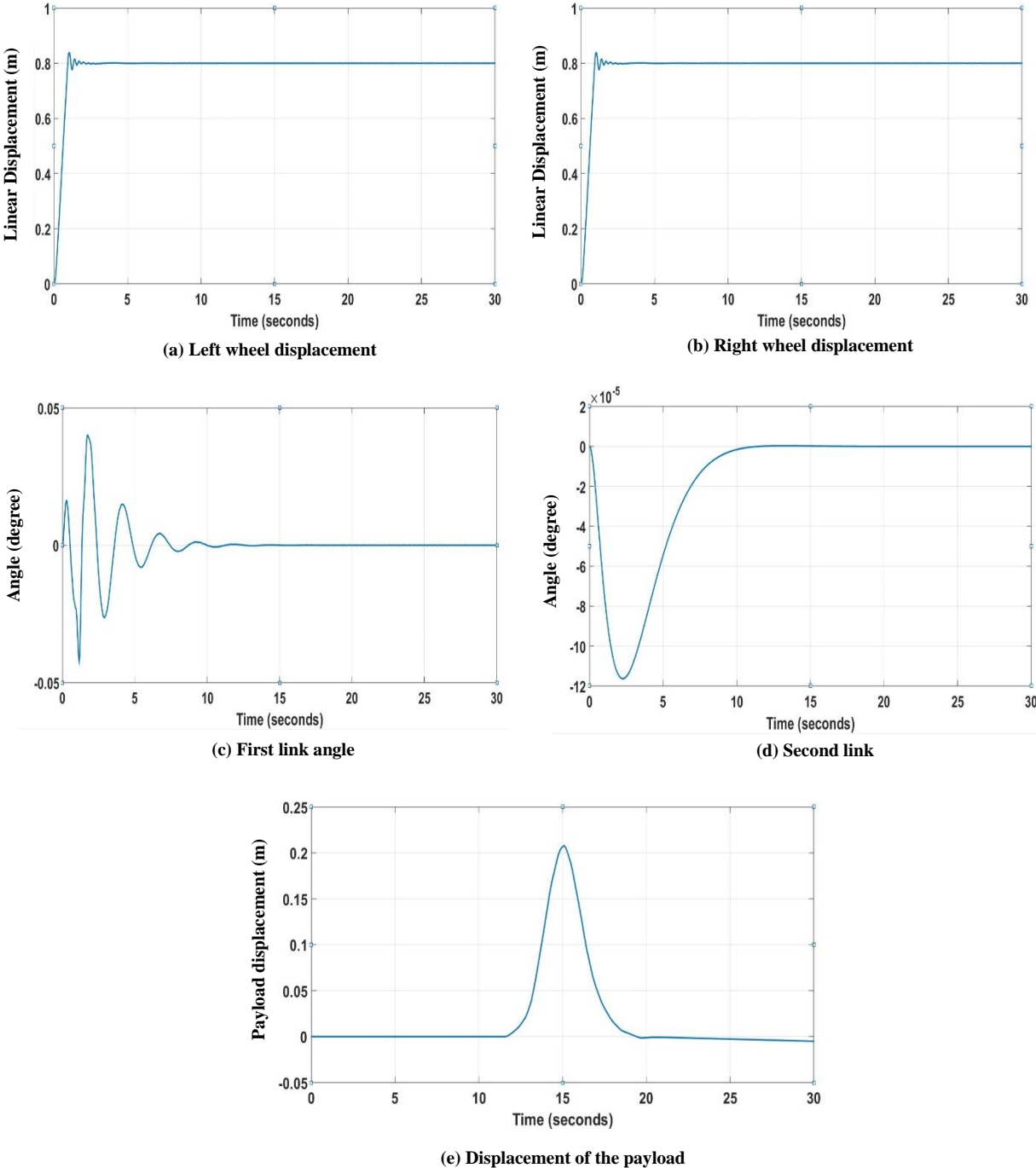


Figure 4. 34: System response using hybrid controllers.

The exerted effort of the controllers required to stabilise the system is represented in Figure 4.35.

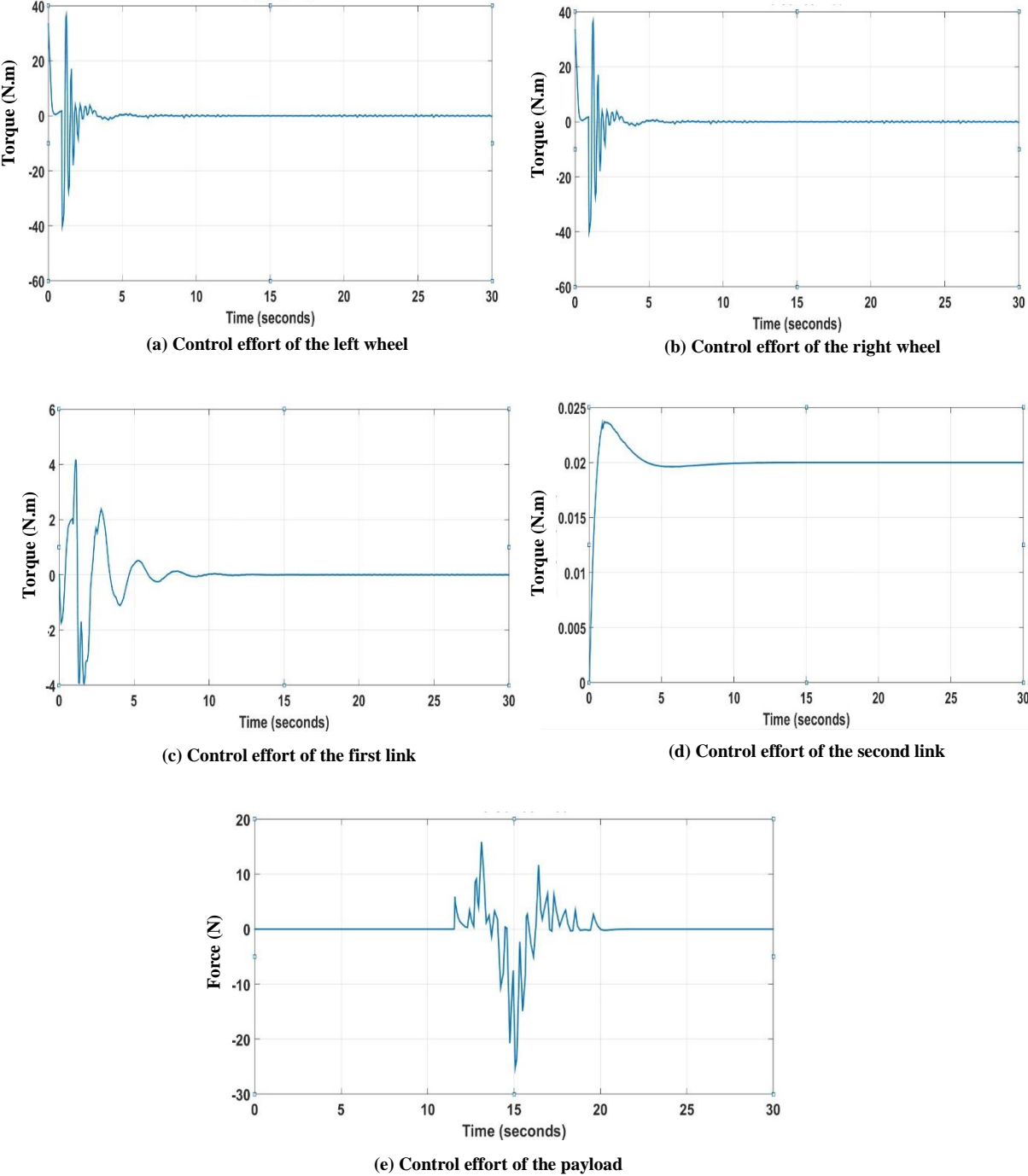


Figure 4. 35: System exerted effort using hybrid controllers.

The system successfully stabilised with the second input signal with less control effort required for the payload stabilisation than the first signal, and the system specifications are illustrated in Table 4.14.

Table 4. 14: System specifications apply the second input signal using hybrid controllers.

	Rise Time	Settling Time	Overshoot	Peak Time	Steady State Error
Left Wheel	0.6694s	1.2682s	4.737%	1.055s	-0.000272
Right Wheel	0.6694s	1.2682s	4.737%	1.055s	-0.000272
First Link	0.0621s	9.5953s	99.960%	1.729s	-1.863e-5
Second Link	4.529s	9.6467s	0.505%	13.255s	6.263e-11
Payload	9.4544s	20.9326s	0.515%	15.074s	1.427e-5

Test 3: Simulation results with third payload input signal

The third input signal using a hybrid controller applied on the payload actuator is illustrated in Figure 4.36.

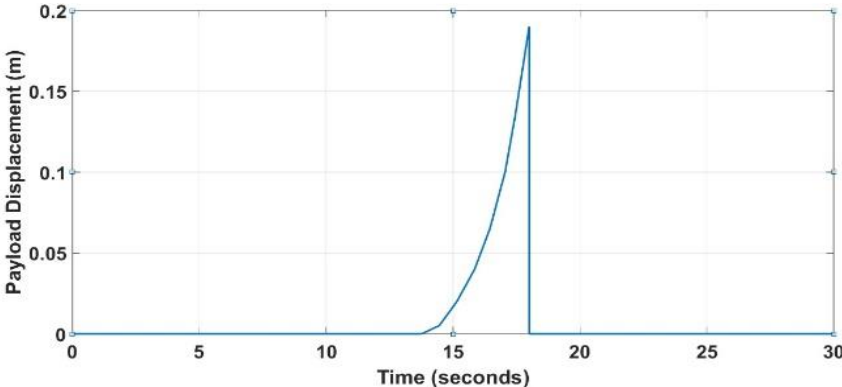


Figure 4. 36: The third input signal applied on the payload.

Simulation results for the system response using the hybrid controllers are illustrated in Figure 4.37.

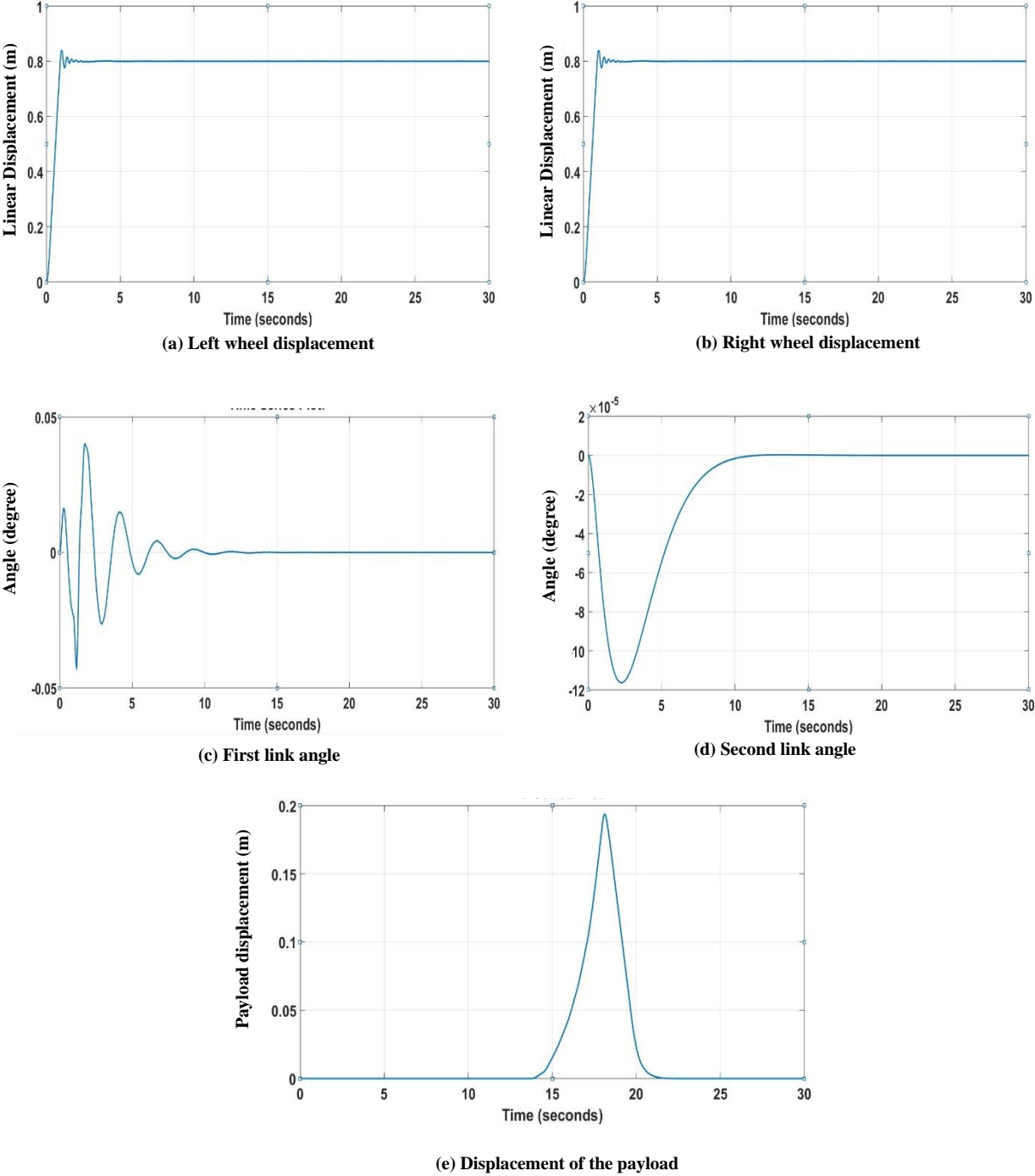
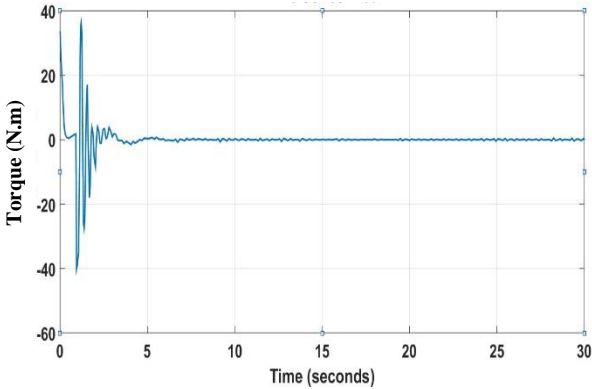
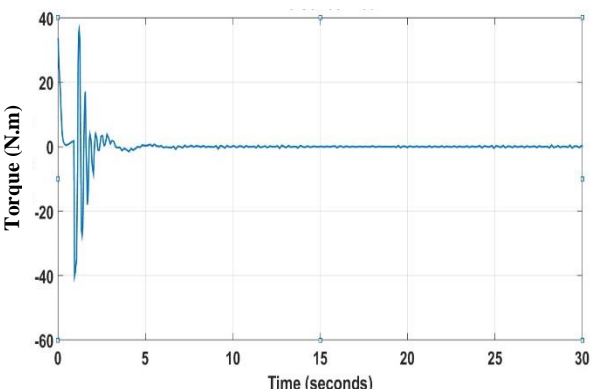


Figure 4. 37: System response using hybrid controllers.

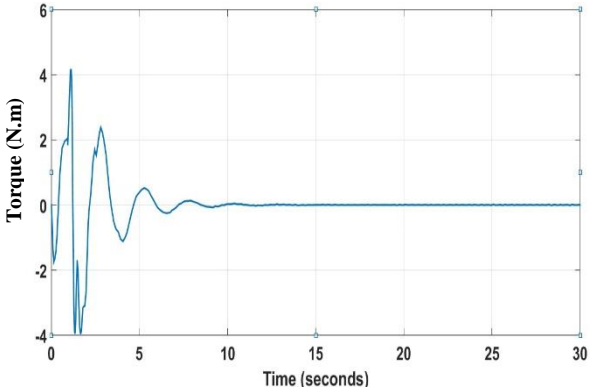
The exerted effort of the controllers required to stabilise the system is represented in Figure 4.38.



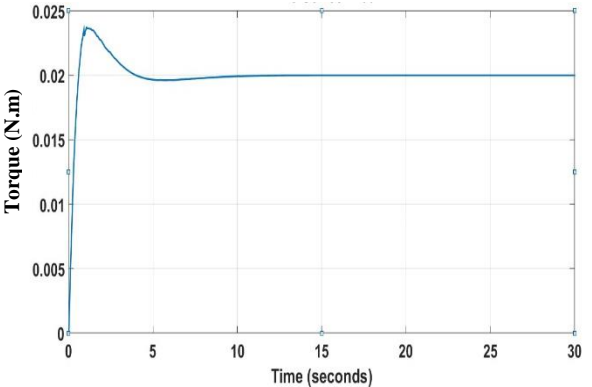
(a) Control effort of the left wheel



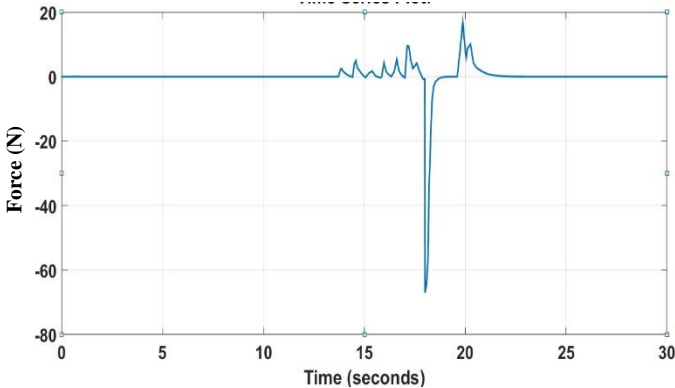
(b) Control effort of the right wheel



(c) Control effort of the first link



(d) Control effort of the second link



(e) Control effort of the payload

Figure 4. 38: System exerted effort using hybrid controllers.

The system successfully stabilised with the third input signal but with higher input signal applied on the payload linear actuator further, the system specifications illustrated in Table 4.15.

Table 4. 15: System specifications apply the third input signal using hybrid controllers

	Rise Time	Settling Time	Overshoot	Peak Time	Steady State Error
Left Wheel	0.6694s	1.2682s	4.737%	1.055s	-2.312e-5
Right Wheel	0.6694s	1.2682s	4.737%	1.055s	-2.312e-5
First Link	0.0621s	9.5953s	99.960%	1.729s	1.762e-5
Second Link	4.529s	9.6467s	0.505%	13.191s	6.3e-11
Payload	2.642s	20.7318s	3.646%	18.147s	1.427e-5

Test 4: Simulation results with fourth payload input signal.

The fourth input signal using a hybrid controller applied on the payload actuator is illustrated in Figure 4.39.

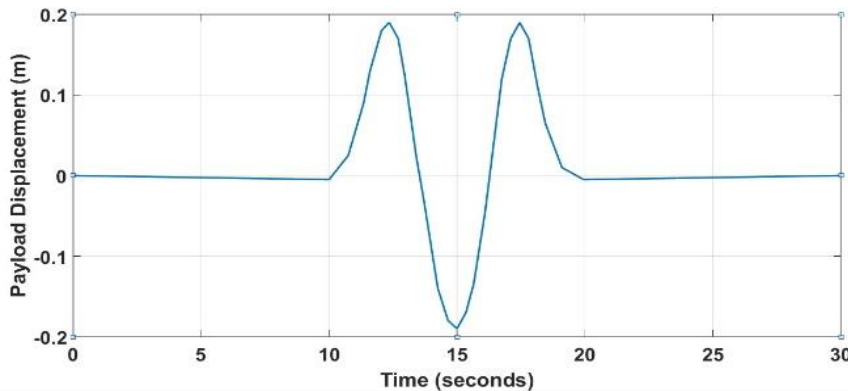


Figure 4. 39: The fourth input signal applied on the payload.

Simulation results for the system response using the hybrid controllers are illustrated in Figure 4.40.

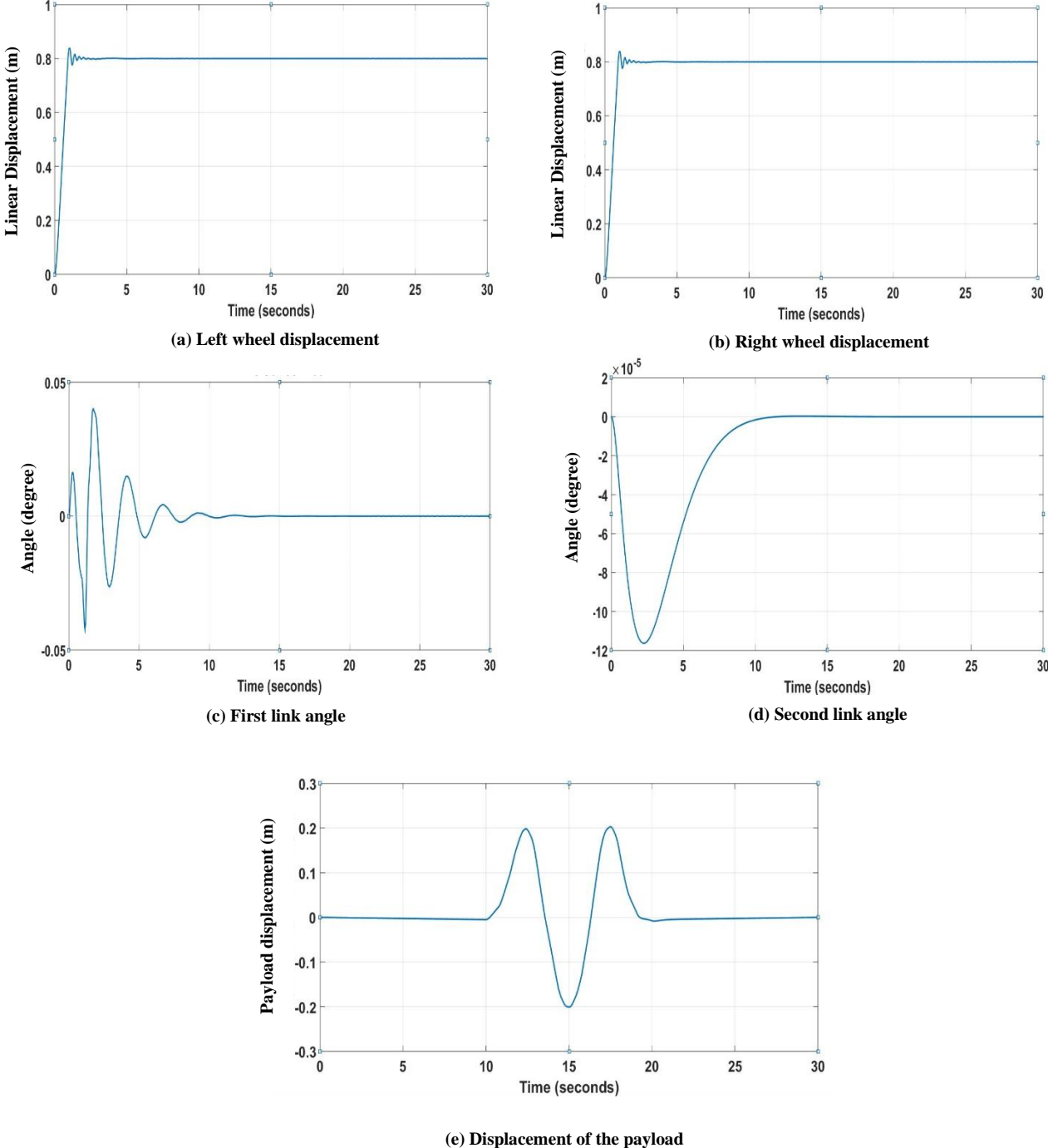


Figure 4. 40: System response using hybrid controllers.

The exerted effort of the controllers required to stabilise the system is represented in Figure 4.41.

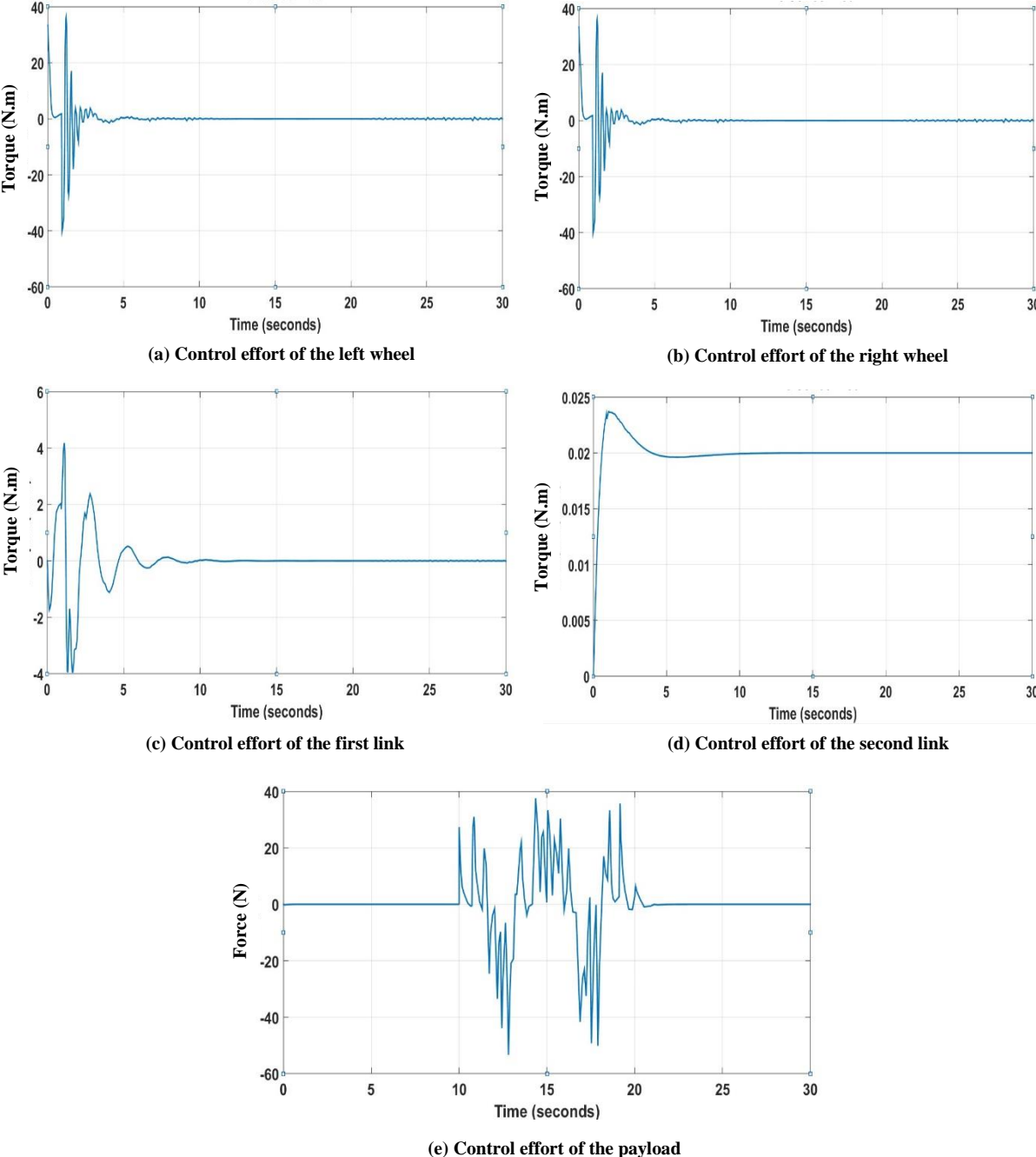


Figure 4. 41: System exerted effort using hybrid controllers.

The last input signal applied on the payload actuator and designed with a hybrid controller successfully stabilised. The system specification of the system is illustrated in Table 4.16.

Table 4. 16: System specifications apply the fourth input signal using hybrid controllers.

	Rise Time	Settling Time	Overshoot	Peak Time	Steady State Error
Left Wheel	0.6694s	1.2682s	4.737%	1.055s	-0.0001553
Right Wheel	0.6694s	1.2682s	4.737%	1.055s	-0.0001553
First Link	0.0621s	9.5953s	99.960%	1.729s	-2.347-5
Second Link	4.529s	9.6467s	0.505%	13.255s	6.542e-11
Payload	10.071s	21.9111s	59.718%	17.530s	1.427e-5

Two hybrid controllers are implemented, including PID with FLC and PD with FLC. The hybrid controllers combined the excellent characteristics of the model designed with the control system.

The hybrid control system successfully stabilised the model, and the linear displacement for both wheels settled with 1.2682s settling time and 4.737% overshoot. The two links of the intermediate body successfully stabilised at the upright position. The first link settled at 9.5953s, while the second link stabilised at 9.6467s with a slight overshoot of 0.505% and small exerted efforts. And the payload produces the same input signal applied on the payload actuator.

In this study, the first procedure was to design the PID-PD controllers that had better system specifications than FLC but exerted higher control efforts for system stabilisation. The reduction of the controller effort was noticed while using the fuzzy logic controller.

None of the studies has used fuzzy logic controllers for two-wheeled robot vehicles with movable payload based on a double inverted pendulum system while moving on flat surfaces. The simulation results using fuzzy controllers give a stable response and are almost the same as the PID-PD controllers but significantly reduce control effort for system stabilisation. However, the fuzzy logic controller has improved the system control effort

exerted. Accordingly, a hybrid control system is designed to combine the best characteristics of two different control systems for better system specifications and appropriate control effort exerted for stabilisation.

Comparing the simulation results to those reported by [37]. The system successfully stabilised with less control effort. The wheels stabilised with 36.4N.m and the first link controller effort is 4.15N.m, which gave a satisfactory response as illustrated in the system specifications tables.

4.3 Summary

The purpose of this chapter was to design different control systems. The model has been simulated and confirmed that the system was unstable. The first type of controller was PID-PD controllers with control parameters tuned manually. The second type is the fuzzy logic controller with 25 rules base and five membership functions. Further work was executed to design a hybrid controller that combined PID, PD, and Fuzzy logic controllers. The control systems were capable of stabilising the system, and simulation results have shown a successful stable response with all controllers with different input signals applied on the payload actuator. The simulation results were satisfactory for the hybrid control techniques that combine excellent specifications from both control approaches with appropriate control effort that provides a stable response. The next procedure is to test the system's robustness by applying external disturbances will be discussed in chapter five.

Chapter Five

Control System Robustness Under Disturbance

5.1 Introduction

This chapter aims to study the validation of the system's control robustness by assessing the designed controller's ability to overcome external disturbances and analysing the robot motion response. Various forces were applied to test system capability to react the external disturbances. The external disturbances applied on vehicle wheels, the two links, and the payload actuator separately. The hybrid controller should cope with disturbance and contact uneven surfaces and different environments. The robot vehicle must successfully reject the disturbances and converge back to the desired set point. The simulation results showed the system behaviour when different forces with different amplitudes were applied to the system component. In addition, there was a detection of the maximum range of applied forces to test the behaviour of the system responses with the disturbances used. Furthermore, the system achieved specifications and control effort to see how much exerted torque and force in system components. Many researchers test the robustness of the designed controllers by applying external disturbances [81] [82] [83][60][84]. Section 5.2 explains the various amplitudes applied on each part and divided into subsections introduced the effect of the disturbance forces and the control action at each part of the designed model.

5.2 Disturbance Force with Various Amplitudes

The robustness of the control system is concerned with applying disturbance of various amplitudes on each part of the robot system. The numerical values of various amplitudes are provided in Table 5.1.

Table 5. 1: The values of the system disturbance force with different amplitudes.

Amplitude	50N, 100N, 250N, 300N, 350N
Period (secs)	25s
Pulse Width (% of period)	0.5
Phase delay (secs)	10s

5.2.1 Disturbance Applied on the Left Wheel

The system response of the left wheel after applying different amplitudes is illustrated in Figure 5.1. The increase of the disturbance affected the peak value that reached 5.13m when maximum disturbance force was applied. The external disturbance makes the vehicle swerve from the path, and it affects the right wheel and tilt angle of the first link, as shown in Figure 5.1. The tilt angle of the second link and payload does not affect by the applied force. The torque exerted to stabilise the system increased with increasing the disturbance force applied.

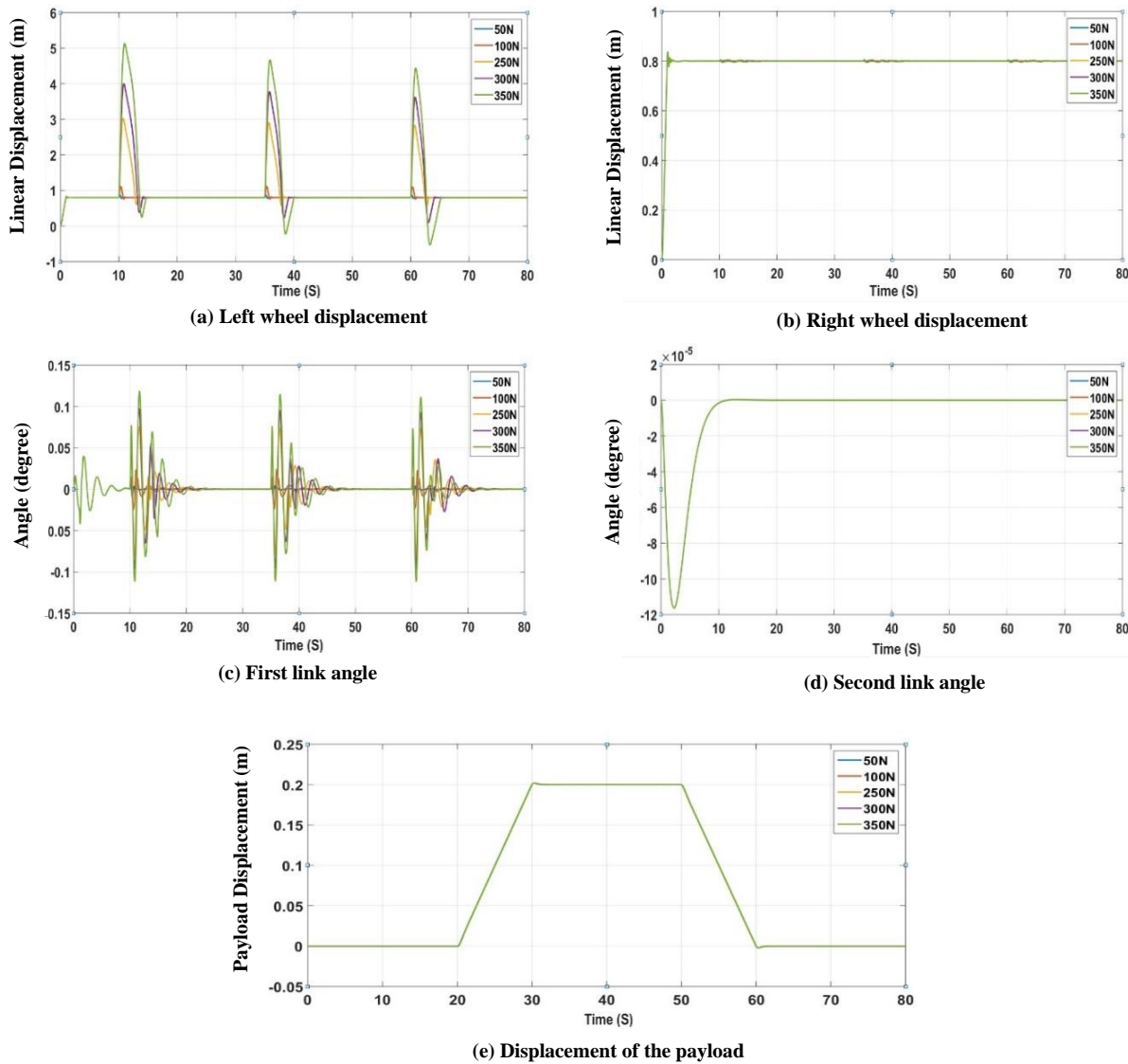
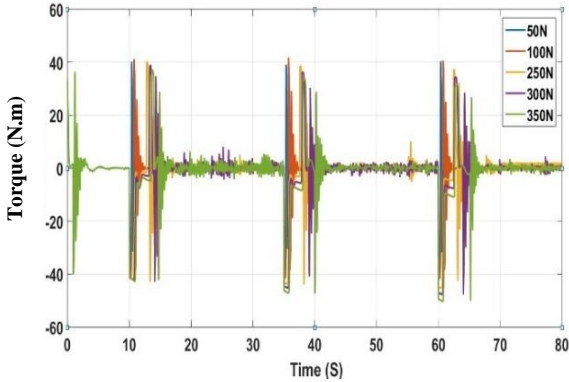
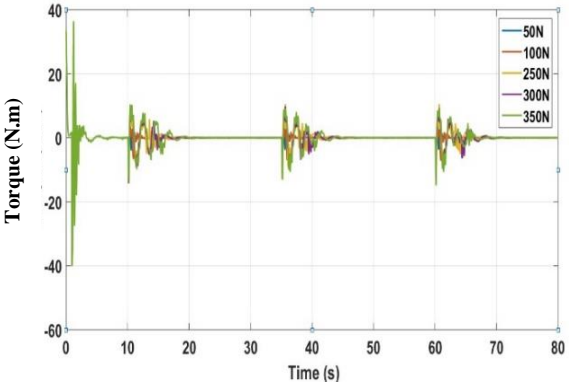


Figure 5. 1: Disturbance applied on the left wheel with different amplitudes.

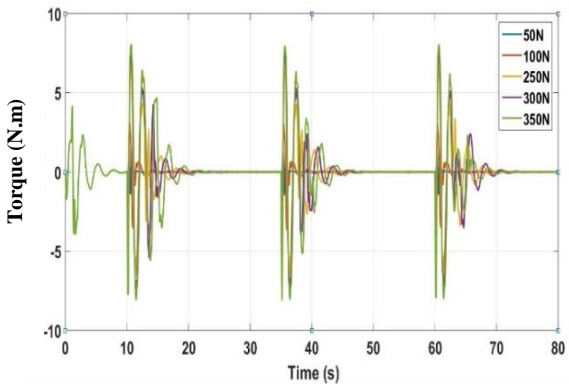
The exerted effort of the controllers required to stabilise the system is represented in Figure 5.2.



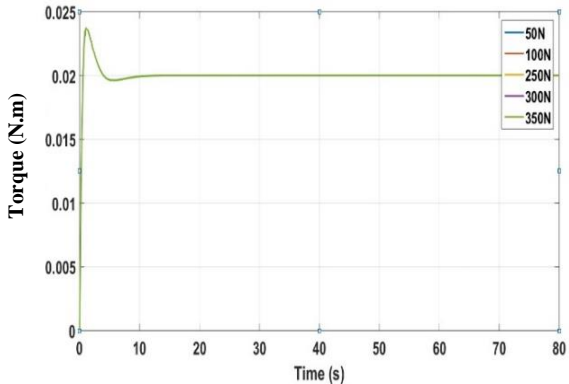
(a) Control effort of the left wheel



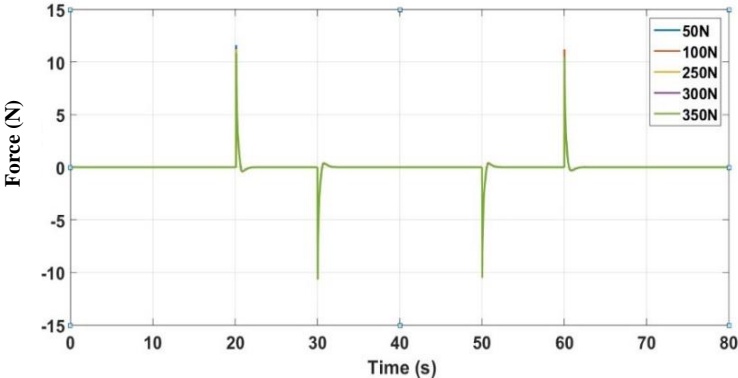
(b) Control effort of the right wheel



(c) Control effort of the first link



(d) Control effort of the second link



(e) Control effort of the payload

Figure 5. 2: The control system effort with disturbance forces applied on the left wheel.

5.2.2 Disturbance Applied on the Right Wheel

The response of the right wheel was the same as the left wheel responses after disturbance forces were applied. The system response in Figure 5.3 explains the system's correspondence when an external disturbance is applied on the left and right wheel. The disturbance on the right wheel also causes fluctuations on the left wheel and tilt angle of the first link while the second link and the payload linear actuator does not affect, as shown in Figure 5.3.

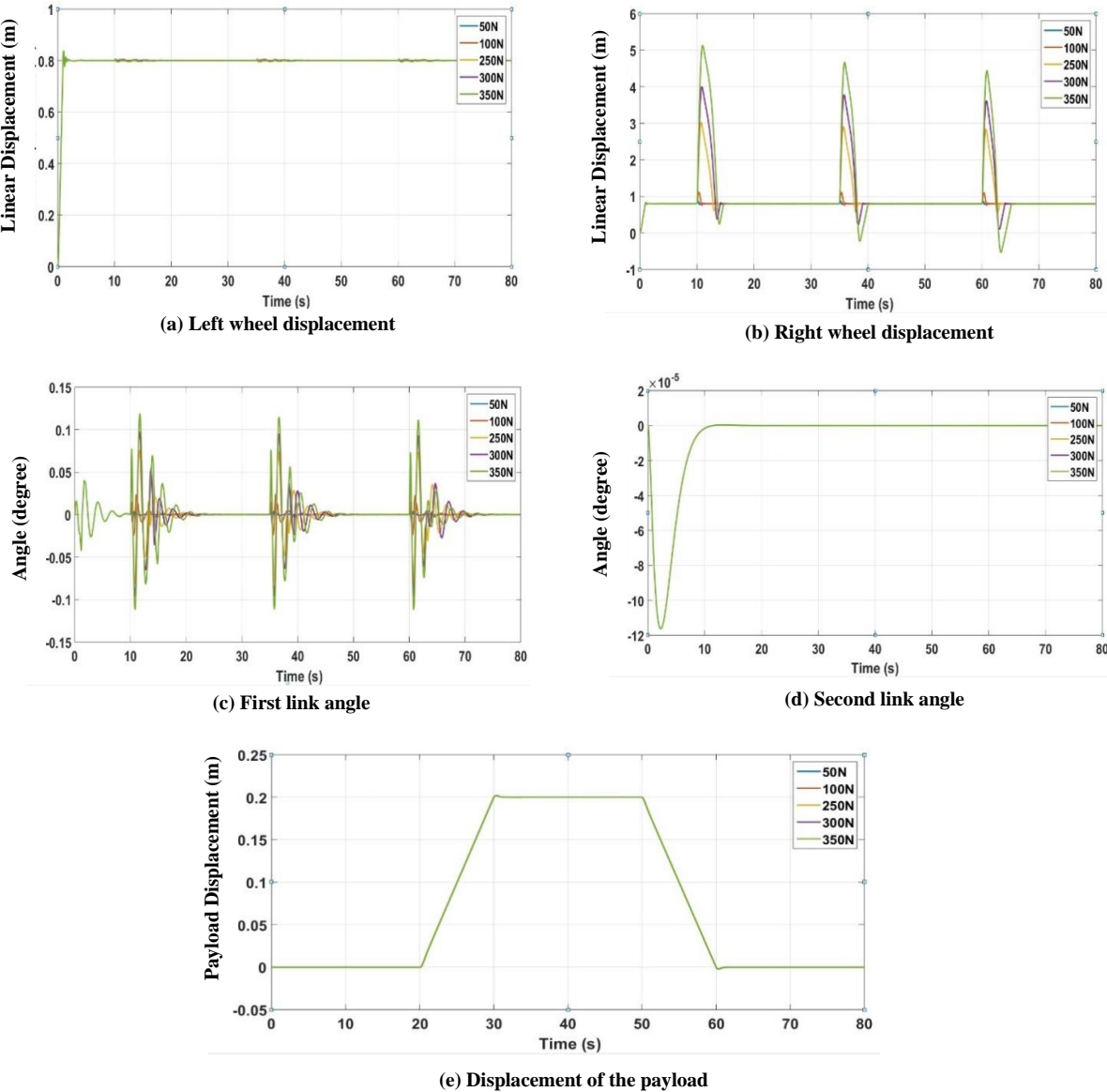
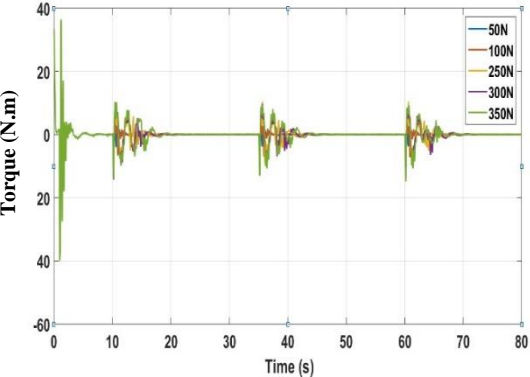
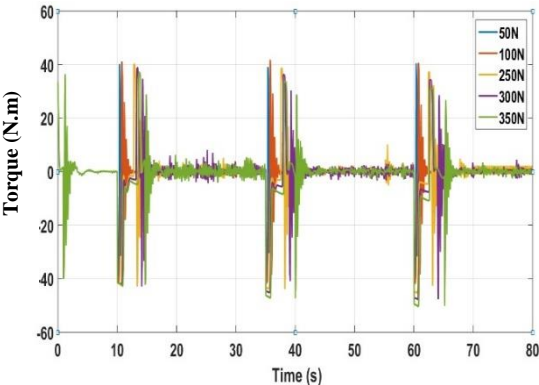


Figure 5. 3: Disturbance applied on the right wheel with different amplitudes.

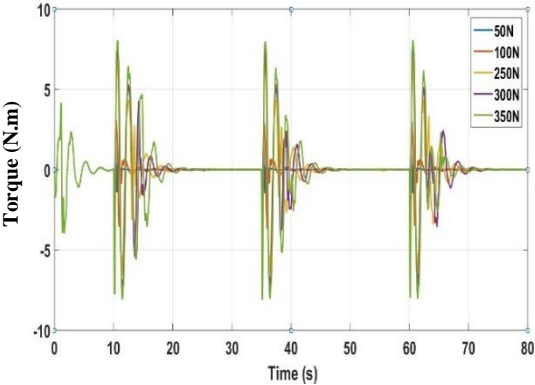
The exerted effort of the controllers required to stabilise the system is represented in Figure 5.4.



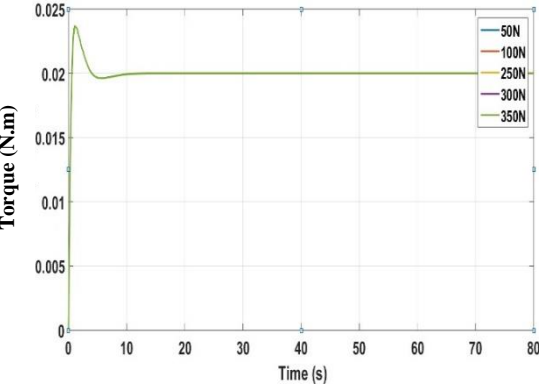
(a) Control effort of the left wheel



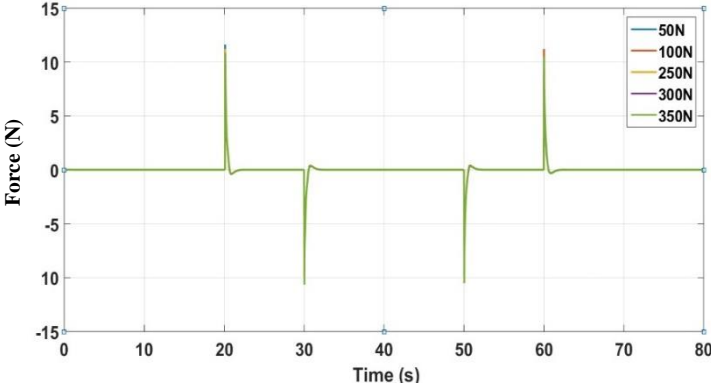
(b) Control effort of the right wheel



(c) Control effort of the first link



(d) Control effort of the second link



(e) Control effort of the payload

Figure 5. 4: The control system effort with disturbance forces applied on the right wheel.

5.2.3 Disturbance Applied on the First Link

The system response when disturbance forces are applied on the first link is illustrated in Figure 5.5. The disturbance applied on the first link yielded negative peaks on the left and right wheels. The negative peaks mean that the vehicle moved in the opposite direction to keep the tilt angles upright. In contrast, the system response of the second link and payload were not affected. The peak value of the first link response reached 0.226° from the steady-state value, as shown in Figure 5.5.

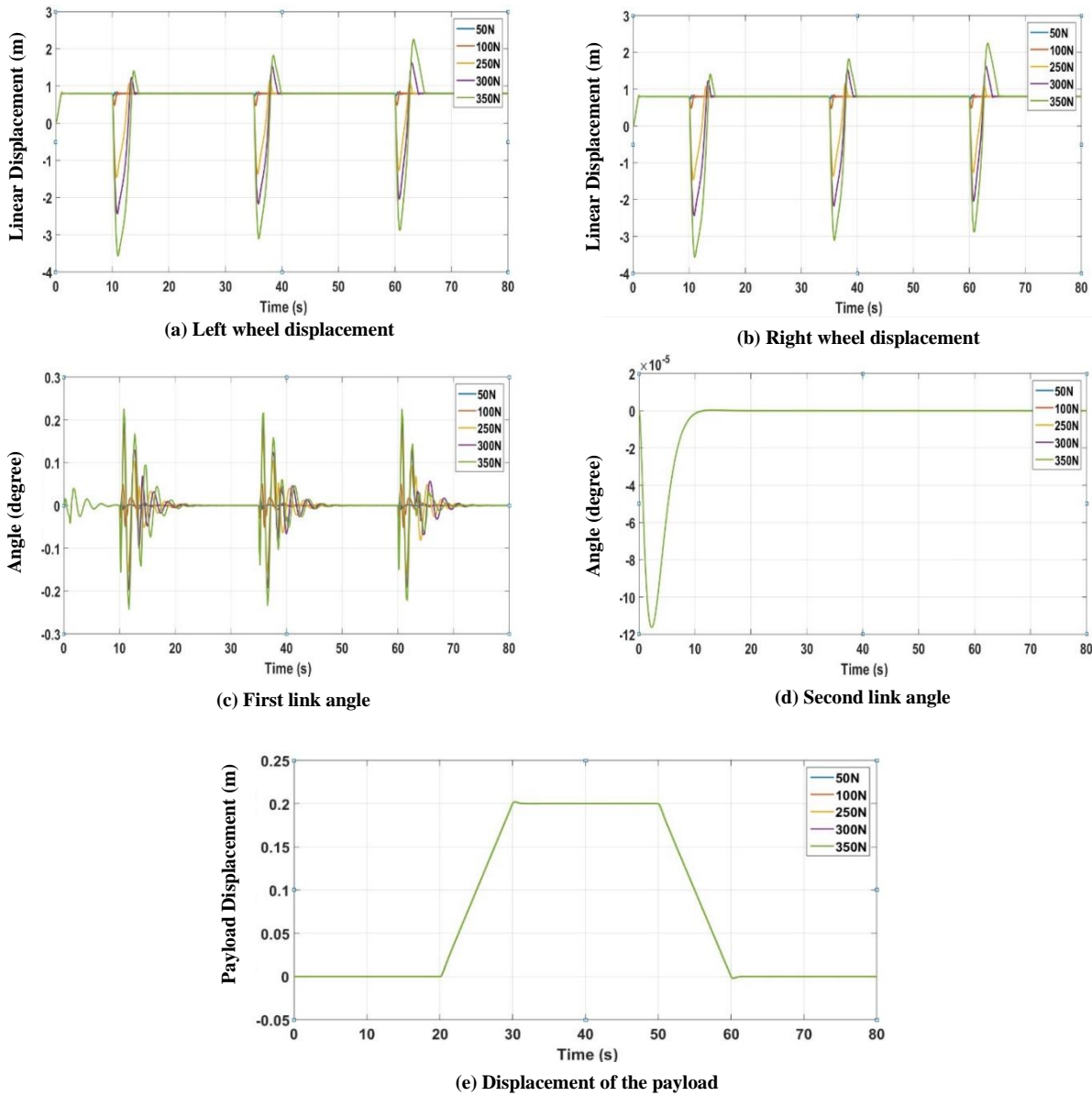
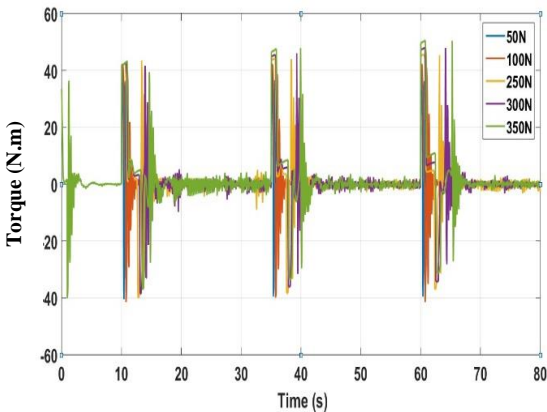
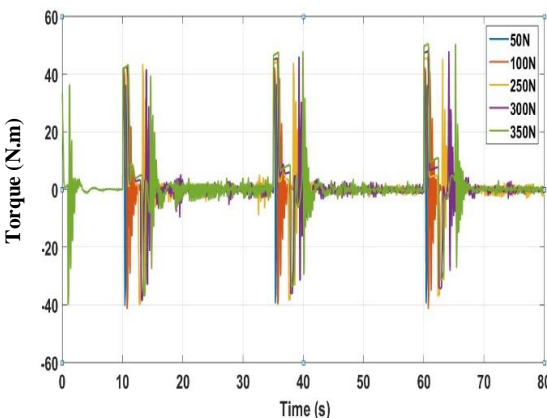


Figure 5. 5: Disturbance applied on the first link with different amplitudes.

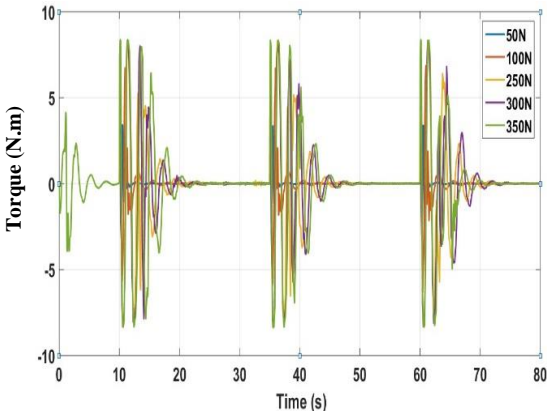
The exerted effort of the controllers required to stabilise the system is represented in Figure 5.6.



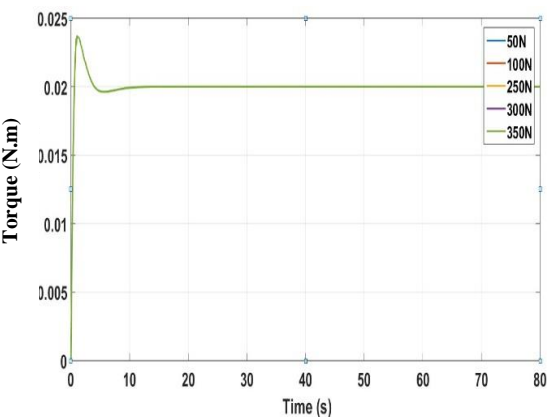
(a) Control effort of the left wheel



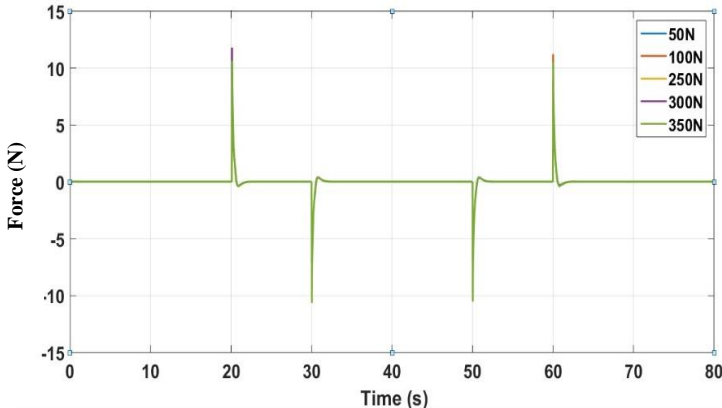
(b) Control effort of the right wheel



(c) Control effort of the first link



(d) Control effort of the second link



(e) Control effort of the payload

Figure 5. 6: The control system effort with disturbance forces applied on the first link.

5.2.4 Disturbance Applied on the Second Link

When disturbance was applied on the second link, it caused oscillation on the tilt angle of the second link. The wheels displacement, the first link, and the payload are not changed; this is due damping effect by vehicle joints and the motor between the two links further, the payload actuator. The disturbance resulted in oscillation in the second link, and peaks value increased with increasing the disturbance force applied, as shown in Figure 5.7.

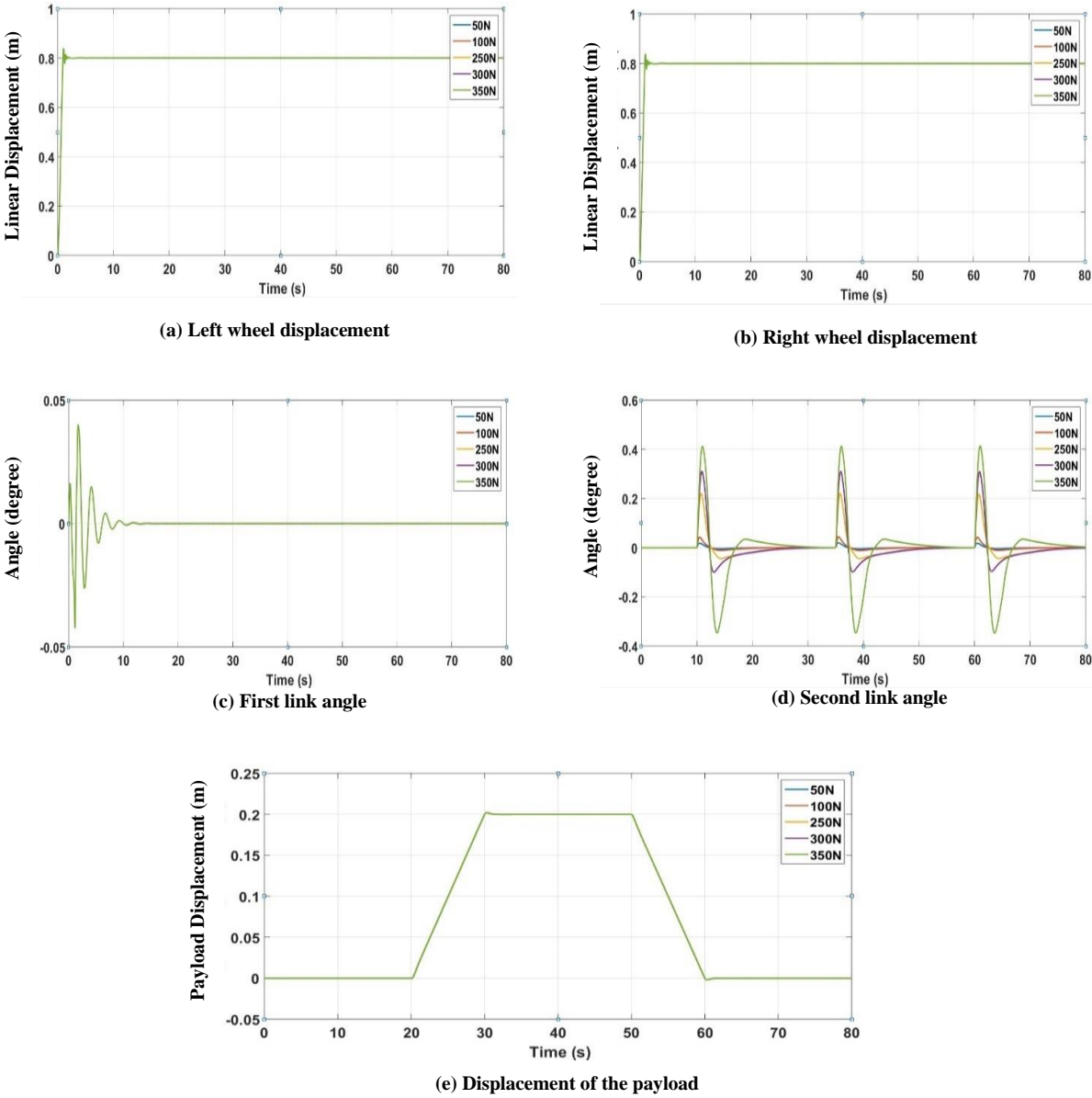


Figure 5. 7: Disturbance applied on the second link with different amplitudes.

The exerted effort of the controllers required to stabilise the system is represented in Figure 5.8.

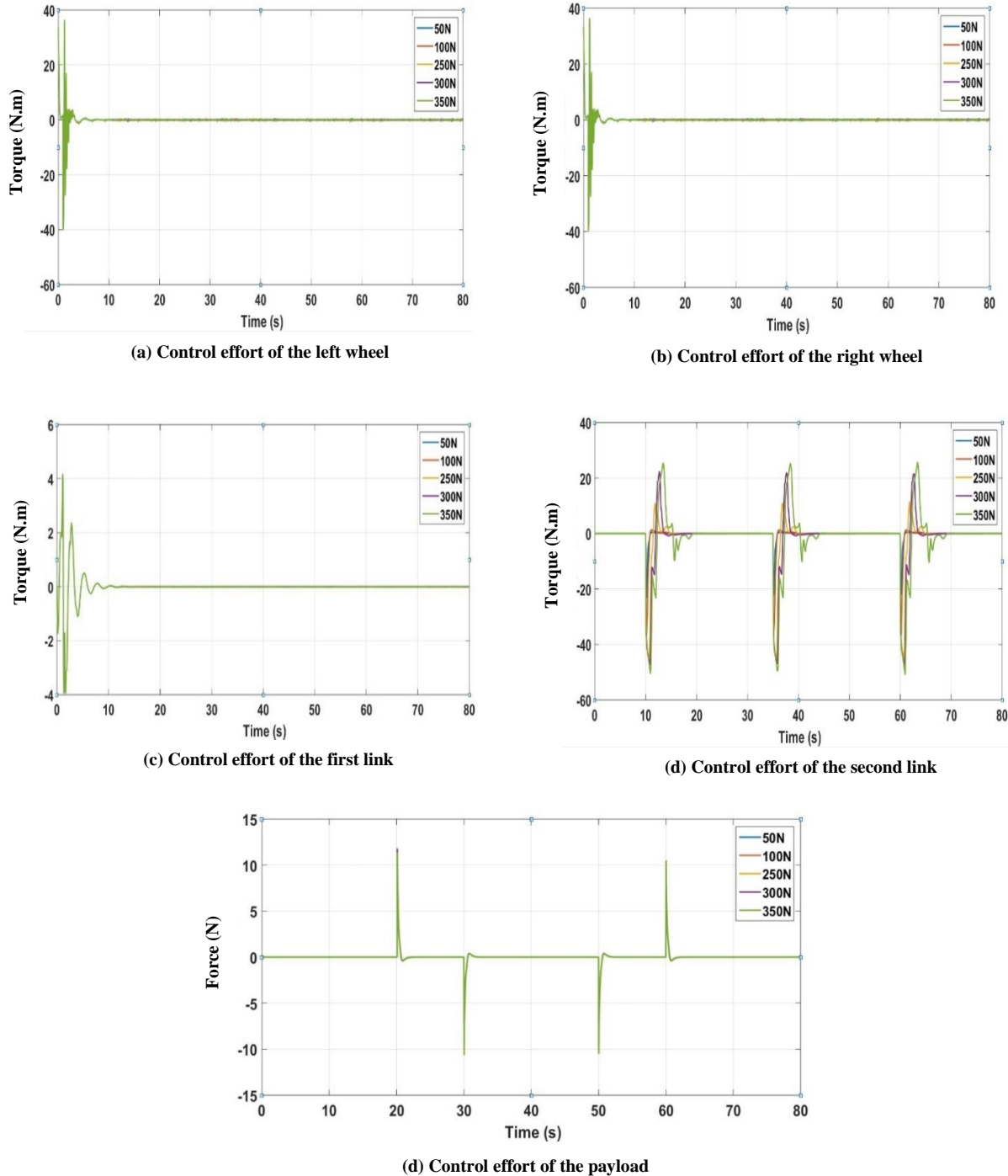


Figure 5. 8: The control system effort with disturbance forces applied on the second link.

5.2.5 Disturbance Applied on the Payload

The disturbance applied on the payload resulted in positive peaks, increased with the increase of the disturbance force applied. The maximum disturbance force applied is illustrated in Figure 5.9, which explains that the peaks value reached 0.378m. Furthermore, the two wheels and the two links of the intermediate body are not affected by the disturbance forces applied.

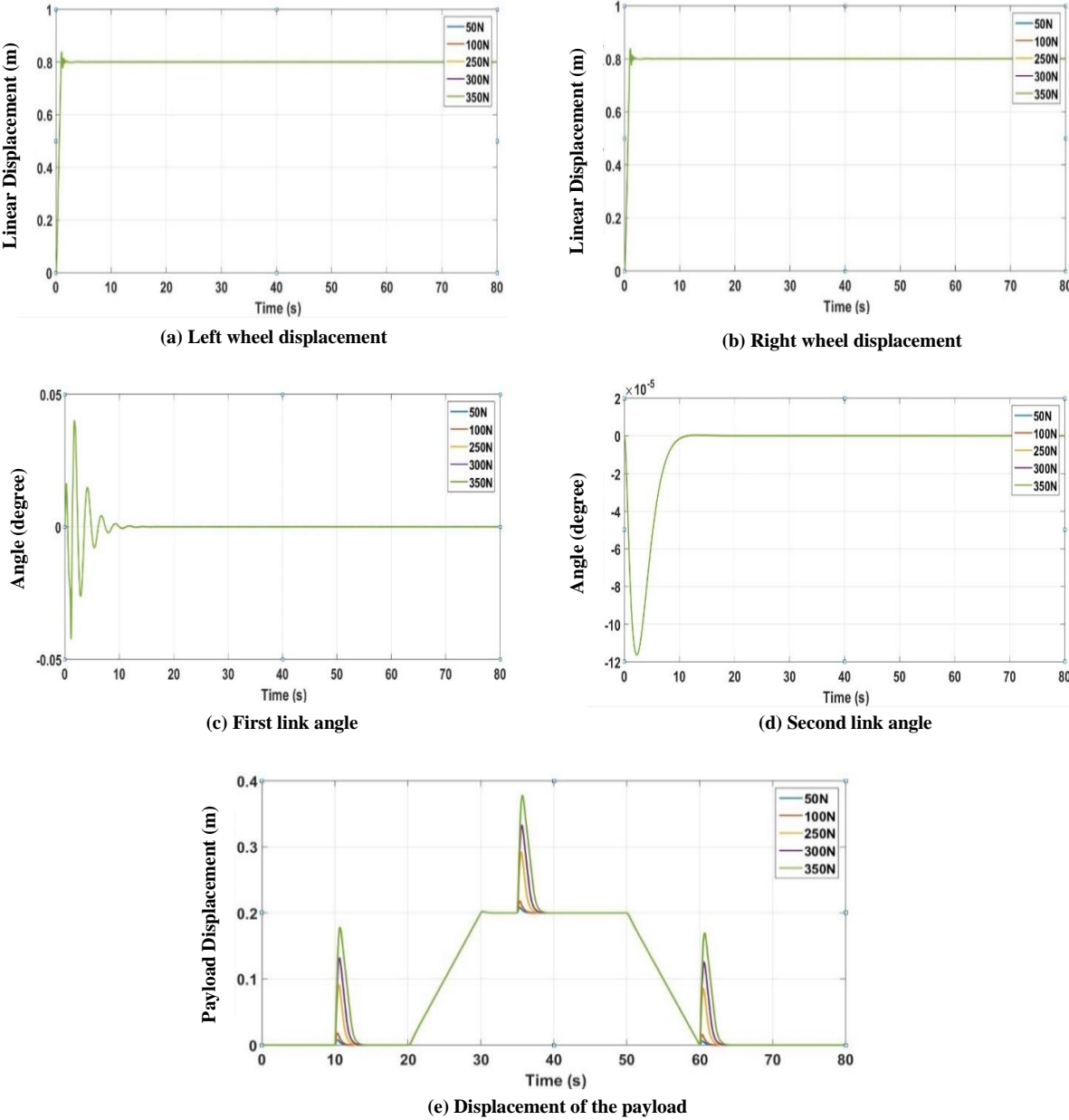


Figure 5. 9: Disturbance applied on the payload with different amplitudes.

The exerted effort of the controllers required to stabilise the system is represented in Figure 5.10.

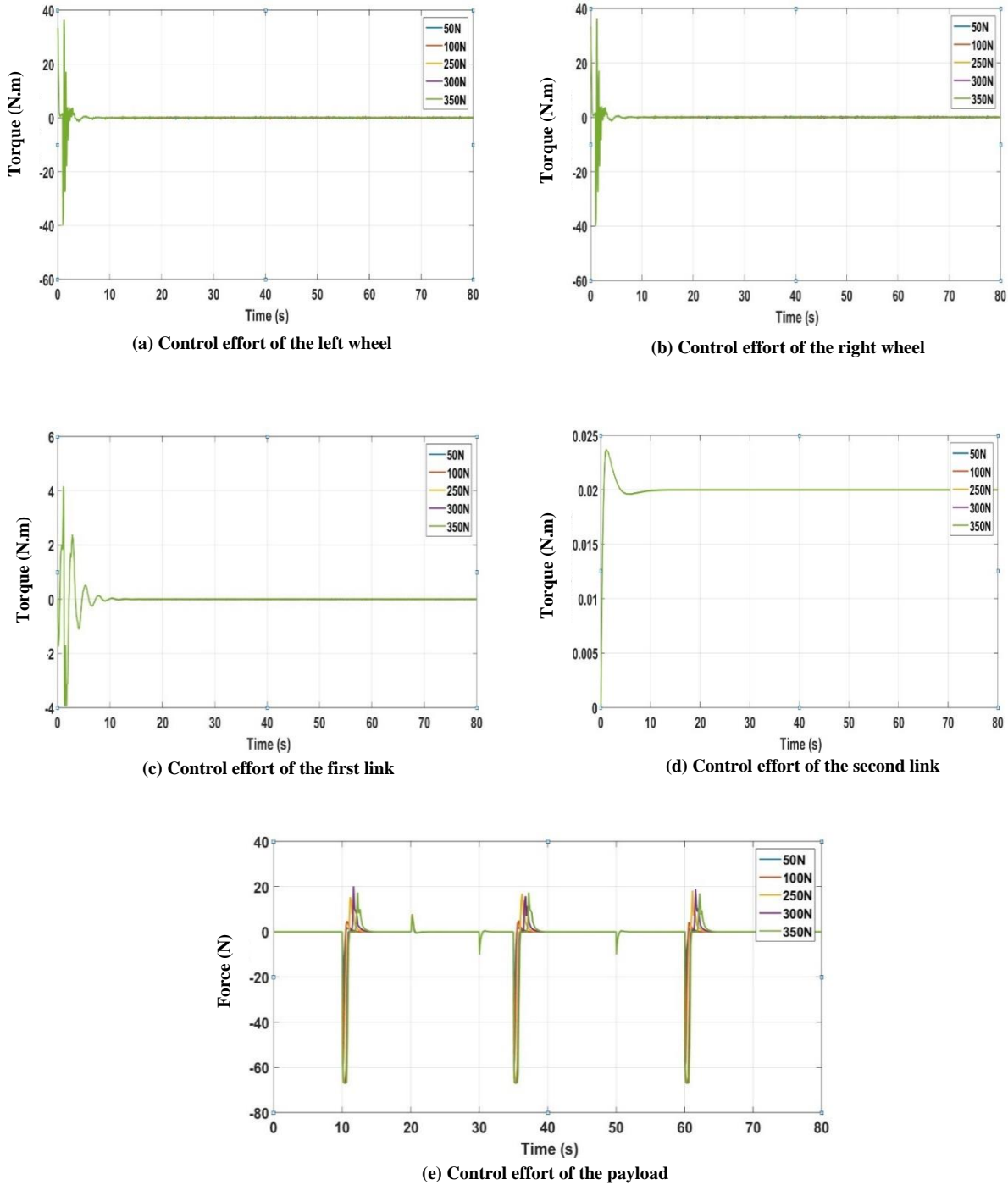


Figure 5. 10: The control system effort with disturbance forces applied on the payload.

The system successfully copes with external disturbance force applied with various amplitudes. The disturbance was applied on the left wheel, right wheel, first link, second link, and payload linear actuator to investigate the hybrid control system robustness. The results demonstrated considerable improvements compared to the previous study. As compared to the authors' previous work [38] the simulation results differ from the previous study in the maximum disturbance force applied. The maximum force applied in the previous work was 300N applied only on the tilt angles of the first link and second link. While in this study the maximum disturbance force was 350N applied on all the system components which successfully cope with an external disturbance with a high degree of robustness. The system specifications for each simulation result when disturbances are applied to each system part separately are provided in APPENDIX-B.

5.3 Summary

This chapter evaluates the two-wheeled robot vehicle robustness by applying external disturbances with different amplitudes. The two-wheeled robot vehicle is simulated to move on flat surfaces. External disturbance forces are applied on each part of the vehicle separately to assess the robustness of the hybrid controllers and study the control system to overcome external disturbances. Simulation results explain the control system's robustness and ability to cope with external disturbance. To validate the system's performance, disturbance forces of various amplitudes were applied. The robot vehicle applied forces measurements of 50N, 100N, 250N, 300N, 350N at all the system components, including the left wheel, right wheel, first link, second link, and the payload linear actuator. The system with different disturbances and related control efforts responses were achieved. From the system response, it can be noticed that the system successfully rejected the external disturbance and back to the desired point. The external disturbances applied on the left wheel produced positive peaks at the left wheel, demonstrating the oscillations at the right wheel and the first link, using more significant disturbance force produced larger peaks. The right wheel responses were precisely the same effect as the left wheel responses, and this explains the correspondence between the wheels when external disturbances were applied. The response of the system with disturbance applied at the first link produces positive peaks at the tilt angle of the first link, and the peaks increase with increasing the disturbance force used. Negative peaks appeared at the displacement of the left wheel and right wheel to keep the vehicle moved in the opposite direction and the tilt angle upright. Applying disturbance on the second link's centre yielded oscillations in the tilt angle of the second link while the other system components do not affect it. The disturbance force is applied at the payload. It was only affected the payload response without changing other system parts. The disturbance force generates positive peaks increased with increasing the force used.

The simulation results showed the ability of the control system to stabilise the robot vehicle and cope with different disturbance forces applied. Chapter six will produce the conclusion, contribution, and future work.

Chapter Six

Conclusion, Contribution, and Future works

6.1 Conclusion

The purpose of this study was to develop control approaches for a two-wheeled robot vehicle with five degrees of freedom. The concept is based on a double inverted pendulum system that has been modified to include the ability to extend the payload to the desired height. The main parts of the robot are the left wheel, right wheel, first link, second link, and movable payload that can move in a variety of situations and different environments. Consequently, to develop appropriate control techniques which are beneficial and effective in dealing with the many conditions encountered in the robot vehicle. The mathematical system model of the robot with two wheels has been presented using the Euler-Lagrange technique that yields five non-linear equations used to describe the suggested model move on flat surfaces. A Proportional Integral Derivative (PID) controller and proportional derivative (PD) controller have stabilised the system, but with higher exerted effort, then a Fuzzy Logic Controller (FLC) was developed for the system stabilisation with fewer torques exerted, so hybrid controllers were designed to include PID with FLC and PD with FLC for vehicle control. The hybrid controller combined the excellent specifications of both control systems used previously moreover, it enhanced the system responses in terms of the system specifications and control effort. The following significant conclusions were obtained:

1. Test the system open-loop response with different force input signals applied to the payload actuator to analyse the system stability.
2. Design PID control system which produces successful stable response but with higher controller effort at each part of the system, especially the wheels that exceeded more than 300N.m.
3. Design FLC controllers that produce a stable response for each part and significantly reduce controller effort exerted for system stabilisation compared with PID controllers.

4. Design hybrid control system includes PID with FLC that improved the system specifications with system controller effort exerted for both wheels 36.45N.m and 4N.m for the first link with 0.0238N.m and 53.3N for the payload actuator.
5. Investigate the system robustness by applying external disturbances with different amplitudes, including 50N, 100N, 250N, 300N and 350N at each part separately.

An external disturbance with various amplitudes is applied to the model parts to test the robustness of the designed controller. The responses show that the designed controller has highly system control robustness that can cope with different forces applied. Thus, concluding and fulfilling the objectives and goals of this research.

6.2 Contribution

The contributions made in this study are:

- Investigating the problem of stabilising the two wheels robot with a movable payload based on a double inverted pendulum system.
- Evaluate and analyse the system performance by applying different input signals at the payload actuator.
- Design and implement different robust controllers and comparison system behaviour considering the proposed control systems used.
- Validate the control systems used by applying various force input signals on the payload to test the control system stability.
- Assess the ability of the designed control system to overcome and reject external disturbances with different amplitudes.

6.3 Future Works

The following recommendations can be considered for future work:

- Apply different optimisation algorithms to improve the control system parameters.
- Balancing the two-wheeled robot vehicle while manoeuvring on inclined surfaces.
- Design different control systems techniques to test the system stability.
- Adding more degrees of freedom to the structure could provide it more mobility and flexibility for application designs.

References

- [1] J. Yi and N. Yubazaki, "Stabilization fuzzy control of inverted pendulum systems," *Artif. Intell. Eng.*, vol. 14, no. 2, pp. 153–163, 2000, doi: 10.1016/S0954-1810(00)00007-8.
- [2] W. Zhong and H. Röck, "Energy and passivity based control of the double inverted pendulum on a cart," *IEEE Conf. Control Appl. - Proc.*, pp. 896–901, 2001, doi: 10.1109/cca.2001.973983.
- [3] M. F. Masrom, N. M. A Ghani, and M. O. Tokhi, "Particle swarm optimization and spiral dynamic algorithm-based interval type-2 fuzzy logic control of triple-link inverted pendulum system: A comparative assessment," *J. Low Freq. Noise Vib. Act. Control*, 2019, doi: 10.1177/1461348419873780.
- [4] K. M. Goher and S. O. Fadlallah, "Control of a Two-wheeled Machine with Two-directions Handling Mechanism Using PID and PD-FLC Algorithms," *Int. J. Autom. Comput.*, vol. 16, no. 4, pp. 511–533, 2019, doi: 10.1007/s11633-019-1172-0.
- [5] S. Ahmad, N. H. Siddique, and M. O. Tokhi, "A modular fuzzy control approach for two-wheeled wheelchair," *J. Intell. Robot. Syst. Theory Appl.*, vol. 64, no. 3–4, pp. 401–426, 2011, doi: 10.1007/s10846-011-9541-0.
- [6] S. Kim and S. J. Kwon, "Dynamic modeling of a two-wheeled inverted pendulum balancing mobile robot," *Int. J. Control. Autom. Syst.*, vol. 13, no. 4, pp. 926–933, 2015, doi: 10.1007/s12555-014-0564-8.
- [7] Y. Liu, Z. Chen, D. Xue, and X. Xu, "Real-time controlling of inverted pendulum by fuzzy logic," *Proc. 2009 IEEE Int. Conf. Autom. Logist. ICAL 2009*, no. August, pp. 1180–1183, 2009, doi: 10.1109/ICAL.2009.5262618.
- [8] J. Wu, W. Zhang, and S. Wang, "A two-wheeled self-balancing robot with the fuzzy PD control method," *Math. Probl. Eng.*, vol. 2012, 2012, doi: 10.1155/2012/469491.
- [9] C. A. Ibañez, O. G. Frias, and M. S. Castañón, "Lyapunov-based controller for the inverted pendulum cart system," *Nonlinear Dyn.*, vol. 40, no. 4, pp. 367–374, 2005,

doi: 10.1007/s11071-005-7290-y.

- [10] S. Rudra and R. K. Barai, “Robust adaptive backstepping control of inverted pendulum on cart system,” *Int. J. Control Autom.*, vol. 5, no. 1, pp. 13–26, 2012.
- [11] M. Bettayeb, C. Boussalem, R. Mansouri, and U. M. Al-Saggaf, “Stabilization of an inverted pendulum-cart system by fractional PI-state feedback,” *ISA Trans.*, vol. 53, no. 2, pp. 508–516, 2014, doi: 10.1016/j.isatra.2013.11.014.
- [12] S. Hanwate, Y. V. Hote, and A. Budhraja, “Design and implementation of adaptive control logic for cart-inverted pendulum system,” *Proc. Inst. Mech. Eng. Part I J. Syst. Control Eng.*, vol. 233, no. 2, pp. 164–178, 2019, doi: 10.1177/0959651818788148.
- [13] S. K. Yadav and Sachin sharma, “Optimal Control of Double Inverted Pendulum Using LQR Controller,” *Int. J. Adv. Res. Comput. Sci. Softw. Eng.*, vol. 2, no. 2, pp. 189–192, 2012, [Online]. Available: <http://www.ijarcse.com/February2012.php>.
- [14] Z. Ben Hazem, M. J. Fotuhi, and Z. Bingül, “Development of a Fuzzy-LQR and Fuzzy-LQG stability control for a double link rotary inverted pendulum,” *J. Franklin Inst.*, vol. 357, no. 15, pp. 10529–10556, 2020, doi: 10.1016/j.jfranklin.2020.08.030.
- [15] H. Su and C. A. Woodham, “On the uncontrollable damped triple inverted pendulum,” *J. Comput. Appl. Math.*, vol. 151, no. 2, pp. 425–443, 2003, doi: 10.1016/S0377-0427(02)00663-5.
- [16] X. L. Zhang, H. M. Fan, J. Y. Zang, L. Zhao, and S. Hao, “Nonlinear control of triple inverted pendulum based on GA–PIDNN,” *Nonlinear Dyn.*, vol. 79, no. 2, pp. 1185–1194, 2015, doi: 10.1007/s11071-014-1735-0.
- [17] S. Kavirayani and U. Salma, *Fuzzy granular computing controls ill-conditioned matrix definitions for triple inverted pendulum*, vol. 758. Springer Singapore, 2018.
- [18] A. Fahmi *et al.*, “Stabilized controller of a two wheels robot,” *Bull. Electr. Eng. Informatics*, vol. 9, no. 4, pp. 1357–1363, 2020, doi: 10.11591/eei.v9i4.1965.

- [19] C. Dias, H. Nishiuchi, S. Hyoudo, and T. Todoroki, “Simulating Interactions between Pedestrians, Segway Riders and Cyclists in Shared Spaces Using Social Force Model,” *Transp. Res. Procedia*, vol. 34, pp. 91–98, 2018, doi: 10.1016/j.trpro.2018.11.018.
- [20] I. Kafetzis and L. Moysis, “Inverted Pendulum: A system with innumerable applications Inverted Pendulum,” *9th Int. Week Dedic. to Maths. Thessaloniki, Greece, March 2017.*, no. February, p. 13, 2017.
- [21] M. Hehn and R. D’Andrea, “A flying inverted pendulum,” *Proc. - IEEE Int. Conf. Robot. Autom.*, no. 2, pp. 763–770, 2011, doi: 10.1109/ICRA.2011.5980244.
- [22] F. M. Phelps and J. H. Hunter, “An Analytical Solution of the Inverted Pendulum,” *Am. J. Phys.*, vol. 33, no. 4, pp. 285–295, 1965, doi: 10.1119/1.1971474.
- [23] Z. Lijuan and T. Yaqing, “Research of car inverted pendulum model based on lagrange equation,” *Proc. World Congr. Intell. Control Autom.*, vol. 1, pp. 820–824, 2006, doi: 10.1109/WCICA.2006.1712457.
- [24] J. Wu, B. Sun, R. Huang, and Z. Peng, “Two-step modeling method for inverted pendulum considering Coulomb friction based on Lagrange equation and its model predictive control,” *Control Eng. Appl. Informatics*, vol. 23, no. 3, pp. 32–41, 2021.
- [25] K. Furuta, H. Kajiwara, and K. Kosuge, “Digital control of a double inverted pendulum on an inclined rail,” *Int. J. Control*, vol. 32, no. 5, pp. 907–924, 1980, doi: 10.1080/00207178008922898.
- [26] H. Niemann and J. K. Poulsen, “Design and analysis of controllers for a double inverted pendulum,” *ISA Trans.*, vol. 44, no. 1, pp. 145–163, 2005, doi: 10.1016/s0019-0578(07)60051-2.
- [27] V. Mohan, A. Rani, and V. Singh, “Robust adaptive fuzzy controller applied to double inverted pendulum,” *J. Intell. Fuzzy Syst.*, vol. 32, no. 5, pp. 3669–3687, 2017, doi: 10.3233/JIFS-169301.
- [28] W. J. Chen, L. Fang, and K. K. Lei, “Fuzzy logic controller for an inverted pendulum

- system,” *Proc. IEEE Int. Conf. Intell. Process. Syst. ICIPS*, vol. 1, no. 2, pp. 185–189, 1998, doi: 10.1109/icips.1997.672762.
- [29] J. J. Wang, “Simulation studies of inverted pendulum based on PID controllers,” *Simul. Model. Pract. Theory*, vol. 19, no. 1, pp. 440–449, 2011, doi: 10.1016/j.simpat.2010.08.003.
- [30] A. Delibasi and I. B. Kucukdemiral, “A robust PID like state-feedback control via LMI approach : An application on a A robust PID like state-feedback control via LMI approach : An,” no. July, 2007, doi: 10.1109/CIRA.2007.382838.
- [31] J. Li, X. Gao, Q. Huang, and O. Matsumoto, “Controller Design of a Two-Wheeled Inverted Pendulum Mobile Robot,” *Proc. 2008 IEEE Int. Conf. Mechatronics Autom. ICMA 2008*, pp. 7–12, 2008, doi: 10.1109/ICMA.2008.4798717.
- [32] Z. Q. Guo, J. X. Xu, and T. H. Lee, “Design and implementation of a new sliding mode controller on an underactuated wheeled inverted pendulum,” *J. Franklin Inst.*, vol. 351, no. 4, pp. 2261–2282, 2014, doi: 10.1016/j.jfranklin.2013.02.002.
- [33] T. J. Ren, T. C. Chen, and C. J. Chen, “Motion control for a two-wheeled vehicle using a self-tuning PID controller,” *Control Eng. Pract.*, vol. 16, no. 3, pp. 365–375, 2008, doi: 10.1016/j.conengprac.2007.05.007.
- [34] K. M. Goher, M. O. Tokhi, and N. H. Siddique, “Dynamic modeling and control of a two wheeled robotic vehicle with a virtual payload,” *ARPJ. Eng. Appl. Sci.*, vol. 6, no. 3, pp. 7–41, 2011.
- [35] A. K. Yadav, P. Gaur, A. P. Mittal, and M. Anzar, “Comparative analysis of various control techniques for inverted pendulum,” *India Int. Conf. Power Electron. IICPE 2010*, no. December 2016, pp. 10–16, 2011, doi: 10.1109/IICPE.2011.5728071.
- [36] J. Wu and W. Zhang, “Design of fuzzy logic controller for two-wheeled self-balancing robot,” *Proc. 6th Int. Forum Strateg. Technol. IFOST 2011*, vol. 2, pp. 1266–1270, 2011, doi: 10.1109/IFOST.2011.6021250.
- [37] A. M. Almeshal, M. O. Tokhi, and K. M. Goher, “Stabilization of a new

configurable two-wheeled machine using a PD-PID and a hybrid FL control strategies: a comparative study,” *Proc. 32nd Int. Conf. Control. Autom. Robot. (ICCAR 2012), Dubai, UAE*, vol. 6, no. 10, pp. 65–72, 2012.

- [38] A. M. Almeshal, M. O. Tokhi, and K. M. Goher, “Robust hybrid fuzzy logic control of a novel two-wheeled robotic vehicle with a movable payload under various operating conditions,” *Proc. 2012 UKACC Int. Conf. Control. Control 2012*, no. September, pp. 747–752, 2012, doi: 10.1109/CONTROL.2012.6334723.
- [39] F. Dai, X. Gao, S. Jiang, Y. Liu, and J. Li, “A multi-DOF two wheeled inverted pendulum robot climbing on a slope,” *2014 IEEE Int. Conf. Robot. Biomimetics, IEEE ROBIO 2014*, pp. 1958–1963, 2014, doi: 10.1109/ROBIO.2014.7090623.
- [40] E. E. Eldukhri and H. G. Kamil, “Optimisation of swing-up control parameters for a robot gymnast using the Bees Algorithm,” *J. Intell. Manuf.*, vol. 26, no. 5, pp. 1039–1047, 2015, doi: 10.1007/s10845-013-0848-5.
- [41] H. G. Kamil, A. A. Ahmed, and A. K. Abbas, “Tuning of Control Motion for a three link robot manipulator using Particle Swarm Optimization Technique,” *J. Univ. Kerbala*, vol. 15, no. 4, pp. 102–110, 2017.
- [42] M. Shehu, M. R. Ahmad, A. Shehu, and A. Alhassan, “LQR, double-PID and pole placement stabilization and tracking control of single link inverted pendulum,” *Proc. - 5th IEEE Int. Conf. Control Syst. Comput. Eng. ICCSCE 2015*, no. November, pp. 218–223, 2016, doi: 10.1109/ICCSCE.2015.7482187.
- [43] A. Kharola, “The control of two-wheeled inverted pendulum robot (TWIPR) using fuzzy logic,” *2015 IEEE Int. Conf. Comput. Intell. Comput. Res. ICCIC 2015*, no. m, pp. 6–9, 2016, doi: 10.1109/ICCIC.2015.7435680.
- [44] A. Kharola, P. Patil, S. Raiwani, and D. Rajput, “A comparison study for control and stabilisation of inverted pendulum on inclined surface (IPIS) using PID and fuzzy controllers,” *Perspect. Sci.*, vol. 8, pp. 187–190, 2016, doi: 10.1016/j.pisc.2016.03.016.

- [45] S. C. & V. V. Shubhank Sondhia, Ranjith Pillai. R, Sharat S. Hegde, “Development of Self Balancing Robot With PID Control,” *Int. J. Robot. Res. Dev. (IJRRD)*, vol. 7, no. 1, pp. 1–6, 2017, [Online]. Available: <http://www.tjprc.org/view-archives.php>.
- [46] R. Eini and S. Abdelwahed, “Indirect Adaptive fuzzy Controller Design for a Rotational Inverted Pendulum,” *Proc. Am. Control Conf.*, vol. 2018-June, pp. 1677–1682, 2018, doi: 10.23919/ACC.2018.8431796.
- [47] K. Pankaj, “A Relative Analysis of PD based Fuzzy , Neural And ANFIS Controller for Balance Control of Inverterd- Pendulum System,” vol. 118, no. 20, pp. 1947–1953, 2018.
- [48] I. Siradjuddin *et al.*, “Stabilising a cart inverted pendulum with an augmented PID control scheme,” *MATEC Web Conf.*, vol. 197, 2018, doi: 10.1051/mateconf/201819711013.
- [49] A. Y. Zimit, H. J. Yap, and M. F. Hamza, “Modelling and Experimental Analysis Two-Wheeled Self Balance Robot Using PID Controller,” vol. 2, pp. 683–698.
- [50] M. Heidar, K. Fadaei, S. Ali, H. Pahnkehkolaei, and M. Jafari, “Design of Hybrid Fuzzy-PD Controller for an Inverted Pendulum,” vol. 10, no. 2, pp. 21–27, 2021.
- [51] N. P. Nguyen, H. Oh, Y. Kim, and J. Moon, “A nonlinear hybrid controller for swinging-up and stabilizing the rotary inverted pendulum,” *Nonlinear Dyn.*, vol. 104, no. 2, pp. 1117–1137, 2021, doi: 10.1007/s11071-021-06317-2.
- [52] A. Shiriaev, A. Pogromsky, H. Ludvigsen, and O. Egeland, “On global properties of passivity-based control of an inverted pendulum,” *Int. J. Robust Nonlinear Control*, vol. 10, no. 4, pp. 283–300, 2000, doi: 10.1002/(SICI)1099-1239(20000415)10:4<283::AID-RNC473>3.0.CO;2-I.
- [53] J. Aminuddin *et al.*, “Estimation of Ideal Configuration and Dimension of Pico Hydropower using Euler-Lagrange Equation and Runge-Kutta Method,” *J. Phys. Conf. Ser.*, vol. 1494, no. 1, 2020, doi: 10.1088/1742-6596/1494/1/012039.

- [54] S. Sheffield, "Development and control of a novel-structure two-wheeled robotic vehicle manoeuvrable in different terrains by," no. December, 2013.
- [55] A. M. Almeshal, K. M. Goher, A. N. K. Nasir, and M. O. Tokhi, "Steering and dynamic performance of a new configuration of a wheelchair on two wheels in various indoor and outdoor environments," *2013 18th Int. Conf. Methods Model. Autom. Robot. MMAR 2013*, pp. 223–228, 2013, doi: 10.1109/mmar.2013.6669910.
- [56] Q. R. Li, W. H. Tao, S. Na, C. Y. Zhang, and L. H. Yao, "Stabilization control of double inverted pendulum system," *3rd Int. Conf. Innov. Comput. Inf. Control. ICICIC'08*, pp. 1–4, 2008, doi: 10.1109/ICICIC.2008.662.
- [57] N. H. Shah and M. Yeolekar, "Pole Placement Approach for Controlling," *Glob. J. Res. Eng. Mech. Mech. Eng.*, vol. 13, no. 2, p. 9, 2013.
- [58] A. N. K. Nasir, M. A. Ahmad, and M. F. Rahmat, "Performance comparison between LQR and PID controllers for an inverted pendulum system," *AIP Conf. Proc.*, vol. 1052, pp. 124–128, 2008, doi: 10.1063/1.3008655.
- [59] J. N. Rai, "Speed Control of Dc Motor Using Fuzzy Logic Technique," *IOSR J. Electr. Electron. Eng.*, vol. 3, no. 6, pp. 41–48, 2012, doi: 10.9790/1676-0364148.
- [60] S. K. Sarkar, F. R. Badal, and S. K. Das, "A comparative study of high performance robust PID controller for grid voltage control of islanded microgrid," *Int. J. Dyn. Control*, vol. 6, no. 3, pp. 1207–1217, 2018, doi: 10.1007/s40435-017-0364-0.
- [61] H. Jafari, G. Nikolakopoulos, and T. Gustafsson, "Stabilization of an inverted pendulum via human brain inspired controller design," *IEEE-RAS Int. Conf. Humanoid Robot.*, vol. 2019-Octob, pp. 433–438, 2019, doi: 10.1109/Humanoids43949.2019.9035019.
- [62] K. M. Elbayomy, Z. Jiao, and H. Zhang, "PID controller optimization by GA and its performances on the electro-hydraulic servo control system," *Chinese J. Aeronaut.*, vol. 21, no. 4, pp. 378–384, 2008, doi: 10.1016/S1000-9361(08)60049-7.
- [63] L. B. Prasad, B. Tyagi, and H. O. Gupta, "Modelling & simulation for optimal

control of nonlinear inverted pendulum dynamical system using PID controller & LQR,” *Proc. - 6th Asia Int. Conf. Math. Model. Comput. Simulation, AMS 2012*, pp. 138–143, 2012, doi: 10.1109/AMS.2012.21.

- [64] O. Of, “Determination of the PID Controller Parameters by Modified Genetic Algorithm for Improved Performance Time,” vol. 1480, pp. 1469–1480, 2007.
- [65] M. Salami and G. Cain, “An Adaptive PID Controller Based on Genetic Algorithm Processor,” no. 414, 1995.
- [66] A. R. Short, O. K. Sayidmarie, S. A. Agouri, M. O. Tokhi, K. M. Goher, and A. M. Almeshal, “Real time PID control of a two-wheeled robot,” *Adapt. Mob. Robot. - Proc. 15th Int. Conf. Climbing Walk. Robot. Support Technol. Mob. Mach. CLAWAR 2012*, pp. 73–80, 2012, doi: 10.1142/9789814415958_0013.
- [67] R. Paz, “The Design of the PID Controller The Design of the PID Controller,” no. April, 2014.
- [68] A. Latif, K. Shankar, and P. T. Nguyen, “Legged fire fighter robot movement using PID,” *J. Robot. Control*, vol. 1, no. 1, pp. 15–18, 2020, doi: 10.18196/jrc.1104.
- [69] B. H. Daulay, M. S. Lydia, and R. W. Sembiring, “Robot Arm Inverse Kinematics Wrist Tilt Repair Using PID Control System (Proportional, Integrative, Derivative),” *J. Phys. Conf. Ser.*, vol. 1898, no. 1, 2021, doi: 10.1088/1742-6596/1898/1/012035.
- [70] L. A. Zadeh, “Fuzzy logic,” *Comput. Complex. Theory, Tech. Appl.*, vol. 9781461418, pp. 1177–1200, 2013, doi: 10.1007/978-1-4614-1800-9_73.
- [71] A. I. Roose, S. Yahya, and H. Al-Rizzo, “Fuzzy-logic control of an inverted pendulum on a cart,” *Comput. Electr. Eng.*, vol. 61, pp. 31–47, 2017, doi: 10.1016/j.compeleceng.2017.05.016.
- [72] A. S. Kedia, K. B. Saw, and B. K. Katti, “Fuzzy logic approach in mode choice modelling for education trips: A case study of Indian metropolitan city,” *Transport*, vol. 30, no. 3, pp. 286–293, 2015, doi: 10.3846/16484142.2015.1081279.

- [73] O. K. Sayidmarie, M. O. Tokhi, A. M. Almeshal, and S. A. Agouri, "Design and real-time implementation of a fuzzy logic control system for a two-wheeled robot," *2012 17th Int. Conf. Methods Model. Autom. Robot. MMAR 2012*, pp. 569–572, 2012, doi: 10.1109/MMAR.2012.6347823.
- [74] K. M. Goher and S. O. Fadlallah, "Control of a led Machine with Two-directions Handling MecTwo-wheehanism Using PID and PD-FLC Algorithms," *Int. J. Autom. Comput.*, vol. 16, no. 4, pp. 511–533, 2019, doi: 10.1007/s11633-019-1172-0.
- [75] X. Li and B. J. Choi, "Design of obstacle avoidance system for mobile robot using fuzzy logic systems," *Int. J. Smart Home*, vol. 7, no. 3, pp. 321–328, 2013.
- [76] M. Rivai, Rendyansyah, and D. Purwanto, "Implementation of fuzzy logic control in robot arm for searching location of gas leak," *2015 Int. Semin. Intell. Technol. Its Appl. ISITIA 2015 - Proceeding*, pp. 69–74, 2015, doi: 10.1109/ISITIA.2015.7219955.
- [77] A. Mohammadzadeh and H. Taghavifar, "A robust fuzzy control approach for path-following control of autonomous vehicles," *Soft Comput.*, vol. 24, no. 5, pp. 3223–3235, 2020, doi: 10.1007/s00500-019-04082-4.
- [78] I. Erenoglu, I. Eksin, E. Yesil, and M. Guzelkaya, "An intelligent hybrid fuzzy PID controller," *20th Eur. Conf. Model. Simul. Model. Methodol. Simul. Key Technol. Acad. Ind. ECMS 2006*, vol. 5, no. Cd, pp. 62–66, 2006, doi: 10.7148/2006-0062.
- [79] P. Pratumswa, S. Thongchai, and S. Tansriwong, "A Hybrid of Fuzzy and Proportional-Integral-Derivative Controller for Electro-Hydraulic Position Servo System," *Energy Res. J.*, vol. 1, no. 2, pp. 62–67, 2010, doi: 10.3844/erjsp.2010.62.67.
- [80] T. L. Grigorie, R. M. Botez, A. V. Popov, M. Mamou, and Y. Mébarki, "A hybrid fuzzy logic proportionalintegral-derivative and conventional on-off controller for morphing wing actuation using shape memory alloy Part 2: Controller implementation and validation," *Aeronaut. J.*, vol. 116, no. 1179, pp. 451–465,

2012, doi: 10.1017/S0001924000006989.

- [81] R. A. Krohling and J. P. Rey, “Design of Optimal Disturbance Rejection PID Controllers Using Genetic Algorithms,” vol. 5, no. 1, pp. 78–82, 2001.
- [82] K. Zheng, H. Liu, and L. Yu, “Robust fuzzy control of a nonlinear magnetic bearing system with computing time delay,” *IEEE/ASME Int. Conf. Adv. Intell. Mechatronics, AIM*, pp. 839–843, 2008, doi: 10.1109/AIM.2008.4601770.
- [83] W. M. Bessa, M. S. Dutra, and E. Kreuzer, “Depth control of remotely operated underwater vehicles using an adaptive fuzzy sliding mode controller,” *Rob. Auton. Syst.*, vol. 56, no. 8, pp. 670–677, 2008, doi: 10.1016/j.robot.2007.11.004.
- [84] L. B. Prasad, H. O. Gupta, and B. Tyagi, “Intelligent control of nonlinear inverted pendulum dynamical system with disturbance input using fuzzy logic systems,” *2011 Int. Conf. Recent Adv. Electr. Electron. Control Eng. IConRAEeCE'11 - Proc.*, pp. 136–141, 2011, doi: 10.1109/ICONRAEeCE.2011.6129799.

APPENDICES

APPENDIX-A

The constants used when the model move on flat surface.

$$C_1 = 2L_{21} + L_{2u}$$

$$C_2 = 2L_{21} + 2L_{2u}$$

$$C_3 = L_1(M_1 + 2(M_m + M_{2l} + M + M_a + M_{2u}))$$

$$C_4 = L_{2l}(M_{2l} + 2M_a)$$

$$C_5 = M_{2u}C_1 + MC_2$$

$$C_6 = C_8 = M_{2u} + M$$

$$C_7 = M_1 + M_m + M + M_{2l} + M_{2u} + M_a$$

$$C_8 = M_{2u} + M$$

$$C_9 = M_1 + 2M_m + 2M_{2l} + 2M + 2M_a + 2M_{2u}$$

$$C_{10} = L_{2l}(M_{2l} + 2M_a) + M_{2u}C_1 + MC_2$$

$$C_{11} = L_{2l}^2(M_{2l} + 4M_a) + M_{2u}C_1^2 + MC_2^2$$

$$C_{12} = 2M_{2u}C_1 + 2MC_2$$

$$C_{13} = L_l(M_1 + 2M_m) + 2L_1(M_{2l} + M_{2u} + M_a + M)$$

$$C_{14} = L_{2l}M_{2u} + 2L_{2l}M_a + M_{2u}C_1 + MC$$

$$C_{15} = C_4 + C_5$$

$$C_{16} = 2J_w + J_{IB}$$

$$C_{17} = M_w R_w^2 + J_w$$

$$C_{18} = 2L_1^2(M_{2l} + M_{2u} + M_a + M) + \frac{1}{2}(M_1 L_1^2 + J_1) + \frac{1}{2}(4M_1 L_1^2 + J_m)$$

$$C_{19} = J_{2l} + J_{2u} + J_a + J_M$$

$$C_{20} = C_{11} + C_{19}$$

$$C_{21} = \frac{1}{2}R_w^2 C_7 + C_{17}$$

$$C_{22} = \frac{1}{4}R_w^2 C_7$$

APPENDIX-B

Table B.1: Disturbance applied on the left wheel.

50N	Rise Time	Settling Time	Overshoot	Peak Time
Left Wheel	0.6730s	60.6467s	4.708%	10.201s
Right Wheel	0.6730s	1.2685s	4.737%	1.0551s
First Link	0.07209s	62.0666s	88.007%	1.1471s
Second Link	4.529s	9.6468s	0.505%	13.187s
Payload	7.904s	59.7980s	0.510%	30.220s

100N	Rise Time	Settling Time	Overshoot	Peak Time
Left Wheel	0.66813s	61.0987s	4.725%	10.344s
Right Wheel	0.66947s	1.2688s	4.737%	1.055s
First Link	0.157911s	66.1863s	146.204%	1.729s
Second Link	4.529s	9.6468s	0.505%	13.138s
Payload	7.977s	59.7980s	0.505%	30.320s

250N	Rise Time	Settling Time	Overshoot	Peak Time
Left Wheel	0.1212s	63.0587s	179.898%	10.742s
Right Wheel	0.66947s	1.2687s	4.737%	1.055s
First Link	0.10868s	70.7000s	145.986%	11.566s
Second Link	4.529s	9.6468s	0.505%	13.170s
Payload	7.910s	59.7980s	0.510%	30.320s

300N	Rise Time	Settling Time	Overshoot	Peak Time
Left Wheel	0.3133s	63.9389s	32.543%	10.822s
Right Wheel	0.669s	1.2687s	4.737%	1.055s
First Link	0.0036s	71.1626s	250.014%	11.580s
Second Link	4.529s	9.6468s	0.505%	13.171s
Payload	7.901s	59.7980s	0510%	30.320s

350N	Rise Time	Settling Time	Overshoot	Peak Time
Left Wheel	0.4636s	65.0493s	9.071%	11.033s
Right Wheel	0.6694s	1.2686s	4.737%	1.055s
First Link	0.0644s	69.3005s	374.054%	11.656s
Second Link	4.529s	9.6468s	0.505%	13.162s
Payload	7.901s	59.7980s	0.510%	30.320s

Table B.2: Disturbance applied on the right wheel.

50N	Rise Time	Settling Time	Overshoot	Peak Time
Left Wheel	0.66947s	1.2685s	4.737%	1.055s
Right Wheel	0.66947s	60.6467s	4.708%	10.201s
First Link	0.070209s	62.0666s	88.007%	1.729s
Second Link	4.529s	9.6468s	0.505%	13.187s
Payload	7.904s	59.7980s	0.510%	30.320s

100N	Rise Time	Settling Time	Overshoot	Peak Time
Left Wheel	0.66813s	61.0987s	4.725%	10.344s
Right Wheel	0.66947s	1.2688s	4.737%	1.055s
First Link	0.157911s	66.1863s	146.204%	1.729s
Second Link	4.529s	9.6468s	0.505%	13.138s
Payload	7.977s	59.7980s	0.505%	30.320s

250N	Rise Time	Settling Time	Overshoot	Peak Time
Left Wheel	0.1212s	63.0587s	179.898%	10.742s
Right Wheel	0.66947s	1.2687s	4.737%	1.055s
First Link	0.10868s	70.7000s	145.986%	11.566s
Second Link	4.529s	9.6468s	0.505%	13.170s
Payload	7.910s	59.7980s	0.510%	30.320s

300N	Rise Time	Settling Time	Overshoot	Peak Time
Left Wheel	0.3133s	63.9389s	32.543%	10.822s
Right Wheel	0.669s	1.2687s	4.737%	1.055s
First Link	0.0036s	71.1626s	250.014%	11.580s
Second Link	4.529s	9.6468s	0.505%	13.171s
Payload	7.901s	59.7980s	0510%	30.320s

350N	Rise Time	Settling Time	Overshoot	Peak Time
Left Wheel	0.4636s	65.0493s	9.071%	11.033s
Right Wheel	0.6694s	1.2686s	4.737%	1.055s
First Link	0.0644s	69.3005s	374.054%	11.656s
Second Link	4.529s	9.6468s	0.505%	13.162s
Payload	7.901s	59.7980s	0.510%	30.320s

Table B.3: Disturbance applied on the first link.

50N	Rise Time	Settling Time	Overshoot	Peak Time
Left Wheel	0.6694s	60.6787s	4.737%	1.055s
Right Wheel	0.6694s	60.6787s	4.737%	1.055s
First Link	0.0612s	63.1500s	141.409%	1.729s
Second Link	4.529s	9.6468s	0.505%	13.186s
Payload	7.903s	59.7980s	0.510%	30.320s

100N	Rise Time	Settling Time	Overshoot	Peak Time
Left Wheel	0.6661s	61.2972s	5.245%	10.830s
Right Wheel	0.6661s	61.2972s	5.245%	10.830s
First Link	0.1430s	67.3355s	316.934%	35.596s
Second Link	4.529s	9.6468s	0.505%	13.154s
Payload	7.902s	59.7980s	0.510%	30.320s

250N	Rise Time	Settling Time	Overshoot	Peak Time
Left Wheel	1.419s	63.0538s	14.848%	37.822s
Right Wheel	1.419s	63.0538s	14.848%	37.822s
First Link	0.0056s	70.6385s	400.007%	60.728s
Second Link	4.528s	9.6468s	0.505%	13.280s
Payload	7.901s	59.7980s	0.510%	30.320s

300N	Rise Time	Settling Time	Overshoot	Peak Time
Left Wheel	1.212s	64.0356s	25.530%	62.939s
Right Wheel	1.212s	64.0356s	25.530%	62.939s
First Link	0.06847s	71.1251s	470.809%	35.830s
Second Link	4.528s	9.6468s	0.505%	13.267s
Payload	7.902s	59.7980s	0.510%	30.320s

350N	Rise Time	Settling Time	Overshoot	Peak Time
Left Wheel	1.296s	65.1262s	26.837%	63.307s
Right Wheel	1.296s	65.1262s	26.837%	63.307s
First Link	0.1321s	69.1453s	161.319%	10.782s
Second Link	4.528s	9.6468s	0.505%	13.245s
Payload	7.901s	59.7980s	0.510%	30.320s

Table B.4: Disturbance applied on the second link.

50N	Rise Time	Settling Time	Overshoot	Peak Time
Left Wheel	0.6694s	1.2677s	4.737%	1.055s
Right Wheel	0.6694s	1.2677s	4.737%	1.055s
First Link	0.0621s	9.6135s	99.960%	1.729s
Second Link	0.1835s	70.7731s	24.224%	35.459s
Payload	7.902s	59.7980s	0.510%	30.320s

100N	Rise Time	Settling Time	Overshoot	Peak Time
Left Wheel	0.6694s	1.2698s	4.737%	1.055s
Right Wheel	0.6694s	1.2698s	4.737%	1.055s
First Link	0.0621s	9.5544s	99.960%	1.729s
Second Link	0.1094s	71.7194s	136.427%	35.459s
Payload	7.902s	59.7980s	0.510%	30.320s

250N	Rise Time	Settling Time	Overshoot	Peak Time
Left Wheel	0.6694s	1.2678s	4.737%	1.055s
Right Wheel	0.6694s	1.2678s	4.737%	1.055s
First Link	0.0621s	9.6062s	99.960%	1.729s
Second Link	0.4720s	75.2021s	-0.309%	35.828s
Payload	7.902s	59.7980s	0.510%	30.320s

300N	Rise Time	Settling Time	Overshoot	Peak Time
Left Wheel	0.6694s	1.2672s	4.737%	1.055s
Right Wheel	0.6694s	1.2672s	4.737%	1.055s
First Link	0.0621s	9.6214s	99.960%	1.729s
Second Link	0.5329s	74.4226s	-0.927%	10.930s
Payload	7.902s	59.7980s	0.510%	30.320s

350N	Rise Time	Settling Time	Overshoot	Peak Time
Left Wheel	0.6694s	1.2685s	4.737%	1.055s
Right Wheel	0.6694s	1.2685s	4.737%	1.055s
First Link	0.0621s	9.5857s	99.960%	1.729s
Second Link	0.9140s	75.2441s	18.049%	60.956s
Payload	7.902s	59.7980s	0.510%	30.320s

Table B.5: Disturbance applied on the payload.

50N	Rise Time	Settling Time	Overshoot	Peak Time
Left Wheel	0.6694s	1.2687s	4.737%	1.055s
Right Wheel	0.6694s	1.2687s	4.737%	1.055s
First Link	0.0621s	9.5806s	99.960%	1.729s
Second Link	4.529s	9.6468s	0.505%	13.234s
Payload	7.815s	60.5946s	4.737%	35.226s

100N	Rise Time	Settling Time	Overshoot	Peak Time
Left Wheel	0.6694s	1.2688s	4.737%	1.055s
Right Wheel	0.6694s	1.2688s	4.737%	1.055s
First Link	0.0621s	9.5751s	99.960%	1.729s
Second Link	4.528s	9.6468s	0.505%	13.206s
Payload	7.846s	60.9714s	9.341%	35.310s

250N	Rise Time	Settling Time	Overshoot	Peak Time
Left Wheel	0.6694s	1.2684s	4.737%	1.055s
Right Wheel	0.6694s	1.2684s	4.737%	1.055s
First Link	0.0621s	9.5751s	99.960%	1.729s
Second Link	4.529s	9.6468s	0.505%	13.221s
Payload	7.865s	61.8512s	46.324%	35.567s

300N	Rise Time	Settling Time	Overshoot	Peak Time
Left Wheel	0.6694s	1.2681s	4.737%	1.055s
Right Wheel	0.6694s	1.2681s	4.737%	1.055s
First Link	0.0621s	9.6014s	99.960%	1.729s
Second Link	4.529s	9.6468s	0.505%	13.270s
Payload	7.900s	62.2652s	65.833%	35.642s

350N	Rise Time	Settling Time	Overshoot	Peak Time
Left Wheel	0.6694s	1.2686s	4.737%	1.055s
Right Wheel	0.6694s	1.2686s	4.737%	1.055s
First Link	0.0621s	9.6041s	99.960%	1.729s
Second Link	4.529s	9.6468s	0.505%	13.253s
Payload	7.781s	62.7554s	91.346%	35.700s

الخلاصة

يهدف هذا العمل الى تحديد نظام التحكم لروبوت ذات العجلتين مع حمولة قابلة للتمديد. يعتمد هذا النظام على آلية البندول المقلوب المزدوج. يتألف النموذج من خمسة أجزاء تتضمن (العجلة اليمنى, العجلة اليسرى, الرابط الأول, الرابط الثاني, والحمولة القابلة للتمديد). يتمتع هذا الروبوت بقدرته على رفع الحمولة حسب الارتفاع المطلوب مما يوفر مزيداً من المرونة والراحة والحماية للمستخدمين مع الحفاظ على استقرار النظام اثناء حركته في بيئات مختلفة.

تم اشتقاق النموذج الرياضي باستخدام معادلات رياضية (Euler-Lagrange equations) للاستفادة منها في بناء المتحكم، و نظراً للاقتران الشديد بين أجزاءه وتعقيده ولكونه غير خطي فقد شكل تحديات للتحكم في أجزاء النظام بما في ذلك موازنة الجسم الوسطي المتألف من جزئين و الإزاحة الزاوية للعجلات بالإضافة الى رفع الحمولة للارتفاع المطلوب.

تم تصميم طرق تحكم مختلفة لدراسة استقرار النظام للمركبة ذات العجلتين. يشمل النوع الأول متحكمين هما Proportional Integral Derivative (PID) و Proportional Derivative (PD). هذه الطرق تم ضبطها تدريجياً حتى وصول أجزاء النظام الى حالة الاستقرار.

النوع الثاني من المسيطرات هو Fuzzy Logic Controller (FLC). بالإضافة الى النوع الثالث وهو مسيطر هجين والذي يشمل كل من النوعين السابقين (PID+FLC) hybrid controller و (PD+FLC).

جميع طرق التحكم المختلفة التي تم استخدامها ساعدت على استقرار النموذج حيث أن النوع الأول (PID-PD) حقق استجابة مستقرة ولكن مع بذل جهد أعلى للمسيطر والتي تصل الى اكثر من 300N.m بالنسبة لمحرك العجلات. مع ذلك من الضروري تقليل جهد المسيطر لتحقيق استقرار النظام وقد لوحظ انخفاض جهد المسيطر في جميع أجزاء النظام ومع استجابة مستقرة عندما تم تصميم مسيطر (FLC). حيث بلغ جهد المسيطر لتحريك العجلات اليمنى و اليسرى اقل من 45N.m.

بعد ذلك تم تصميم مسيطر هجين يجمع بين الطريقتين السابقتين والذي بدوره ساعد على جمع الخصائص الجيدة بين الطريقتين مما أدى الى تحسين الاستجابة الكلية لجميع الأجزاء دون التأثير على استقرارية النظام.

تم تطبيق المقارنة بين النتائج النظرية بناءً على جهد المسيطر ومواصفات النظام والتي تتضمن (settling time, rise time, overshoot, peak time, and steady-state error) للحصول على أفضل وحدات تحكم للنظام المقترح.

تم تسليط قوى خارجية ذات قيم مختلفة من أجل اختبار متانة نظام التحكم وكانت أقصى قوى تم تسليطها بقيمة 350N على كل جزء من أجزاء الروبوت لدراسة قدرة النظام على التعامل مع مختلف القوى الخارجية التي قد يتعرض لها النموذج.

بغية الحصول على النتائج آنفة الذكر تم تنفيذ محاكاة النموذج ذات العجلتين مع الحمولة المنقولة المصممة بأنظمة تحكم مختلفة باستخدام برنامج الماتلاب (MATLAB/Simulink).



جمهورية العراق
وزارة التعليم العالي والبحث العلمي
جامعة كربلاء/كلية الهندسة
قسم الهندسة الكهربائية والإلكترونية

تصميم وحدة التحكم للمركبة الآلية ذات العجلتين بناءً على تقنية المنطق الضبابي

رسالة مقدمة الى

كلية الهندسة/ جامعة كربلاء

كجزء من متطلبات نيل شهادة الماجستير في علوم الهندسة الكهربائية

من قبل

يمنى صباح حسين

تحت اشراف

أ.م.د. حيدر جليل كامل

أ.م.د. أحمد عبدالهادي أحمد

1443هـ

2022م